

SULPHIDE ZONING AT THE LAKESHORE COPPER DEPOSIT,  
PINAL COUNTY, ARIZONA

by

David Long South

---

A Thesis Submitted to the Faculty of the  
DEPARTMENT OF GEOSCIENCES  
In Partial Fulfillment of the Requirements  
For the Degree of  
MASTER OF SCIENCE  
In the Graduate College  
THE UNIVERSITY OF ARIZONA

1 9 7 2

STATEMENT BY AUTHOR

This thesis has been submitted in partial fulfillment of requirements for an advanced degree at The University of Arizona and is deposited in the University Library to be made available to borrowers under rules of the Library.

Brief quotations from this thesis are allowable without special permission, provided that accurate acknowledgment of source is made. Requests for permission for extended quotation from or reproduction of this manuscript in whole or in part may be granted by the head of the major department or the Dean of the Graduate College when in his judgment the proposed use of the material is in the interests of scholarship. In all other instances, however, permission must be obtained from the author.

SIGNED:

David L. South

APPROVAL BY THESIS DIRECTOR

This thesis has been approved on the date shown below:

John M. Guilbert  
JOHN M. GUILBERT  
Associate Professor of Geosciences

July 4, 1972  
Date

## ACKNOWLEDGMENTS

Many people provided assistance without which this thesis would not have been possible. Especial thanks go to the Hecla Mining Company for providing access to information and for funds to finance the work and to the Department of Geosciences, The University of Arizona, for providing computer time and funds for drafting. Much of the computer programming was done by Carlos Aiken, and his assistance throughout the computer programming phase of this project made the project possible. John Kaur of Digitgraph Computer Systems Company, Tucson, Arizona, was most helpful in explaining the intricacies of the double-Fourier trend surface analysis program, and Dr. J. R. Sturgul was helpful in determining parameters to be used in the trend surface analysis.

Many thanks go to the geologic staff at Lakeshore for their time and patience. Mr. James J. Quinlan, Chief Geologist, in particular, spent many hours discussing the geology of the Lakeshore area and critically reviewing the manuscript. Dr. William P. Johnston also reviewed the manuscript and made helpful suggestions.

My committee members, Dr. J. M. Guilbert, Dr. K. L. Zonge, and Dr. William B. Bull, reviewed the manuscript to check for clarity and accuracy. Dr. J. M. Guilbert, my thesis director, provided assistance and direction throughout the project. Illustrations were done by Carolyn Shakel.

## TABLE OF CONTENTS

	Page
LIST OF ILLUSTRATIONS . . . . .	vi
ABSTRACT . . . . .	x
INTRODUCTION . . . . .	1
Purpose of Study and Method of Data Handling . . . . .	3
Data-handling Techniques . . . . .	5
Types of Maps Generated . . . . .	8
Rock-type Maps . . . . .	8
Level Maps . . . . .	10
GEOLOGY OF THE LAKESHORE MINE . . . . .	12
General Geologic Setting . . . . .	12
Geology of the Mine Area . . . . .	15
SULFIDE ZONING PATTERNS . . . . .	21
Sulfide Zoning at Lakeshore . . . . .	22
Sulfide Zoning by Rock Type . . . . .	26
Overall Zoning Pattern . . . . .	26
Upper Porphyry . . . . .	30
Lower Porphyry . . . . .	30
Cretaceous Volcanic and Sedimentary Rocks . . . . .	39
Tactite . . . . .	44
Dripping Spring Quartzite . . . . .	49
Diabase . . . . .	49
Sulfide Zoning by Level . . . . .	58
Chalcopyrite Zoning . . . . .	63
Pyrite-chalcopyrite Ratio Zoning . . . . .	76
Pyrite Zoning . . . . .	76
Summary of Sulfide Zoning Patterns at the Lakeshore Mine . . . . .	77
Overall Zoning Pattern . . . . .	78
Upper Porphyry . . . . .	78
Lower Porphyry . . . . .	78
Cretaceous Volcanic and Sedimentary Rocks . . . . .	78
Tactite . . . . .	78
Dripping Spring Quartzite . . . . .	79
Diabase . . . . .	79
Level Maps . . . . .	79

TABLE OF CONTENTS--Continued

	Page
COMPARISON OF ZONING AT LAKESHORE WITH HYPOTHETICAL ZONING IN PORPHYRY COPPER DEPOSITS . . . . .	80
APPENDIX: TREND SURFACE ANALYSIS . . . . .	84
Statistical Measures--Goodness of Fit . . . . .	94
Percent Sum of the Squares Contribution. . . . .	94
F Ratio . . . . .	98
REFERENCES . . . . .	102

## LIST OF ILLUSTRATIONS

Figure	Page
1. Location Map of the Lakeshore Mine, Arizona . . . . .	2
2. Surface Geology, Lakeshore Mine Area . . . . .	13
3. Geology of Section AA', Figure 2 . . . . .	17
4. Location of Drill Holes from Which Data Were Obtained .	19
5. Contour Map of the Top of the Sulfide Zone, Lakeshore Mine . . . . .	24
6. Geologic Map of the 700 Level, Lakeshore Mine. . . . .	25
7. Overall Zoning Pattern of Pyrite, Lakeshore Mine . . . . .	27
8. Overall Zoning Pattern of Chalcopyrite, Lakeshore Mine .	28
9. Overall Zoning Pattern of Pyrite-chalcopyrite Ratio, Lakeshore Mine . . . . .	29
10. Isopach Map of the Upper Porphyry within the Sulfide Zone, Lakeshore Mine . . . . .	31
11. Zoning Pattern of Pyrite in Upper Porphyry, Lakeshore Mine . . . . .	32
12. Zoning Pattern of Chalcopyrite in Upper Porphyry, Lakeshore Mine . . . . .	33
13. Zoning Pattern of Pyrite-chalcopyrite Ratio in Upper Porphyry, Lakeshore Mine . . . . .	34
14. Isopach Map of the Lower Porphyry, Lakeshore Mine . . .	35
15. Zoning Pattern of Pyrite in Lower Porphyry, Lakeshore Mine . . . . .	36
16. Zoning Pattern of Chalcopyrite in Lower Porphyry, Lakeshore Mine . . . . .	37
17. Zoning Pattern of Pyrite-chalcopyrite Ratio in Lower Porphyry, Lakeshore Mine . . . . .	38

LIST OF ILLUSTRATIONS--Continued

Figure	Page
18. Isopach Map of the Cretaceous Volcanic and Sedimentary Rocks within the Sulfide Zone, Lakeshore Mine . . . . .	40
19. Zoning Pattern of Pyrite in Cretaceous Volcanic and Sedimentary Rocks, Lakeshore Mine. . . . .	41
20. Zoning Pattern of Chalcopyrite in Cretaceous Volcanic and Sedimentary Rocks, Lakeshore Mine . . . . .	42
21. Zoning Pattern of Pyrite-chalcopyrite Ratio in Cretaceous Volcanic and Sedimentary Rocks, Lakeshore Mine . . . . .	43
22. Isopach Map of the Tactite within the Sulfide Zone, Lakeshore Mine . . . . .	45
23. Zoning Pattern of Pyrite in Tactite, Lakeshore Mine . . . . .	46
24. Zoning Pattern of Chalcopyrite in Tactite, Lakeshore Mine . . . . .	47
25. Zoning Pattern of Pyrite-chalcopyrite Ratio in Tactite, Lakeshore Mine . . . . .	48
26. Isopach Map of the Dripping Spring Quartzite within the Sulfide Zone, Lakeshore Mine. . . . .	50
27. Zoning Pattern of Pyrite in Dripping Spring Quartzite, Lakeshore Mine. . . . .	51
28. Zoning Pattern of Chalcopyrite in Dripping Spring Quartzite, Lakeshore Mine. . . . .	52
29. Zoning Pattern of Pyrite-chalcopyrite Ratio in Dripping Spring Quartzite, Lakeshore Mine. . . . .	53
30. Isopach Map of the Diabase within the Sulfide Zone, Lakeshore Mine. . . . .	54
31. Zoning Pattern of Pyrite in Diabase, Lakeshore Mine . . . . .	55
32. Zoning Pattern of Chalcopyrite in Diabase, Lakeshore Mine . . . . .	56
33. Zoning Pattern of Pyrite-chalcopyrite Ratio in Diabase, Lakeshore Mine . . . . .	57

LIST OF ILLUSTRATIONS--Continued

Figure		Page
34.	Geologic Map of the 100 Level, Lakeshore Mine. . . . .	59
35.	Geologic Map of the 200 Level, Lakeshore Mine. . . . .	60
36.	Geologic Map of the 300 Level, Lakeshore Mine. . . . .	61
37.	Geologic Map of the 400 Level, Lakeshore Mine. . . . .	62
38.	Zoning Pattern of Chalcopyrite in the 100 Level, Lakeshore Mine . . . . .	64
39.	Zoning Pattern of Chalcopyrite in the 200 Level, Lakeshore Mine . . . . .	65
40.	Zoning Pattern of Chalcopyrite in the 300 Level, Lakeshore Mine . . . . .	66
41.	Zoning Pattern of Chalcopyrite in the 400 Level, Lakeshore Mine . . . . .	67
42.	Zoning Pattern of Pyrite-chalcopyrite Ratio in the 100 Level, Lakeshore Mine . . . . .	68
43.	Zoning Pattern of Pyrite-chalcopyrite Ratio in the 200 Level, Lakeshore Mine . . . . .	69
44.	Zoning Pattern of Pyrite-chalcopyrite Ratio in the 300 Level, Lakeshore Mine . . . . .	70
45.	Zoning Pattern of Pyrite-chalcopyrite Ratio in the 400 Level, Lakeshore Mine . . . . .	71
46.	Zoning Pattern of Pyrite in the 100 Level, Lakeshore Mine . . . . .	72
47.	Zoning Pattern of Pyrite in the 200 Level, Lakeshore Mine . . . . .	73
48.	Zoning Pattern of Pyrite in the 300 Level, Lakeshore Mine . . . . .	74
49.	Zoning Pattern of Pyrite in the 400 Level, Lakeshore Mine . . . . .	75
50.	Sulfide Zoning at the San Manuel-Kalamazoo Deposit. . .	81



LIST OF ILLUSTRATIONS--Continued

Figure		Page
51.	Least-squares Fit of Plane to Points . . . . .	86
52.	Least-squares Fit of a Line . . . . .	96

## ABSTRACT

The Lakeshore copper deposit is located in Pinal County, south-central Arizona, approximately 28 miles south of Casa Grande. This study deals with the districtwide sulfide zoning pattern at Lakeshore. Assay data obtained from diamond drilling were used in a double-Fourier trend surface analysis to generate zoning maps of chalcopyrite, pyrite, and pyrite-chalcopyrite ratio for the different rock types at the mine and for selected levels of the mine.

Lakeshore is typical of porphyry copper deposits of southwestern North America. A Laramide quartz monzonite porphyry has intruded Precambrian and Cretaceous sedimentary rocks in the Lakeshore area. Sulfide mineralization in the form of pyrite and chalcopyrite is associated with the intrusion.

The sulfide zoning at Lakeshore is centered on the quartz monzonite porphyry and extends into the adjacent host rocks, having a pronounced northwest trend. The pyrite-chalcopyrite ratio was found to be the most sensitive indicator of sulfide zoning. The quartz monzonite porphyry has a low-grade, low pyrite-chalcopyrite ratio core with increasing chalcopyrite occurring on the margin of the quartz monzonite porphyry and in the host rocks adjacent to it. Away from the margin, the pyrite-chalcopyrite ratio increases as chalcopyrite drops off and pyrite increases, forming a pyrite halo. This sulfide zoning pattern agrees well with hypothetical zoning patterns described in the literature. The intrusion of quartz monzonite porphyry apparently acted as a heat source,

setting up pressure and temperature gradients, and the mineralizing fluids moved outward from the intrusion, depositing sulfides in zones defined by the pressure and temperature gradients.

## INTRODUCTION

The Lakeshore copper deposit is located 28 miles south of Casa Grande, Pinal County, Arizona, along the highway connecting Casa Grande with Quijotoa. The deposit lies within the Papago Indian Reservation just north of the Pinal-Pima county line on the southwest flank of the Slate Mountains (Fig. 1). The property consists of 6 patented and 19 unpatented lode claims, encompassing 462 acres and 10,142 acres leased from the Papago Indians. The claims and leases are held jointly by the El Paso Natural Gas Company and the Hecla Mining Company; Hecla is the operator.

Lakeshore is a porphyry copper deposit and has much in common with many of the other porphyry copper deposits in southwestern North America. A Laramide quartz monzonite porphyry, which has intruded sedimentary, volcanic, and intrusive rocks, is believed to be the source of sulfide mineralization which is disseminated throughout both the porphyry and the adjacent host rocks. Among the host rocks for the Laramide quartz monzonite porphyry is the Mescal Limestone, which has been highly metasomatized by the porphyry to form a tactite horizon containing high-grade copper mineralization. The major ore mineral is chalcopryrite.

Whereas most porphyry copper deposits in the Southwest are mined by open-pit methods, the Lakeshore mine will be entirely underground. Twin declines are currently being drive to provide access to the ore body.

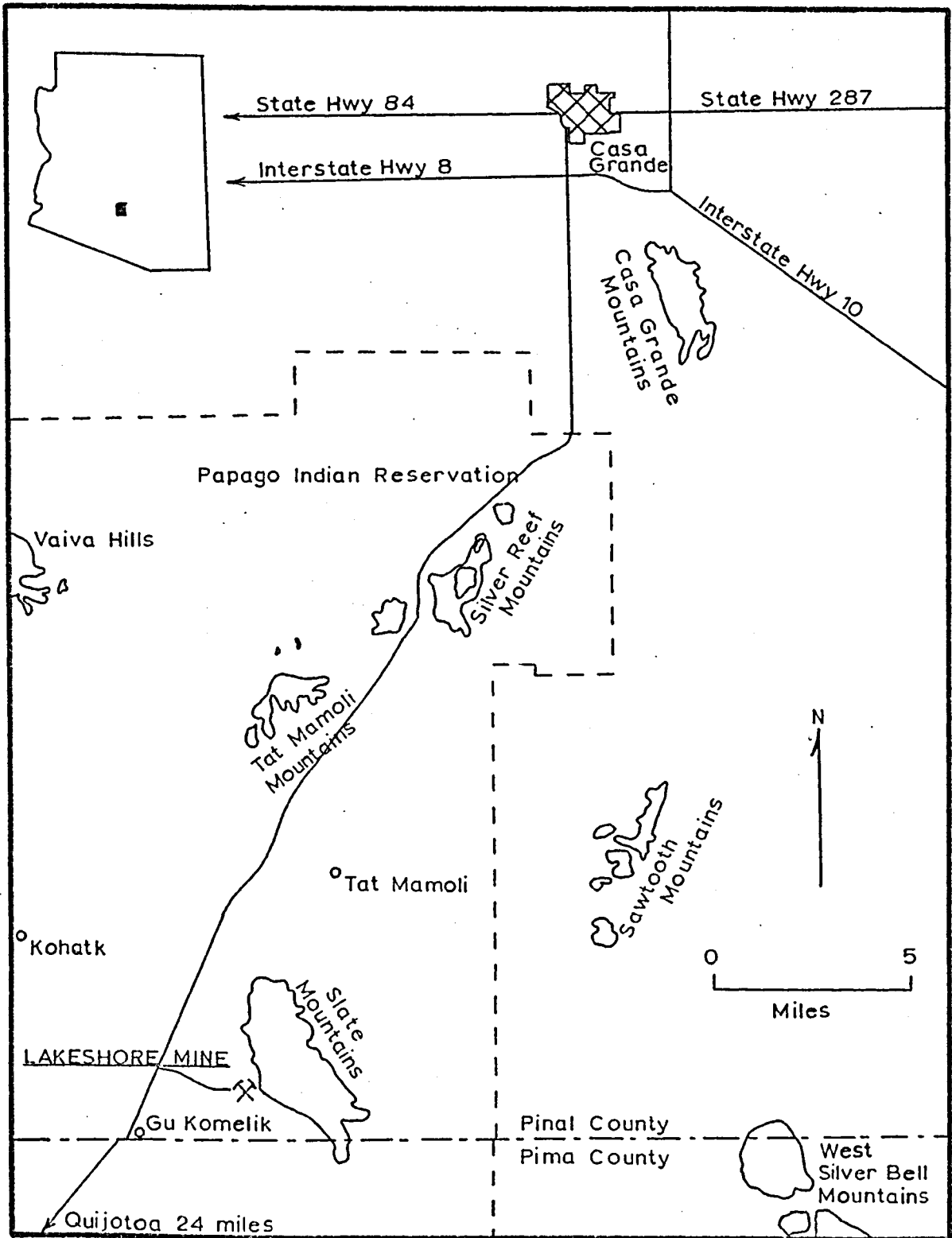


Figure 1. Location Map of the Lakeshore Mine, Arizona

### Purpose of Study and Method of Data Handling

The purpose of this study is to show the pattern of primary sulfide zoning at the Lakeshore deposit and to compare it with the pattern of sulfide zoning at other porphyry copper deposits. In most porphyry copper deposits, the main primary Cu-Fe-S system minerals present are chalcopyrite and pyrite, with pyrite generally in excess of chalcopyrite. These minerals show a similar zoning pattern in many of the deposits, namely, a low-chalcopyrite, low-pyrite, low-total sulfide core, a halo surrounding the core in which chalcopyrite is higher relative to the chalcopyrite content of the core and pyrite is still low, and a second halo containing high pyrite, low chalcopyrite, and high total sulfides (Rose, 1970). This idealized pattern of sulfide zoning is modified by the particulars of the local geology at any given deposit and is perhaps best seen in the Kalamazoo portion of the San Manuel deposit as described by Lowell and Guilbert (1970).

Assay data are used in this study to determine the pattern of primary sulfide zoning at the Lakeshore deposit. The assay data were obtained from diamond drill coring by the Hecla Mining Company and supplied to the author by Hecla. Data for assay intervals used were recorded by the author from the diamond drill core logs and included drill hole number, drill hole coordinates, collar elevation, depth of assay interval, rock type, weight percentage total copper, weight percentage sulfide sulfur, and weight percentage molybdenum. The assay interval was 5 feet. Each 5-foot interval of drill core was split in half lengthwise; one half was sent to be assayed, and the other half was retained in storage at the deposit. Weight percentage copper content

was determined for each 5-foot assay interval, whereas weight percentage sulfide sulfur and weight percentage molybdenum contents were determined only for every fifth 5-foot assay interval. Only intervals which were assayed for weight percentage sulfide sulfur and weight percentage molybdenum, as well as for weight percentage copper, were used in this study. The assays were done by Southwestern Assayers & Chemists, Inc., Tucson, Arizona, and by the Hecla assay laboratory at Lakeshore. A sodium carbonate leach was used to dissolve sulfate from the samples, and the residues were assayed for sulfide sulfur. This technique insured that the weight percentage sulfur reported was from sulfide minerals and not from rare sulfates, such as anhydrite, gypsum, or barite.

The copper mineralization at Lakeshore is divided into an oxide zone and a sulfide zone. Since the purpose of this study is to show the primary sulfide zoning pattern, only the sulfide zone was considered, since supergene enrichment in the oxide zone has modified the primary sulfide zoning. One basic assumption was made: the only sulfide minerals present in significant quantities within the sulfide zone are pyrite, chalcopyrite, and molybdenite. Other sulfides, such as sphalerite, galena, and bornite, are locally present, but they occur in such small quantities as to have no effect on the method of analysis used to determine the zoning pattern. This assumption was verified by the geologic staff at Lakeshore and by examination of the core.

Included within the sulfide zone, however, is a supergene chalcocite blanket. Since the chalcocite blanket obviously contains a sulfide mineral other than pyrite, chalcopyrite, or molybdenite, namely

chalcocite, and moreover since the chalcocite blanket is due to supergene enrichment and is not a feature of primary sulfide zoning, it was necessary to determine the vertical extent of the chalcocite blanket so that data from the chalcocite blanket portion of the sulfide zone could be omitted from the study. The presence of the chalcocite blanket was determined in two ways:

1. If chalcocite was noted in the drill log, or
2. Where chalcocite was not noted in the log but copper was in excess of sulfur, it was assumed that chalcocite or other copper oxide minerals were present, since copper cannot be in excess of sulfur if chalcopyrite is the only copper mineral present.

If either of these conditions was met for a particular assay interval, that interval was omitted from the data used in the study.

#### Data-handling Techniques

The weight percentages of chalcopyrite and pyrite were calculated from the copper, sulfide sulfur, and molybdenum assay data. By knowing the content by weight of copper and molybdenum in chalcopyrite and molybdenite, it proved a simple matter to calculate weight percentage in the rock from weight percentage copper in the rock and to calculate weight percentage molybdenite in the rock from the weight percentage molybdenum in the rock. Once the weight percentage of chalcopyrite and molybdenite in the rock are known, the weight percentage sulfur contained in both minerals may be determined. This weight percentage sulfur contained in chalcopyrite and molybdenite may then be subtracted from the total weight percentage sulfide sulfur. Since it has



been assumed that chalcopyrite, molybdenite, and pyrite are the only sulfide minerals present and since the weight percentage sulfur contained in the chalcopyrite and molybdenite has been accounted for, the remaining sulfur must be contributed by the pyrite. By knowing the content by weight of sulfur in pyrite, the weight percentage pyrite in the rock may be determined. Pyrite-chalcopyrite ratio in the rock is then determined by dividing weight percentage pyrite content by weight percentage chalcopyrite content.

The above calculations provide weight percentage chalcopyrite content, weight percentage pyrite content, and pyrite-chalcopyrite ratio for each assay interval used in the study. By knowing the coordinates and collar elevation of the drill hole from which each assay interval was taken and the depth of each assay interval, the different chalcopyrite and pyrite contents by weight of the rock and the pyrite-chalcopyrite ratio in the rock at each assay location in space are known. Distribution maps may be prepared to show the sulfide zoning pattern.

The distribution maps were produced by a double-Fourier trend surface analysis, using the University of Arizona CDC 6400 computer. Trend surface analysis is a mathematical surface-fitting technique which uses the least-squares criterion to fit a surface to a set of data points. This is done using some equation for a surface, here a double-Fourier series. The observed value of, for example, chalcopyrite at a given point is used, along with all the other observed values at other points, to calculate coefficients to the Fourier series. The north and east coordinates of a particular point may then be used as independent variables and be substituted into the Fourier series with the coefficients obtained

from the observed values. This substitution will yield a trend value of chalcopyrite at those coordinates. A map is generated by doing this for successive points.

Note that the trend value calculated from the double-Fourier equation will be different from the observed value at any particular point. As mentioned, the least-squares criterion is used to fit the trend surface to the observed points. Using this criterion, a trend surface is passed through the observed values such that the sum of the squared differences between the observed values and the trend values is minimized.

Trend surfacing of data smooths out variations within the data. It was this smoothing characteristic which was sought in this study in order to remove random variation in the data and to obtain a valid representation of the spatial distribution of the sulfides. The Fourier series is such, however, that a surface may be fitted to any set of points, whether they represent a surface or not. It is necessary to have some statistical measure of how well a trend surface fits the data from which it was derived.

One such measure is the percent sum of the squares contribution (percent SS contribution), which measures how much of the total variation in a data set is accounted for by the trend surface. When the percent SS contribution is 50 percent, half of the variation from the mean in the data is represented by the trend surface and the other half is due to factors not represented by the trend surface. When the percent SS contribution is low, say 15 to 30 percent, most of the variation present in the data is not represented by the trend function. However, this does not

necessarily invalidate the surface generated. In this study, the purpose was to determine sulfide zoning on a districtwide basis. Local factors which cause variations in sulfide content are filtered out by the Fourier analysis. A low percent SS contribution indicates that a large part of the variation in sulfide content is due to local controls rather than district-wide zoning. Another measure of the validity of a trend surface is its significance level, which reflects the probability of the correctness of the trend surface. If the significance level is 95 percent, then 95 percent of the values on a trend surface are related to the observed values and 5 percent of the values are due to random variation in the fitting technique.

A comprehensive discussion of the double-Fourier trend-surfacing method and associated statistical measures is given in the Appendix.

### Types of Maps Generated

Two sets of maps were generated with the Fourier trend-surface technique. In one set, the percentage chalcopyrite, percentage pyrite, and pyrite-chalcopyrite ratio are mapped according to rock type; in the other set, the percentage chalcopyrite, percentage pyrite, and pyrite-chalcopyrite ratio are mapped on different levels within the sulfide zone.

#### Rock-type Maps

The rock-type maps show the sulfide distribution for the different rock types at the deposit. The rocks at the deposit have been divided into six types: upper porphyry, lower porphyry, Cretaceous volcanic and sedimentary rocks, tactite, Dripping Spring Quartzite, and

diabase. These rocks will be discussed in more detail in the next chapter. Chalcopyrite, pyrite, and pyrite-chalcopyrite ratio maps were generated for each rock type, as well as for the entire district without regard for rock type.

Several operations preceded the trend surface analysis in order to convert the raw data into a form useable by the Fourier analysis program. As previously described, the weight percentage chalcopyrite, weight percentage pyrite, and pyrite-chalcopyrite ratio were calculated for each assay interval, and each assay interval was located in space by drill hole coordinates and depth. The mean weight percentage of chalcopyrite and pyrite and the mean pyrite-chalcopyrite ratio for each rock type in each drill hole was then determined. For example, a single hole may pass through three different rock types: upper porphyry, Cretaceous volcanic and sedimentary rocks, and tactite. The mean weight percentage chalcopyrite for the tactite in that hole is taken as the mean value of the weight percentage chalcopyrite contents of all assay intervals taken in tactite in that hole. Assay intervals taken in upper porphyry are used to determine the mean weight percentage chalcopyrite content for the upper porphyry in that hole, and assay intervals taken in Cretaceous volcanic and sedimentary rocks are used to determine the mean weight percentage chalcopyrite content for the Cretaceous volcanic and sedimentary rocks in that hole. The same procedure is used to determine mean weight percentage pyrite contents and mean pyrite-chalcopyrite ratios for each rock type in the hole. The procedure is followed for all holes. Thus, each hole has mean weight percentage contents of chalcopyrite and pyrite and mean pyrite-chalcopyrite ratios

according to rock type. Mean contents and ratios were also determined for the entire hole, without regard to rock type.

The trend surfaces are generated from the data derived by the foregoing procedure. The data used to produce on chalcopyrite map consist of drill hole numbers, drill hole coordinates, and mean chalcopyrite contents of the drill holes for one individual rock type.

This method of data handling works quite well for determining lateral zoning. The main drawback is that it completely masks any vertical zoning. Level maps were generated in order to look at vertical zoning as well as to gain a more detailed look at lateral zoning.

#### Level Maps

The level maps show the distribution of chalcopyrite, pyrite, and the pyrite-chalcopyrite ratio on four levels within the sulfide zone. In order to generate these maps, a least-squares curve fit was run for the chalcopyrite, pyrite, and pyrite-chalcopyrite ratio values in each hole, using the Fourier analysis. This fit resulted in a series of curves showing the weight percentage chalcopyrite, weight percentage pyrite, or pyrite-chalcopyrite ratio versus depth for each hole. Weight percentage chalcopyrite, weight percentage pyrite, and pyrite-chalcopyrite ratios could then be picked for a given elevation in all holes, and maps showing their distribution could be generated with the trend surface program.

The least-squares curve fit was done for the same reason that the trend surfacing was done: to smooth the data in a given hole and to obtain a statistically representative value for the sulfide content at a

particular level within that hole. This process for determining the sulfide content at a particular level is far better statistically than averaging the values nearest the desired level as representative of the sulfide content, because the Fourier least-squares curve fit takes into account all values in the hole.

## GEOLOGY OF THE LAKESHORE MINE

The Lakeshore mine is located on the southwest flank of the Slate Mountains in south-central Arizona. Physiographically, the area is typical of the desert region of the Basin and Range Province in southern Arizona with many elongate northwest-trending mountain ranges separated by large expanses of alluvial-filled basins. In the area of Lakeshore, the desert floor lies at an elevation of around 1,800 feet, and the Slate Mountains rise 1,500 feet above the desert floor to attain a maximum elevation of 3,332 feet at Prieta Peak (Fig. 1).

McClymonds (1959) has described the Precambrian and Paleozoic rocks of the Papago Indian Reservation, which includes the Slate Mountains. Hogue (1940) has described the general geology of the north end of the Slate Mountains, and Hammer (1961) has described the general geology of the same area as well as the geology of several small gold-silver occurrences on the north end of the Slate Mountains. Hammer included a detailed stratigraphic section measured in the north end of the Slate Mountains. Regional geologic relations are described by Wilson (1962). Harper and Reynolds (1969) have described the geology of the Lakeshore mine. This description has been modified in the light of geologic information collected by the Lakeshore staff during the last two years.

### General Geologic Setting

The Slate Mountains (Fig. 2) trend north-northwest and are composed predominantly of Older Precambrian Pinal Schist. Younger

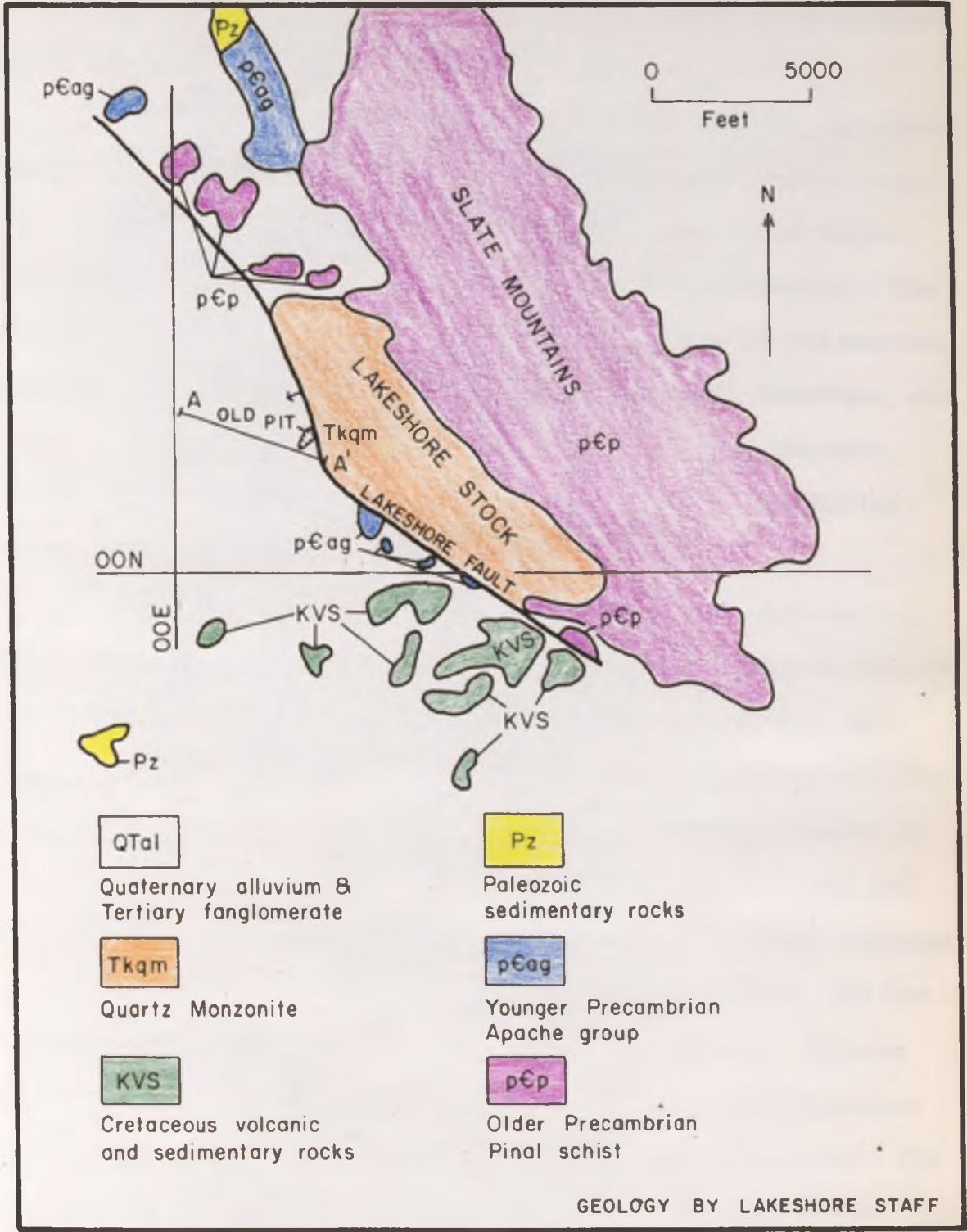


Figure 2. Surface Geology, Lakeshore Mine Area



Precambrian Apache Group and Paleozoic sedimentary rocks are exposed on the north end of the Slate Mountains.

The Apache Group overlies the Pinal Schist with angular unconformity. On the north end of the Slate Mountains where Hammer measured his stratigraphic section, the Apache Group consists of Pioneer Shale (oldest), Dripping Spring Quartzite, and Mescal Limestone. The Pioneer Shale consists of 374 feet of interbedded siltstone and quartzite, the Dripping Spring Quartzite of 1,179 feet of quartzite, sandstone, and siltstone, and the Mescal Limestone of 193 feet of cherty dolomite (Hammer, 1961). Upper Precambrian diabase sills have intruded the units in many places.

Disconformably overlying the Apache Group is a sequence of Cambrian to Mississippian rocks, consisting of Bolsa Quartzite (oldest), Abrigo Formation, Martin Formation, and Escabrosa Limestone. The Bolsa Quartzite disconformably overlies the Mescal Limestone and consists of 463 feet of quartzite and sandstone. It is Middle Cambrian in age and is overlain by the Upper Cambrian Abrigo Formation, 448 feet of interbedded mudstone, quartzite, and dolomite. The Abrigo Formation is disconformably overlain by the Devonian Martin Formation, 208 feet of muddy dolomite interbedded with siltstone and quartzite. Capping the units in the northern Slate Mountains is 150 feet of Mississippian Escabrosa Limestone, a fossiliferous, somewhat cherty limestone. The top of the Escabrosa is an erosion surface. About two miles to the southeast of the Slate Mountains, the Escabrosa is 400 feet thick, and the lower part of the Pennsylvanian Horquilla Limestone caps the Paleozoic sedimentary sequence. Unconformably overlying the Paleozoic

rocks is a sequence of Cretaceous volcanic and terrestrial sedimentary rocks. The volcanic units consist of andesite flows and pyroclastic andesitic agglomerates; the sedimentary rocks are conglomeratic clastics derived from the volcanic rocks.

During Laramide time, an equigranular quartz monzonite stock, the Lakeshore stock, intruded all formations up to and including the Cretaceous volcanic and sedimentary rocks. The stock crops out over an area of about two square miles on the central part of the southwest flank of the Slate Mountains (Fig. 2). Isotopic potassium-argon age dating indicates the age of the Lakeshore stock to be 67 m.y. This determination was made by the Geochron Laboratories, Inc., Cambridge, Massachusetts. The mineralization at the Lakeshore mine is related to this stock.

Finally, Tertiary conglomerate covering the older units occupies most of the basin area. Quaternary alluvium occurs in the desert washes and on the pediment surrounding the Slate Mountains.

#### Geology of the Mine Area

The Lakeshore deposit is a typical porphyry copper deposit which exhibits many features common to other porphyry copper deposits in Arizona. Primary copper ore can be divided into two types: (1) lower grade disseminated chalcopyrite in quartz monzonite porphyry, Cretaceous volcanic and sedimentary rocks, and Precambrian diabase, and (2) higher grade tabular bodies of chalcopyrite associated with magnetite and silicate minerals in the Mescal Limestone. This latter type is generally termed the "tactite" ore. Hydrothermal alteration zones typical of

most of the porphyry copper deposits have been recognized at Lakeshore and include potassic, phyllic, argillic, and propylitic zones, although these zones have not as yet been delineated.

Structural and stratigraphic relationships at the Lakeshore deposit are shown in Figure 3, a cross section through the ore body. The dominating structural feature is the Lakeshore fault, a post-ore normal fault striking north-northwest and dipping  $50^{\circ}$ - $80^{\circ}$  W. The equigranular quartz monzonite Lakeshore stock crops out over an area of about two square miles in the footwall area of the Lakeshore fault. It is interpreted by the geologic staff at Lakeshore that major normal displacement on the Lakeshore fault has dropped the presumed cupola portion of the Lakeshore stock down to the west to its present position, thus preserving the main Lakeshore ore body from erosion. This cupola portion is a quartz monzonite porphyry. For this study, the quartz monzonite porphyry has been divided into two units: the lower porphyry, which occurs below the tactite horizon; and the upper porphyry, which occurs within and above the tactite horizon. The upper and lower porphyries are probably continuous; however, the upper porphyry contains ore-grade mineralization whereas the lower porphyry is essentially barren. The term "quartz monzonite porphyry" as used in this paper refers to both the upper porphyry and the lower porphyry taken together. The lower porphyry appears to grade into the equigranular quartz monzonite Lakeshore stock, and isotopic age dating indicates that both the quartz monzonite porphyry and the Lakeshore stock have the same 67 m.y. age (J. J. Quinlan, 1972, oral communication).

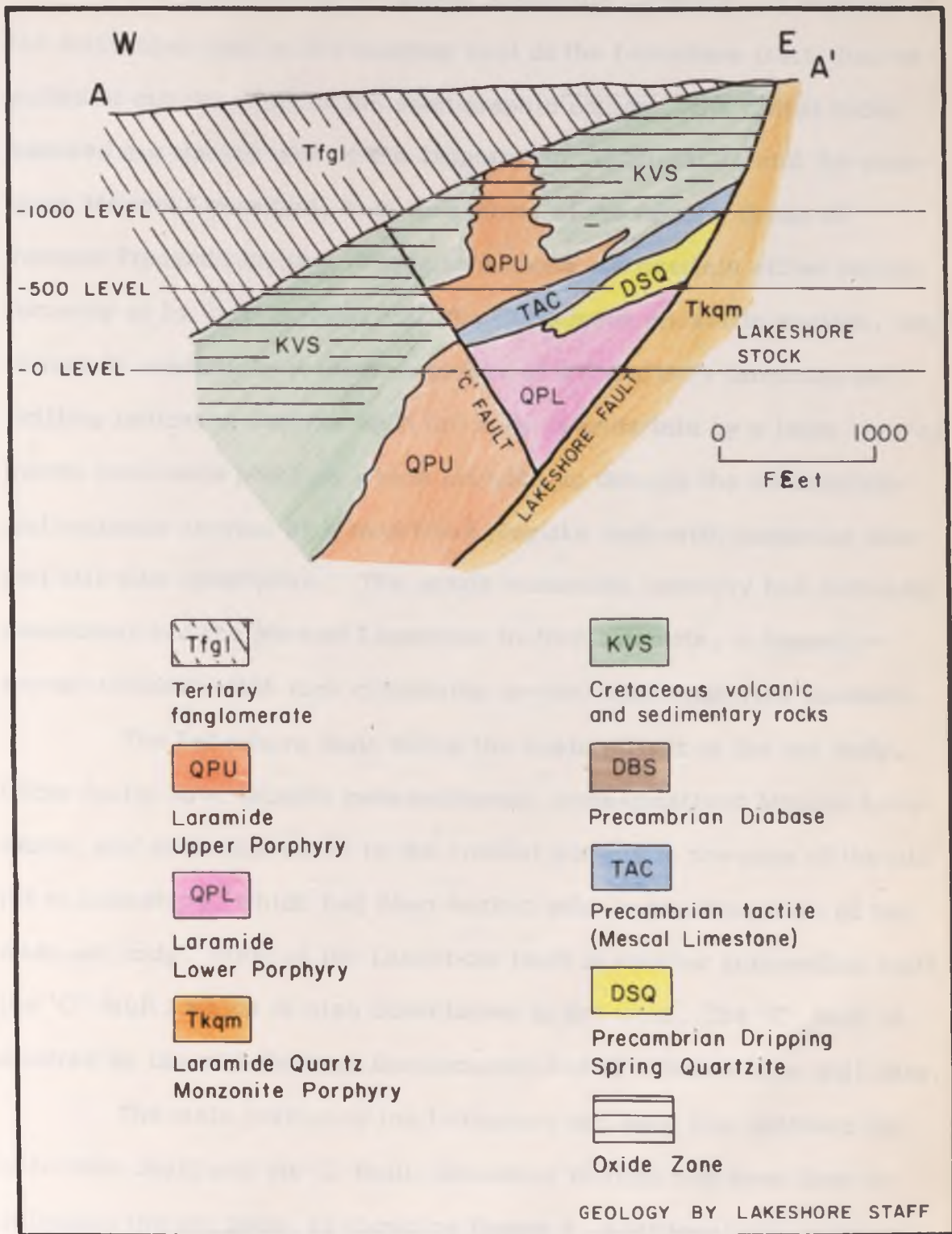


Figure 3. Geology of Section AA', Figure 2

The intrusion of the quartz monzonite porphyry, as exposed in the main mine area on the hanging wall of the Lakeshore fault, has engulfed or cut out much of the stratigraphic column. The oldest rocks exposed are the top part of the Dripping Spring Quartzite and the overlying Mescal Limestone, both formations of the Apache Group of Younger Precambrian age. These formations are overlain either unconformably or by fault contact with the Cretaceous andesitic section, which in turn is overlain by a thick sequence of mid-Tertiary fanglomerate. Drilling indicates that the main ore body is underlain by a large body of quartz monzonite porphyry which intruded up through the sedimentary and volcanic section as a restricted pluglike body with numerous dike and sill-like apophyses. The quartz monzonite porphyry has intensely metasomatized the Mescal Limestone to form a tactite, a diopside-garnet-tremolite-rich rock containing several magnetite-rich horizons.

The Lakeshore fault marks the eastern limit of the ore body. Older faults have brought metasediments, metasomatized Mescal Limestone, and andesitic rocks to the present surface in the area of the old pit at Lakeshore, which had been worked prior to the discovery of the main ore body. West of the Lakeshore fault is another subparallel fault, the 'C' fault, which is also downthrown to the west. The 'C' fault is covered by the mid-Tertiary fanglomerate and is inferred from drill data.

The main portion of the Lakeshore ore body lies between the Lakeshore fault and the 'C' fault. Extensive drilling has been done to delineate the ore body, as shown by Figure 4. Additional ore is present west of the 'C' fault, and exploration in the area is proceeding. This

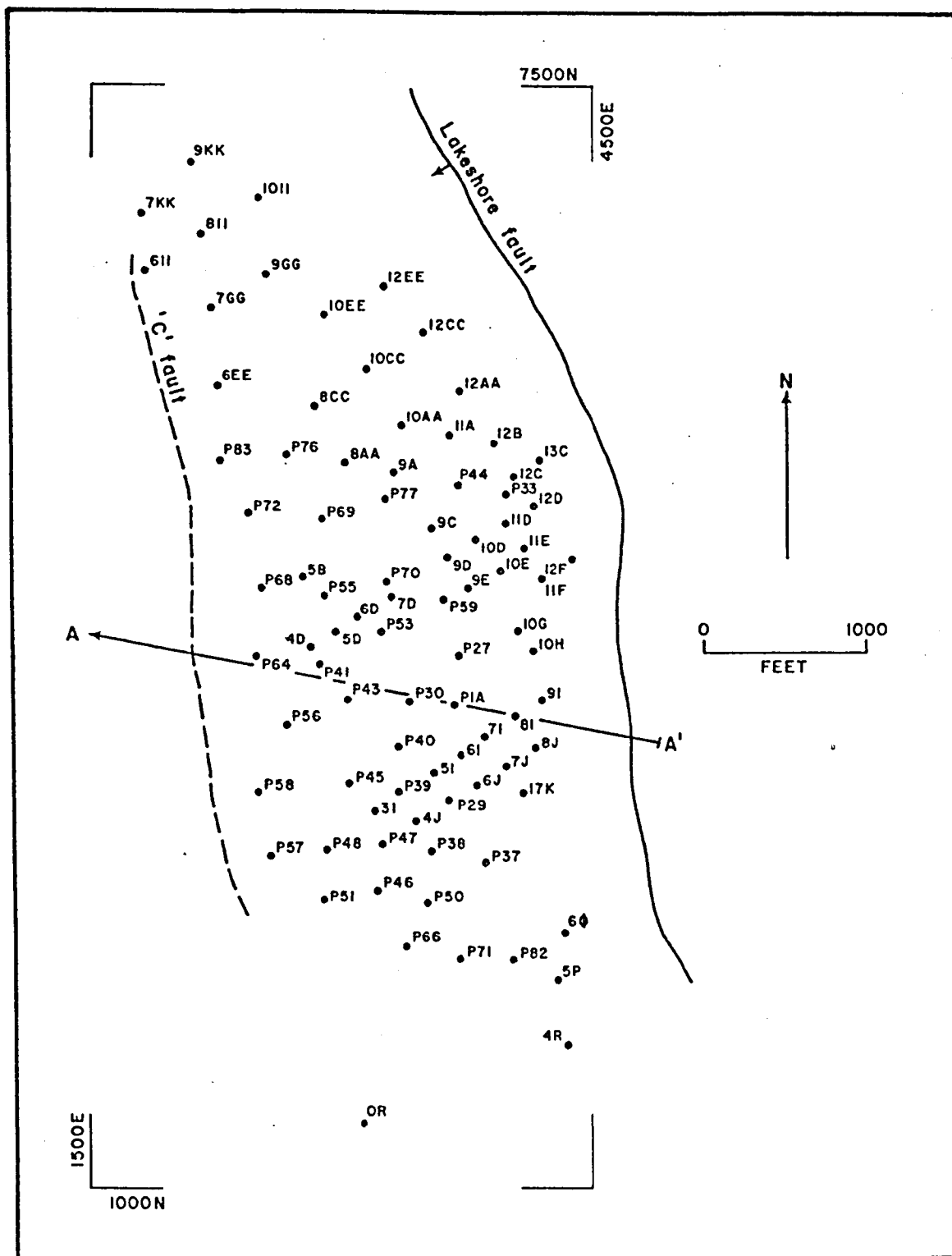


Figure 4. Location of Drill Holes from Which Data Were Obtained.

study deals only with the main portion of the ore body between the Lakeshore and 'C' faults.

The deposit is separated into an upper oxide zone, a transition zone, and an underlying sulfide zone. The oxide zone, in which chrysocolla, brochantite, and tenorite are the principal copper minerals, is highly irregular, extending to depths of as much as 1,400 feet in the area of the main ore body. The transition zone is the area where both sulfide and oxide minerals can be observed in the drill core. Its thickness is highly variable and the zone is not always present.

The sulfide zone begins below the point where the last oxides are observed. A supergene chalcocite blanket is locally present which is included as part of the sulfide zone. The blanket is irregular and discontinuous in the central part of the deposit but attains considerable thickness to the northwest. Below the chalcocite blanket, the primary sulfides are chalcopyrite and pyrite. The host rocks for the sulfide ores are the upper porphyry, the Cretaceous andesitic rocks, the Mescal Limestone, and the diabase sills. The upper porphyry, andesite, and diabase have been extensively fractured, and the sulfides occur as disseminations and fracture fillings throughout the rock. The Mescal Limestone has been intensely metasomatized to form a tactite, a diopside-garnet-tremolite-rich rock with magnetite-rich horizons. The sulfides appear to prefer the magnetite-rich horizons. Much of the lower porphyry and Dripping Spring Quartzite is essentially barren.

## SULFIDE ZONING PATTERNS

The porphyry copper deposits as a class have been extensively studied, and an idealized sulfide zoning pattern has been determined. Two of the more recent papers dealing with zoning patterns, both of hydrothermal alteration and of sulfide minerals, in porphyry coppers are by Lowell and Guilbert (1970) and by Rose (1970).

Zoning is generally centered on a porphyritic quartz dioritic to quartz monzonitic stock. Ore fluids appear to have moved outward from the stock through highly fractured country rock, depositing sulfides as both disseminations and fracture coatings in the margin of the stock and in the adjacent country rock, although the source of the water and metals is still a subject of lively debate. According to Lowell and Guilbert (1970) and Rose (1970), the hypogene sulfides in the central portion of the stock have a low pyrite-chalcopyrite ratio and a low total sulfide content. In the margin of the stock and in the adjacent country rock, chalcopyrite and pyrite increase, the pyrite-chalcopyrite ratio is still low, and the sulfide content is moderate. A pyrite halo surrounds the ore deposit with high pyrite-chalcopyrite ratio and high total sulfides grading outward to lower total sulfides.

The pattern for idealized zoning is a set of concentric rings centered on the stock. In practice, the zoning pattern is modified by the degree to which the rock has been shattered and thereby obtained secondary permeability. In areas of relatively unfractured rock (low permeability) ore fluids have not been able to move through the rock,



and zoning patterns are likely not to be well developed. Conversely, where the rock has been highly fractured, free movement of ore fluids will allow good development of zoning patterns.

Of less importance than permeability, but still a significant parameter in sulfide zoning, is the chemical composition of the host rock for the sulfides. In low-reactivity rocks, such as quartzites, the ore fluid tends to move through the rock without either altering it or depositing much ore, and the zoning patterns tend to be poorly developed. In moderately reactive rocks, such as andesite, the effect of the ore fluid is pronounced, and zoning is well developed. In highly reactive rocks, such as limestone, the zoning is telescoped and obscured by metasomatic effects.

#### Sulfide Zoning at Lakeshore

In the following pages, maps illustrating the sulfide zoning pattern at Lakeshore, both by rock type and by level as determined by the double-Fourier analysis described previously, will be presented. On the maps, the drill holes used in making the maps are shown by the black dots. There are generally less holes than are shown on Figure 4, the drill hole map, since a given rock type was not encountered in every hole. Naturally, contours in areas where not much drilling has been done are more speculative than contours in areas where drilling has been extensive. In addition, pertinent statistics are shown on all maps. The accuracy of the map can be judged from these statistics. For most maps, the significance level is greater than 90 percent, and all pyrite-chalcopyrite ratio maps have a significance level greater than 90 percent.

Other maps which are useful in interpreting zoning are also included. Figure 5 is a contour map of the top of the sulfide zone. Rocks above the sulfide zone were not included in the data used for this study, since oxidation and supergene enrichment have largely destroyed the hypogene mineral zoning. Isopach maps of the various rock types, which are shown with the zoning maps of the particular rock types, show thicknesses of the rock type within the sulfide zone. Where a value of zero thickness for a rock type is shown, it does not mean that there is no rock of that type present; rather, it means that there is no rock of that type within the sulfide zone at that point. This omission of rocks in the oxide zone actually applies mainly to the Cretaceous volcanic and sedimentary rocks and, to a lesser extent, to the upper porphyry, since these are the only rocks significantly affected by oxidation. The rest of the rocks are below the oxidation zone.

Most importantly, a set of level maps, including the geology of the 100, 200, 300, 400, and 700 levels of the deposit are shown. At Lakeshore, designations indicate elevation; thus, the 700 level is 700 feet above sea level. The 100, 200, 300, and 400 level maps are shown with the mineral zoning maps for those levels, but the 700 level (Fig. 6) is presented here to show the geologic relations of the upper portion of the ore body. Although much of the rock on the 700 level is in the oxide zone, it must be remembered that there was no oxide zone when the ore body was emplaced and the geometry of the zoning was affected by the geologic relations of the rocks in what is now the oxide zone as well as the relations of the rocks in the oxide zone.

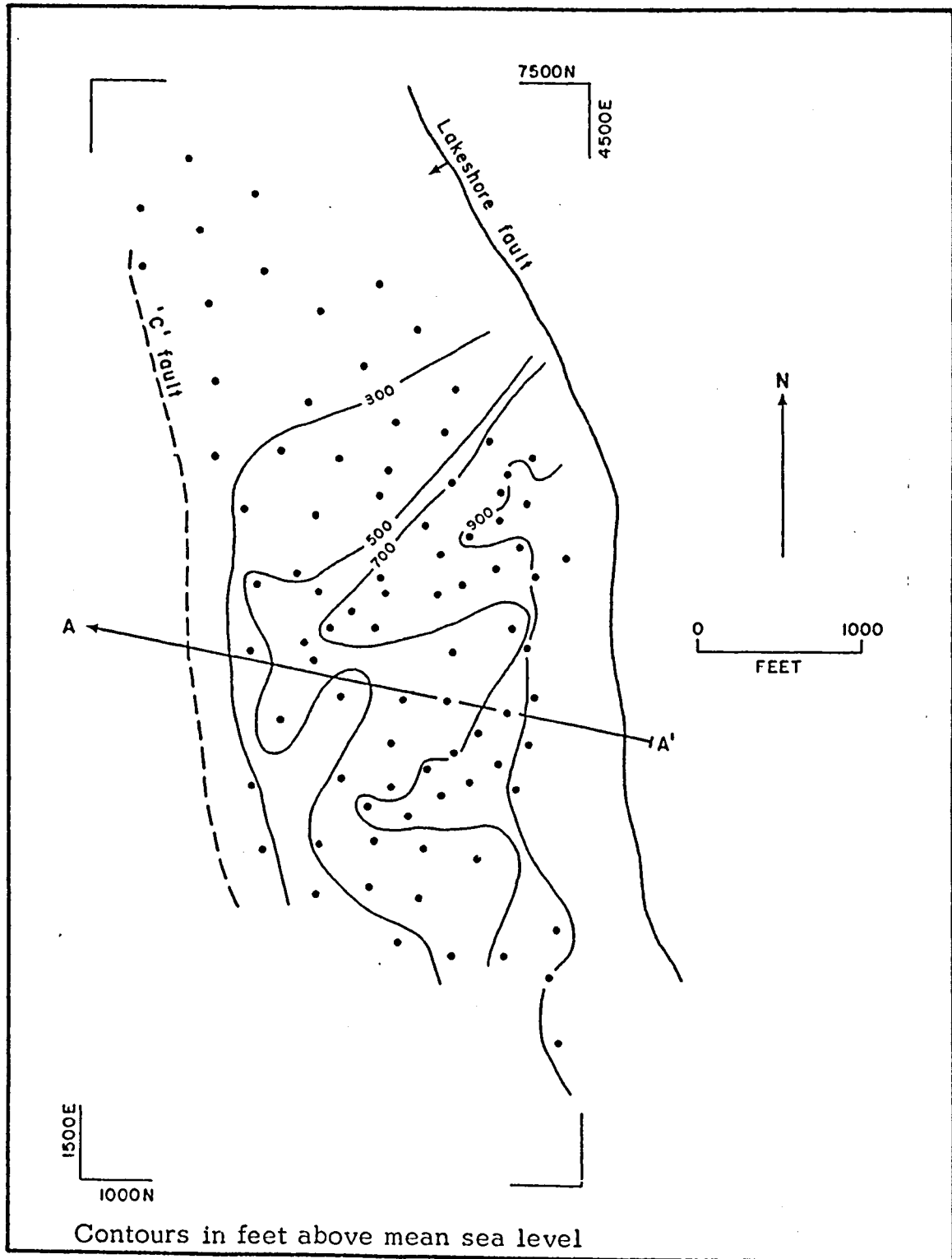


Figure 5. Contour Map of the Top of the Sulfide Zone, Lakeshore Mine

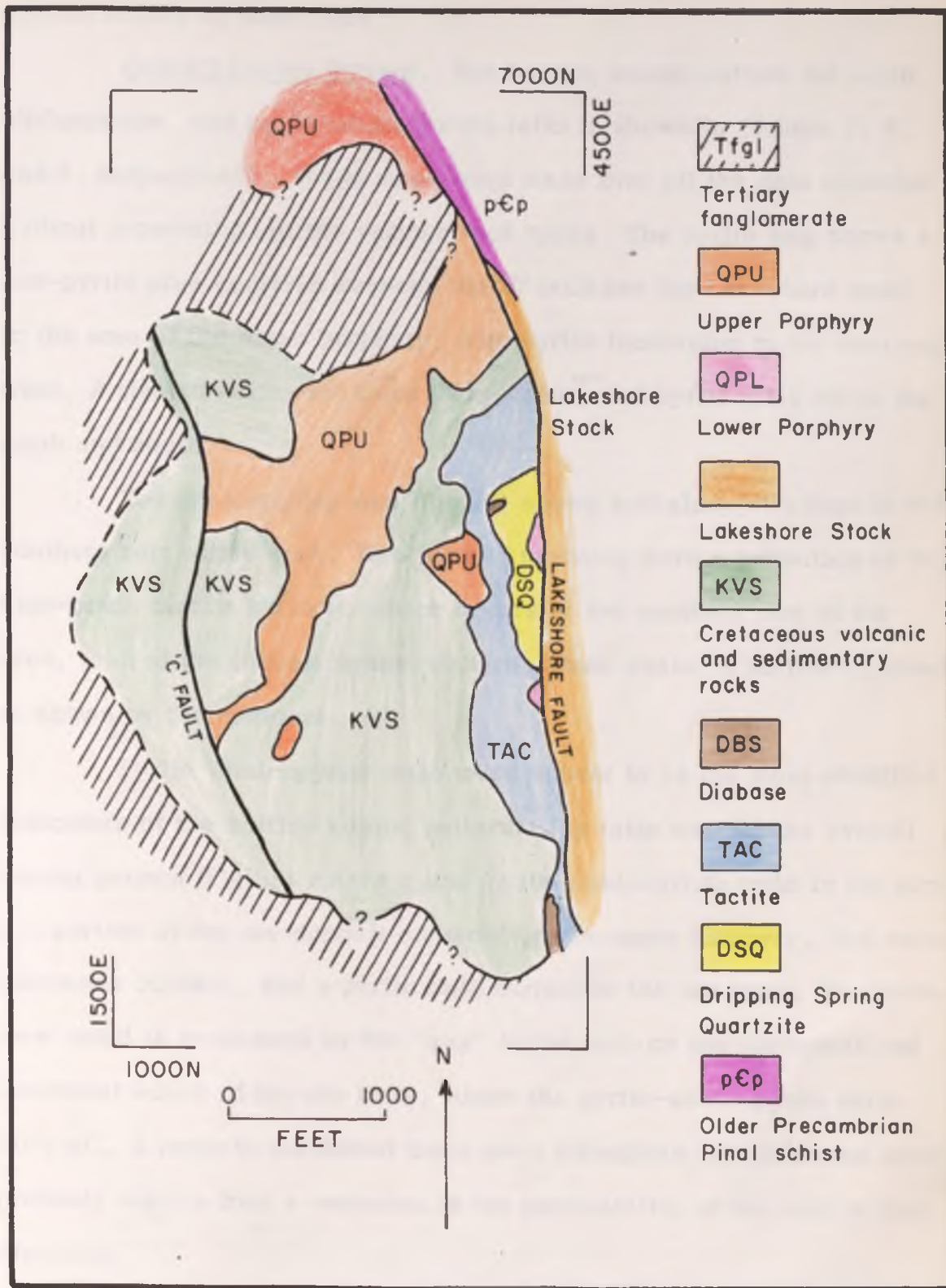


Figure 6. Geologic Map of the 700 Level, Lakeshore Mine

## Sulfide Zoning by Rock Type

Overall Zoning Pattern. The overall zoning pattern for pyrite, chalcopyrite, and pyrite-chalcopyrite ratio is shown in Figures 7, 8, and 9, respectively. These maps were made from all the data recorded without separating out the various rock types. The pyrite map shows a low-pyrite area centered between the 'C' fault and the Lakeshore fault, in the area of the upper porphyry, with pyrite increasing to the east and west. A marked northwest trend is apparent, and pyrite falls off to the north and south.

The chalcopyrite map (Fig. 8) shows a chalcopyrite high in the southern part of the area. This high is probably more a reflection of the high-grade tactite horizon, which occurs in the southern part of the area, than of the overall zoning pattern. Once again, a northwest trend is shown by the contours.

Pyrite-chalcopyrite ratio maps appear to be the most sensitive indicators of the sulfide zoning pattern. The ratio map for the overall zoning pattern (Fig. 9) shows a low pyrite-chalcopyrite ratio in the central portion of the ore deposit centered on the upper porphyry. The ratio increases outward, and a pyrite halo surrounds the ore body. The northwest trend is evidenced by the "gap" in the halo on the northwest and southeast edges of the ore body, where the pyrite-chalcopyrite ratio falls off. A north to northwest trend seen throughout the following maps probably results from a variation in the permeability of the rock in that direction.

The overall zoning pattern agrees well with the idealized pattern described by Rose (1970), with a low pyrite-chalcopyrite ratio in the

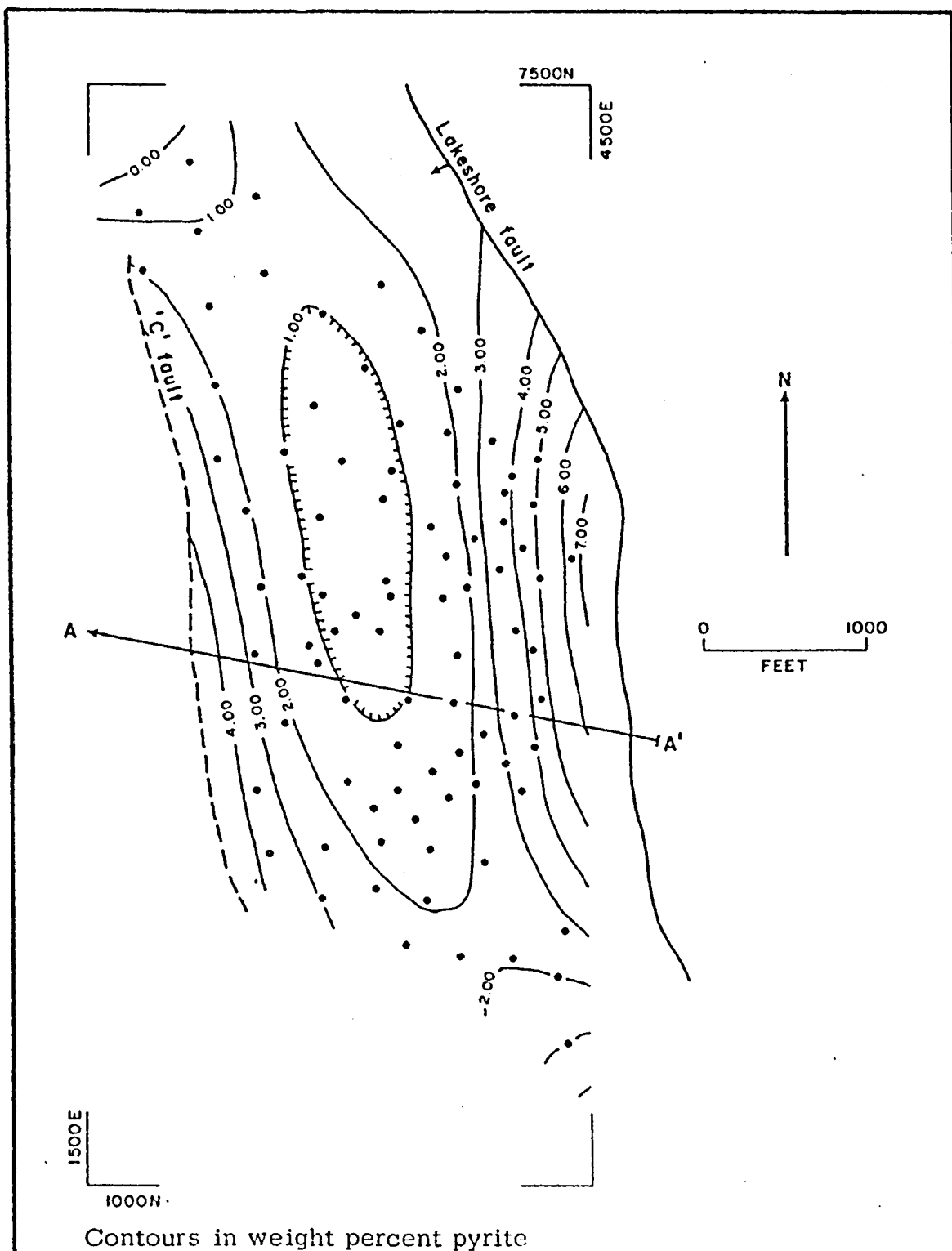
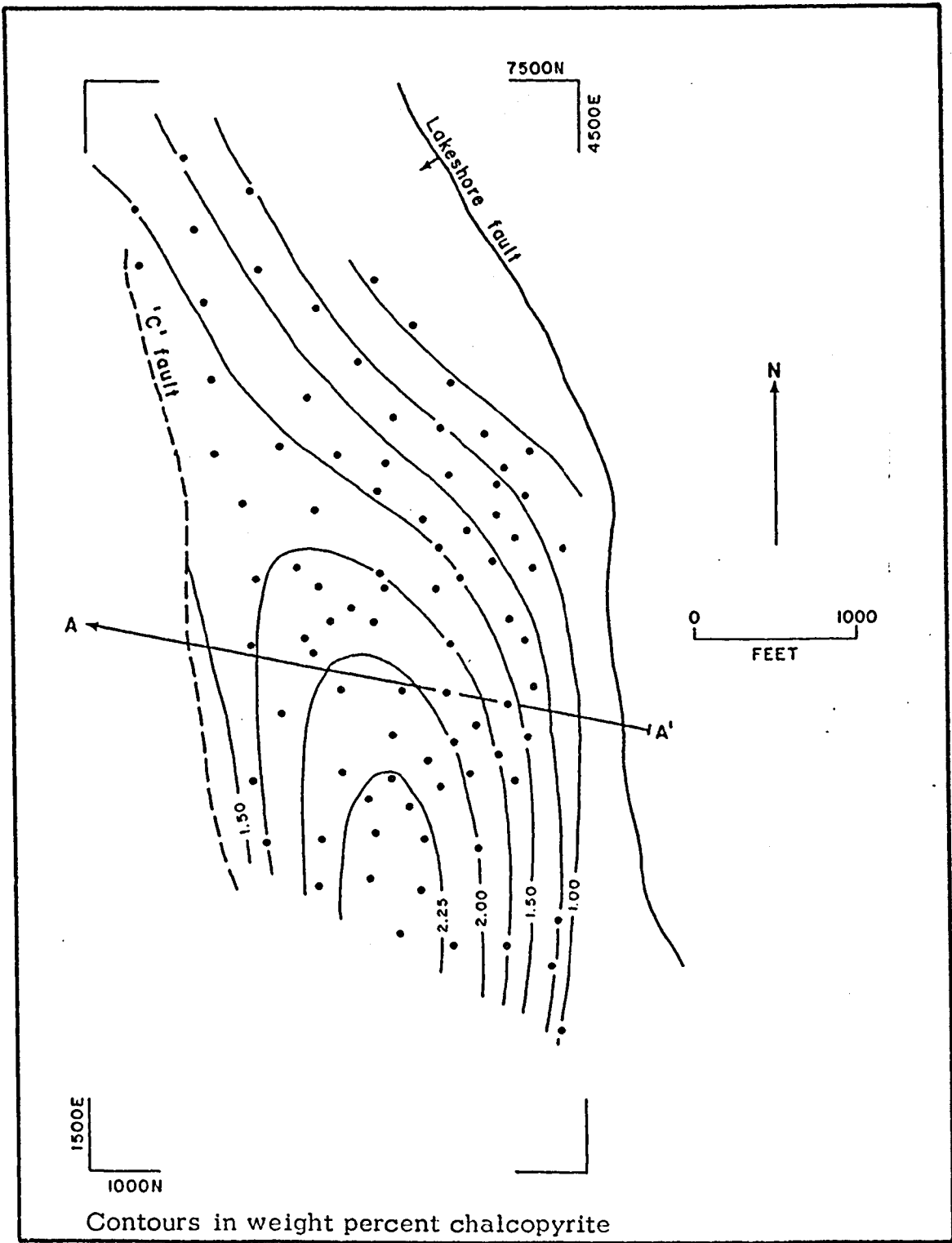


Figure 7. Overall Zoning Pattern of Pyrite, Lakeshore Mine  
 Percent SS contribution: 26.90; significance level: +90%.



Mine Figure 8. Overall Zoning Pattern of Chalcopyrite, Lakeshore

Percent SS contribution: 20.77; significance level: +90%.

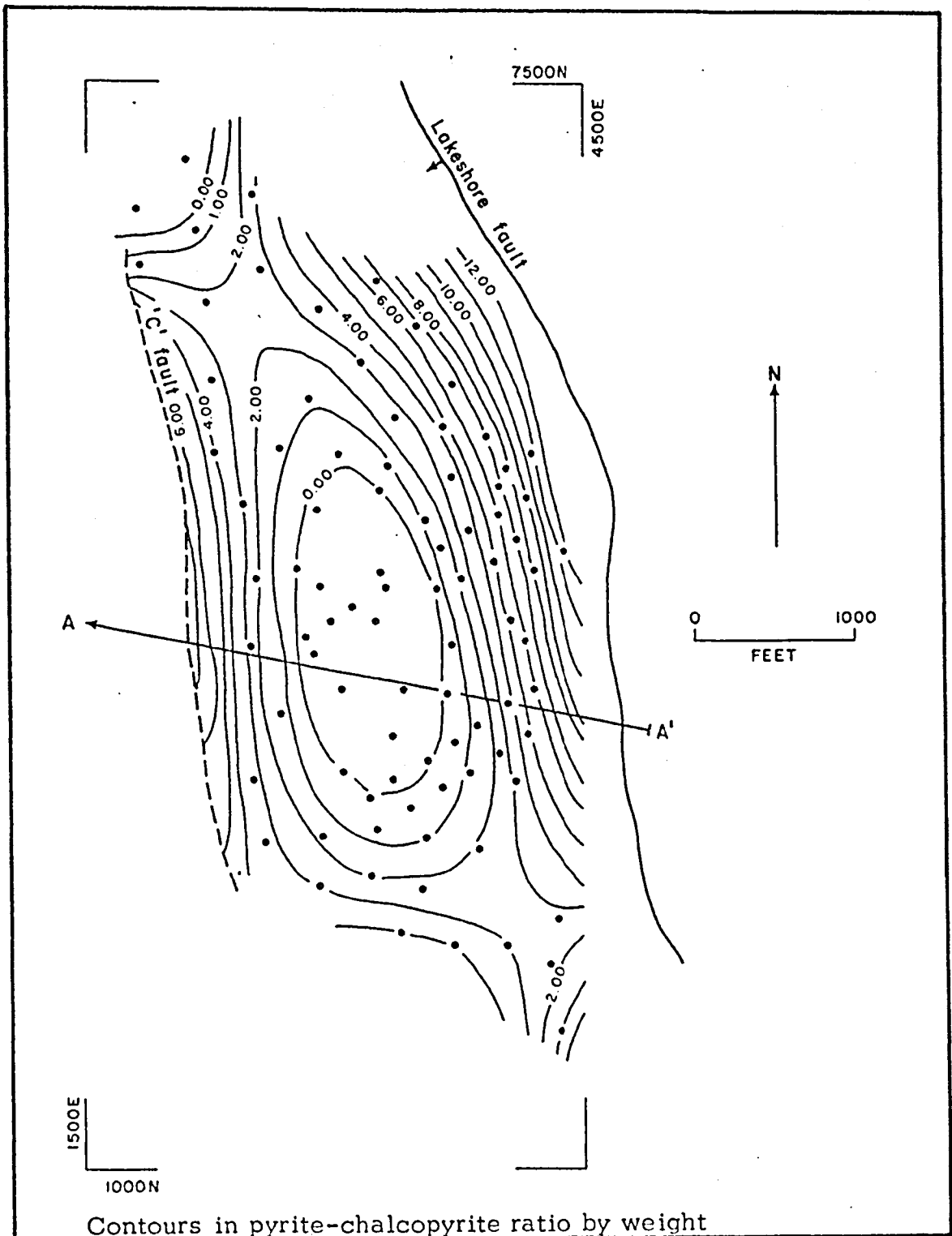


Figure 9. Overall Zoning Pattern of Pyrite-chalcopyrite Ratio, Lakeshore Mine

Percent SS contribution: 20.55; significance level: +90%.



central portion of the deposit and a pyrite halo on the margin of the deposit.

Upper Porphyry. Figure 10 is an isopach map of the upper porphyry and Figures 11, 12, and 13 show the sulfide zoning pattern. The upper porphyry is thickest to the west, with a broad "saddle area" in the west-central portion of the area. The porphyry thins to the east.

The pyrite and chalcopyrite maps have significance levels of 70 and 50 percent respectively. These rather low significance levels indicate that some factors other than simple districtwide zoning patterns are influencing sulfide distribution. The pyrite map shows a low centered on the upper porphyry with increasing values to the north and south and decreasing values to the east and west. The chalcopyrite map shows a high in the southeast margin of the porphyry. Note again the northerly component to the maps, especially on the pyrite map.

The pyrite-chalcopyrite ratio map has a significance level of 90 percent and is the best indicator of zoning in the upper porphyry. The map shows a pyrite-chalcopyrite ratio low centered on the upper porphyry with a pyrite halo to the north and south. The dropping off in the ratio to the east probably reflects an area of increasing chalcopyrite in the east margin of the upper porphyry, which thins to the east.

Lower Porphyry. Figure 14 is the isopach map of the lower porphyry and Figures 15, 16, and 17 show the zoning pattern. The lower porphyry is thickest to the southeast and to the north. The thinning to the northeast represents the truncation of the porphyry by the Lakeshore fault, and the thinning to the southwest is probably due to the fact that holes were not drilled as deeply into the lower porphyry as in other areas.

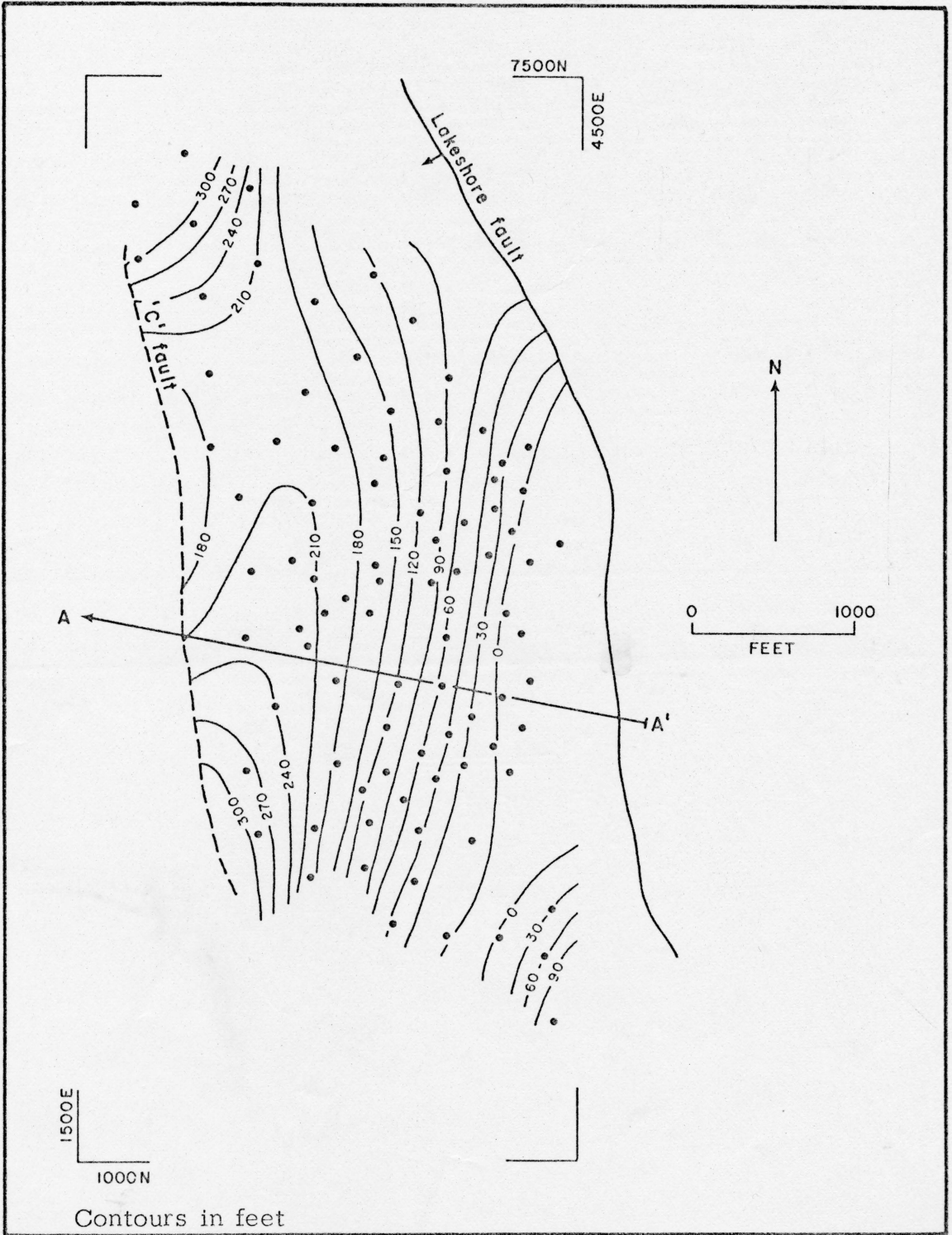


Figure 10. Isopach Map of the Upper Porphyry within the Sulfide Zone, Lakeshore Mine

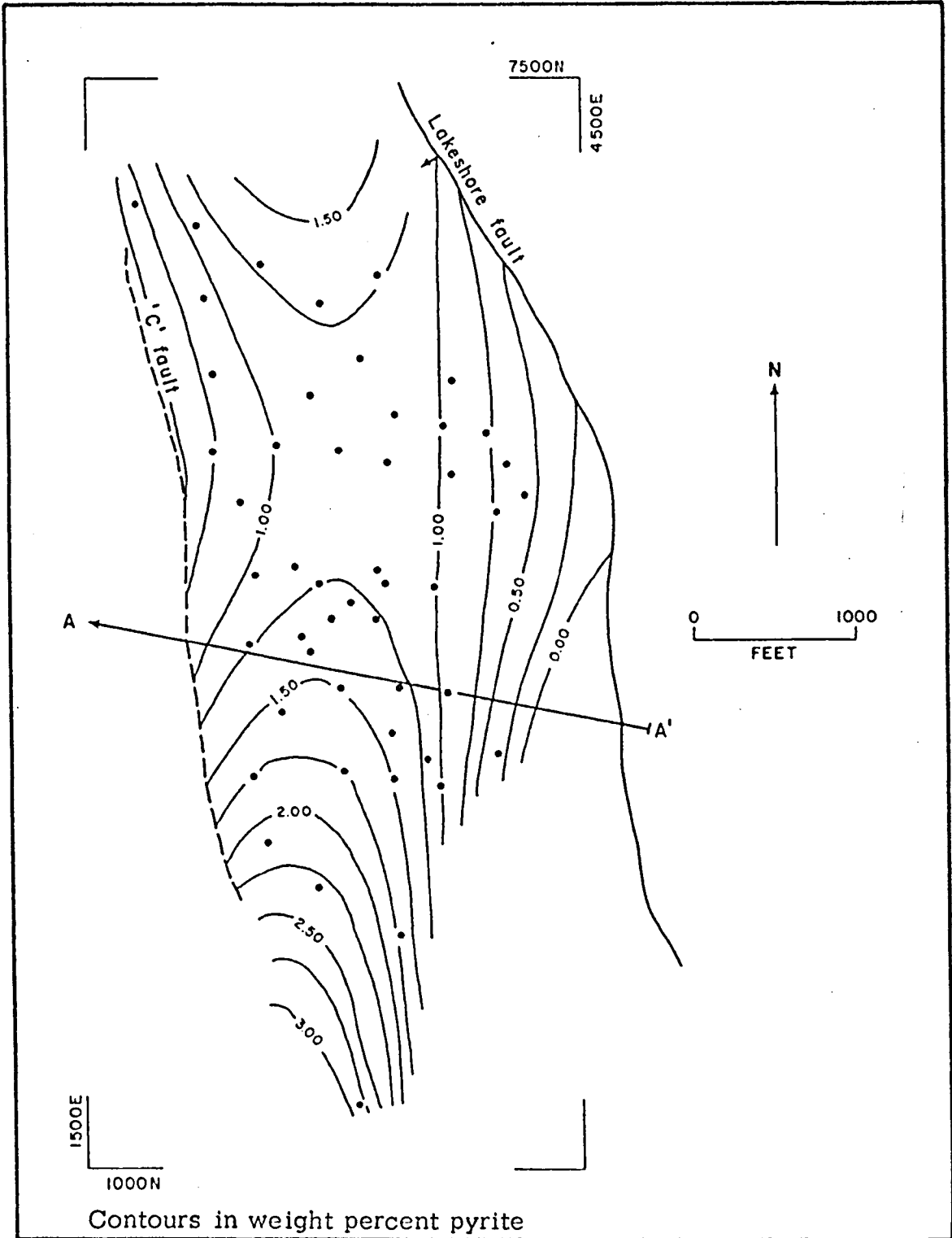


Figure 11. Zoning Pattern of Pyrite in the Upper Porphyry, Lakeshore Mine

Percent SS contribution: 20.11; significance level: +70%.

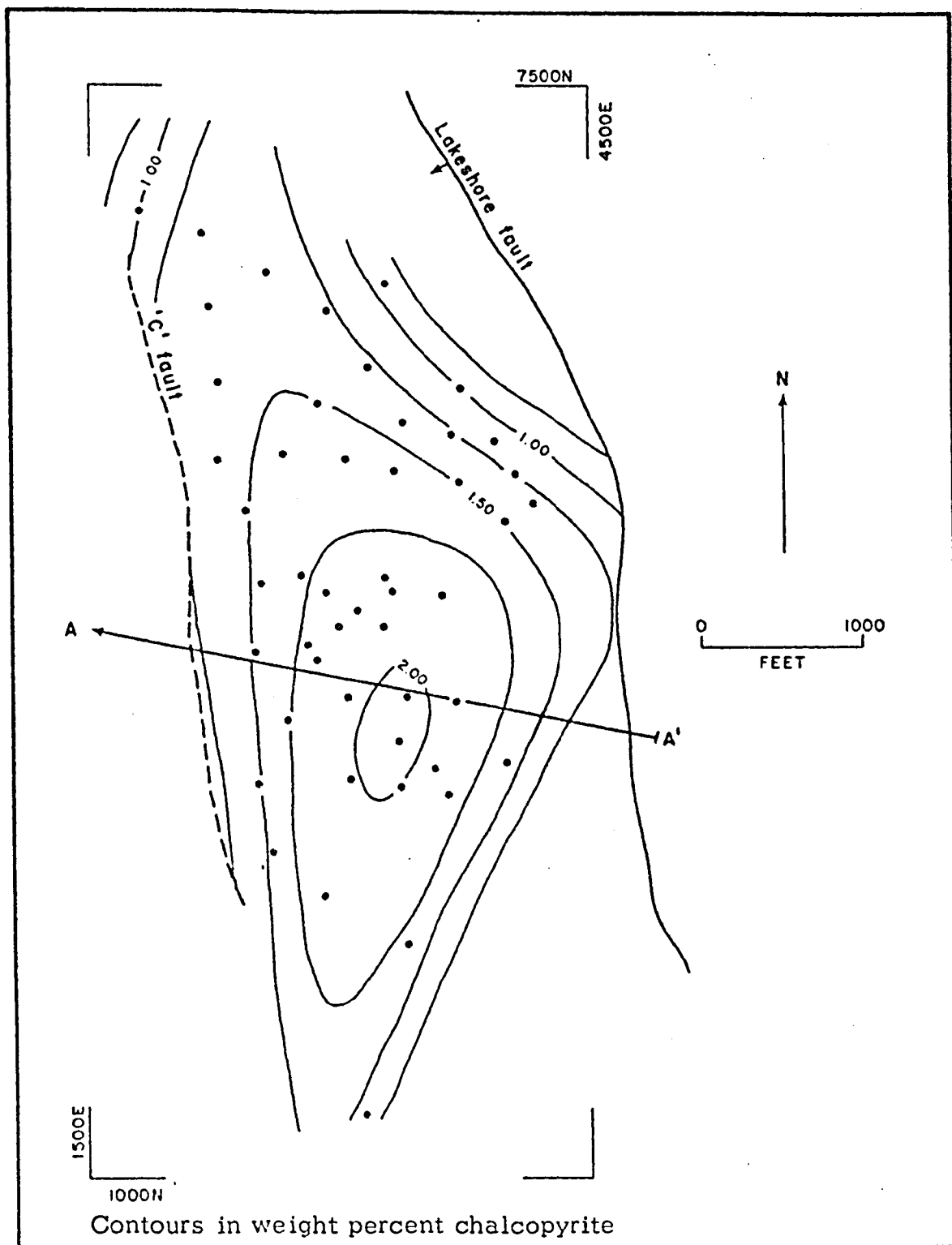


Figure 12. Zoning Pattern of Chalcopyrite in Upper Porphyry, Lakeshore Mine

Percent SS contribution: 16.04; significance level: +50%.

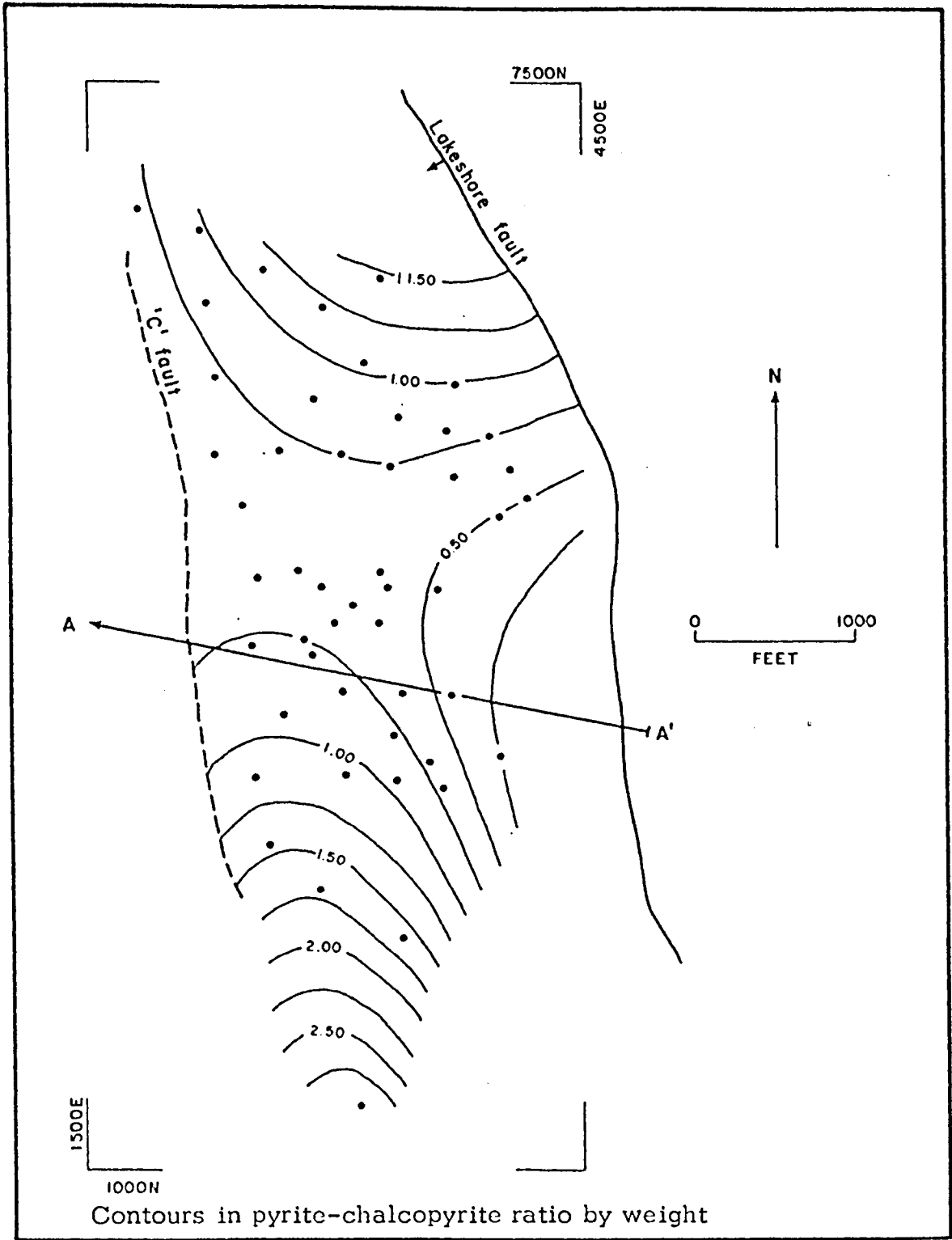


Figure 13. Zoning Pattern of Pyrite-chalcopyrite Ratio in Upper Porphyry, Lakeshore Mine

Percent SS contribution: 32.55; significance level: +90%.

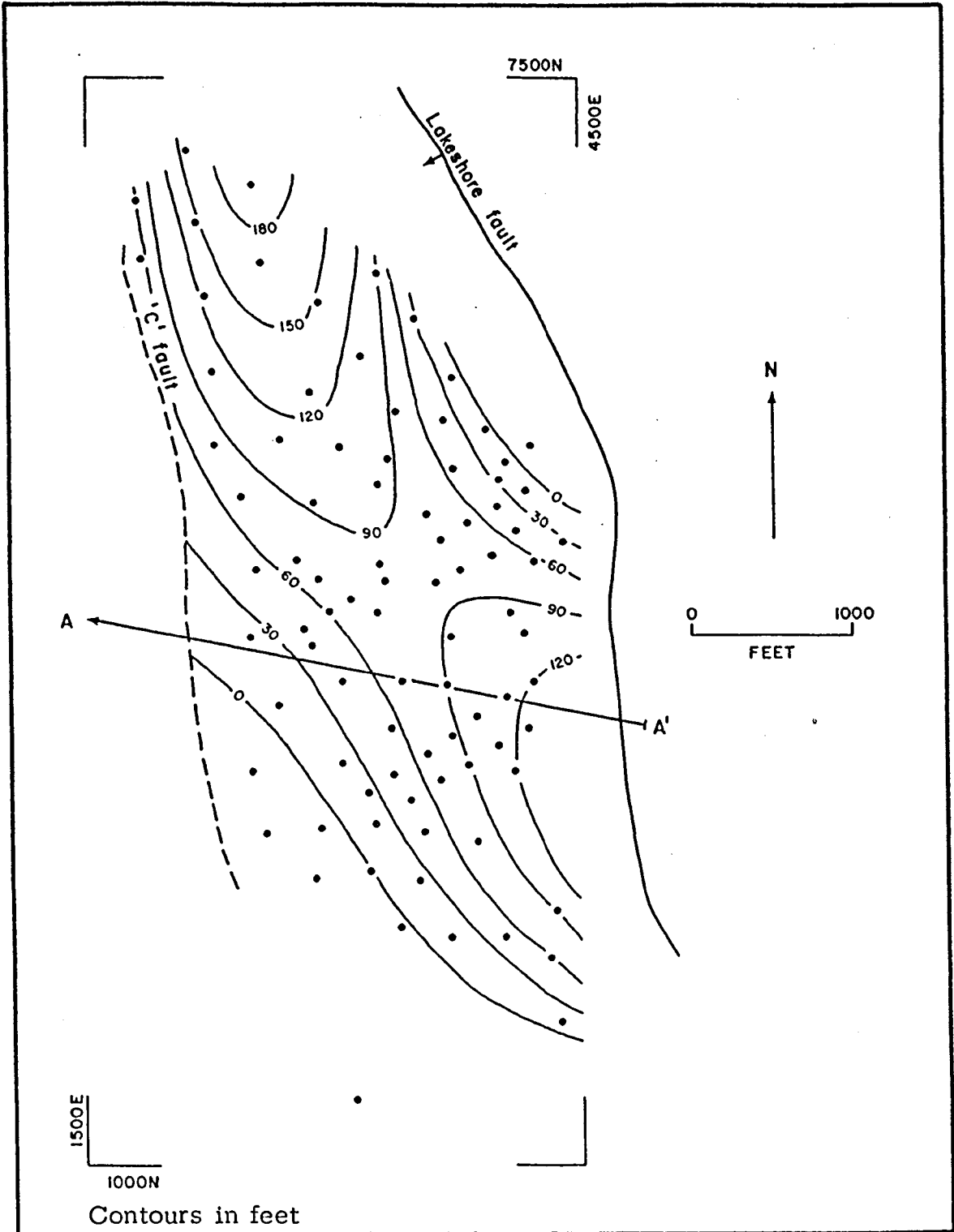


Figure 14. Isopach Map of the Lower Porphyry, Lakeshore Mine

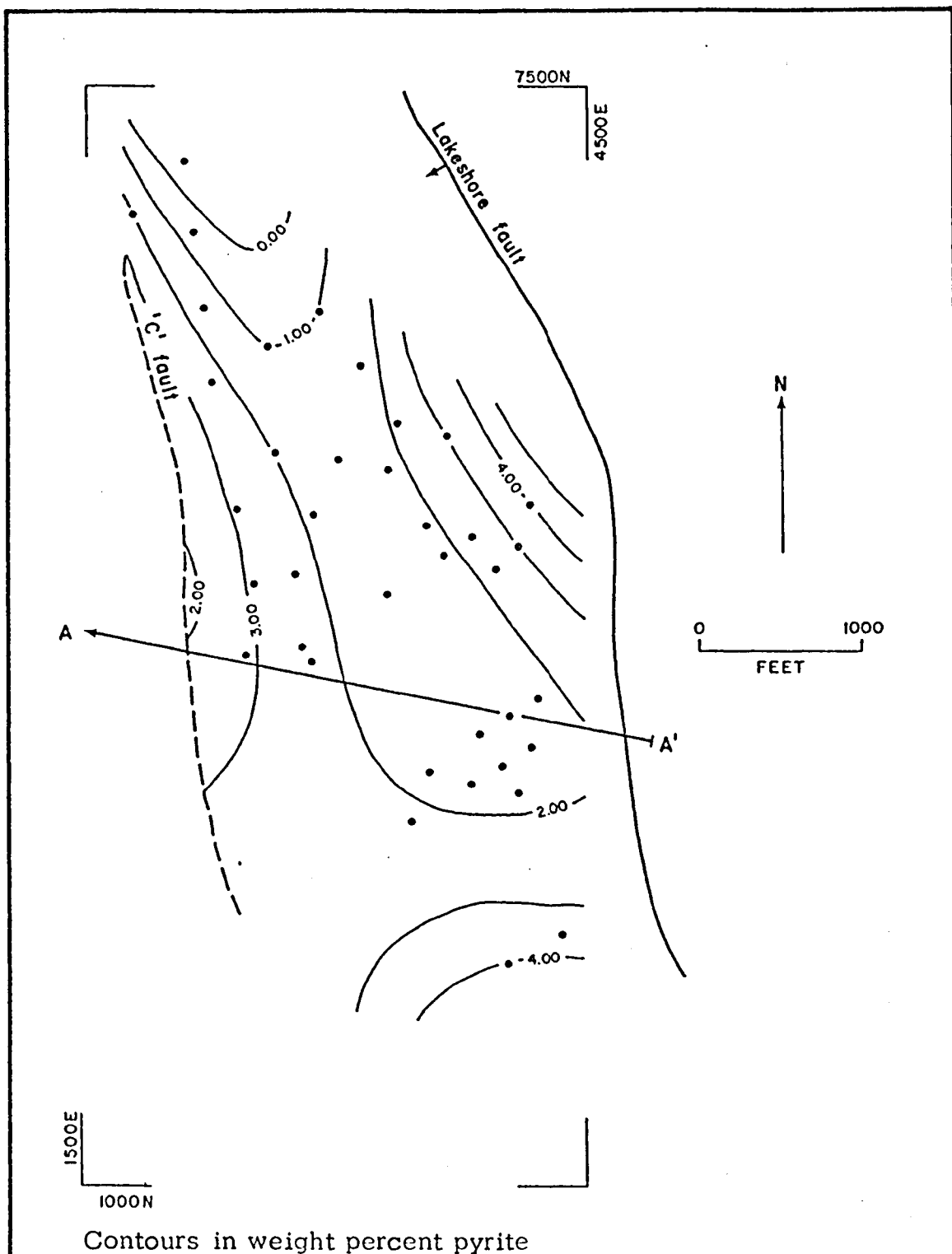


Figure 15. Zoning Pattern of Pyrite in Lower Porphyry, Lakeshore Mine

Percent SS contribution: 27.71; significance level: +75%.

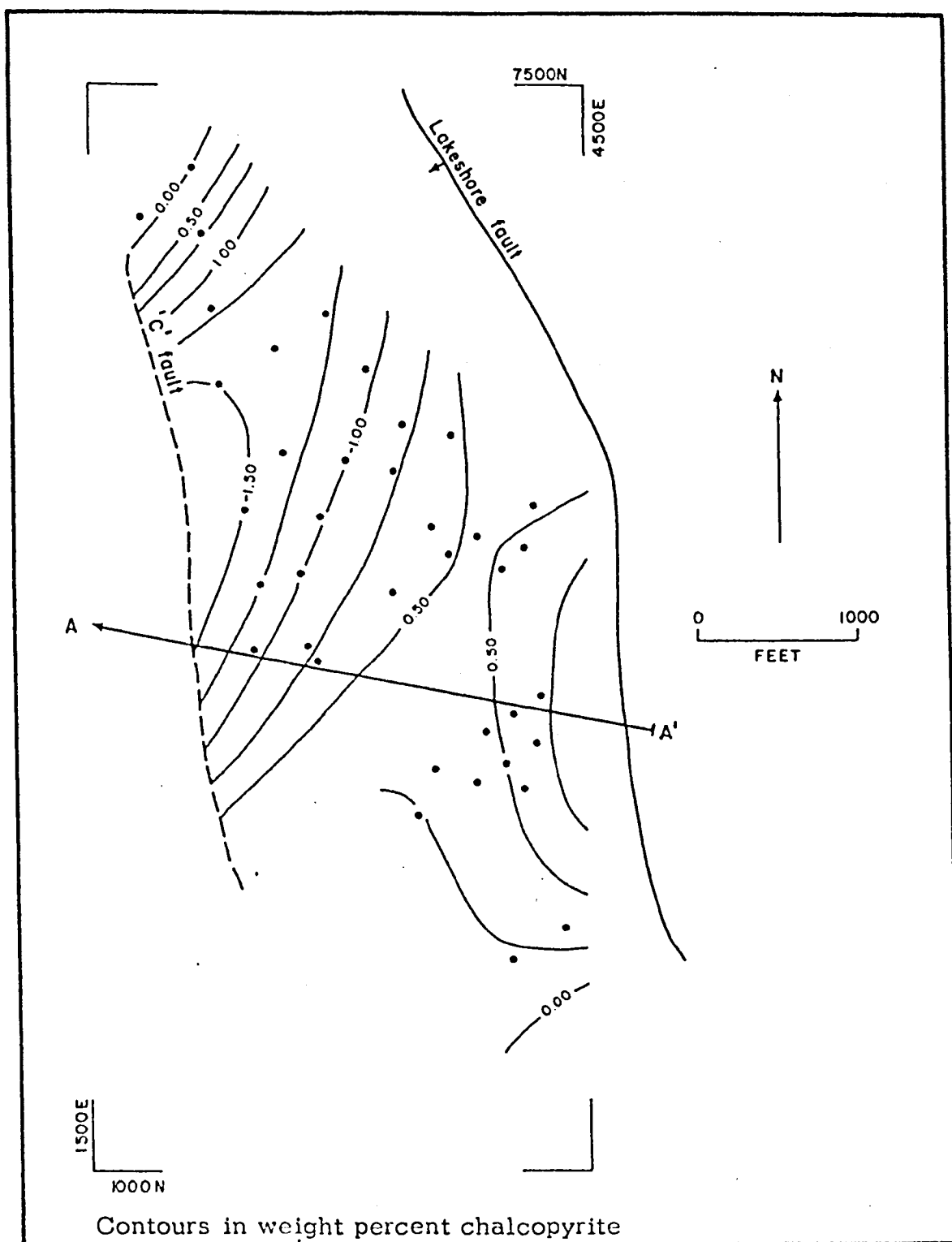
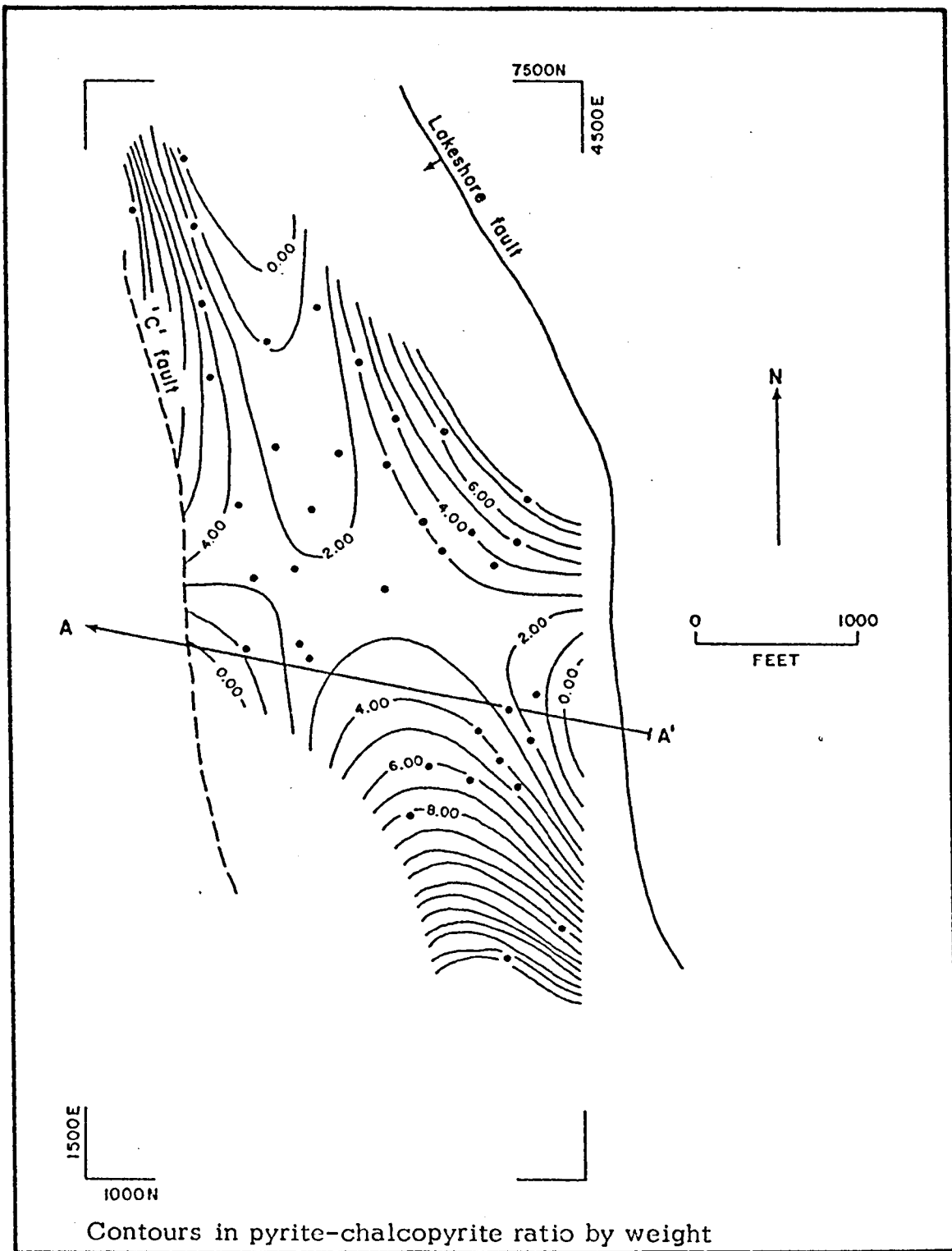


Figure 16. Zoning Pattern of Chalcopyrite in Lower Porphyry, Lakeshore Mine

Percent SS contribution: 46.88; significance level: +90%.





Contours in pyrite-chalcopyrite ratio by weight

Figure 17. Zoning Pattern of Pyrite-chalcopyrite Ratio in Lower Porphyry, Lakeshore Mine  
Percent SS contribution: 54.17; significance level: +90%.

The pyrite map (Fig. 15) shows a low in the central part of the porphyry extending as a trough to the north. The chalcopyrite map (Fig. 16) is especially interesting, for it shows a chalcopyrite high in the west-central part of the deposit which is truncated by the 'C' fault. Although much of the lower porphyry is essentially barren, there could be a down-dropped center of mineralization west of the 'C' fault.

The pyrite-chalcopyrite ratio map (Fig. 17) shows a central low with a pyrite halo. There are gaps in the halo to the north, southeast, and southwest.

Cretaceous Volcanic and Sedimentary Rocks. The isopach map for the Cretaceous volcanic and sedimentary rocks is shown in Figure 18, and the zoning pattern is shown in Figures 19, 20, 21. On the isopach map (Fig. 18), an elongate northwest-trending zone in which the Cretaceous volcanic and sedimentary rocks are relatively thin represents the portion of the andesite overlying the upper porphyry which has deleted much of the Cretaceous volcanic and sedimentary rocks. To the west, along the 'C' fault, the upper porphyry has cut out the Cretaceous volcanic and sedimentary rocks.

The pyrite map (Fig. 19) shows a low centered on the underlying porphyry. Pyrite increases outward to form the pyrite halo, with gaps once again to the northwest and southeast reflecting the common trend.

The chalcopyrite map (Fig. 20) shows a strong northerly trend, with a high beginning to form to the southwest. This high coincides with the margin of the upper porphyry and represents higher grade mineralization in the Cretaceous volcanic and sedimentary rocks adjacent to the upper porphyry.

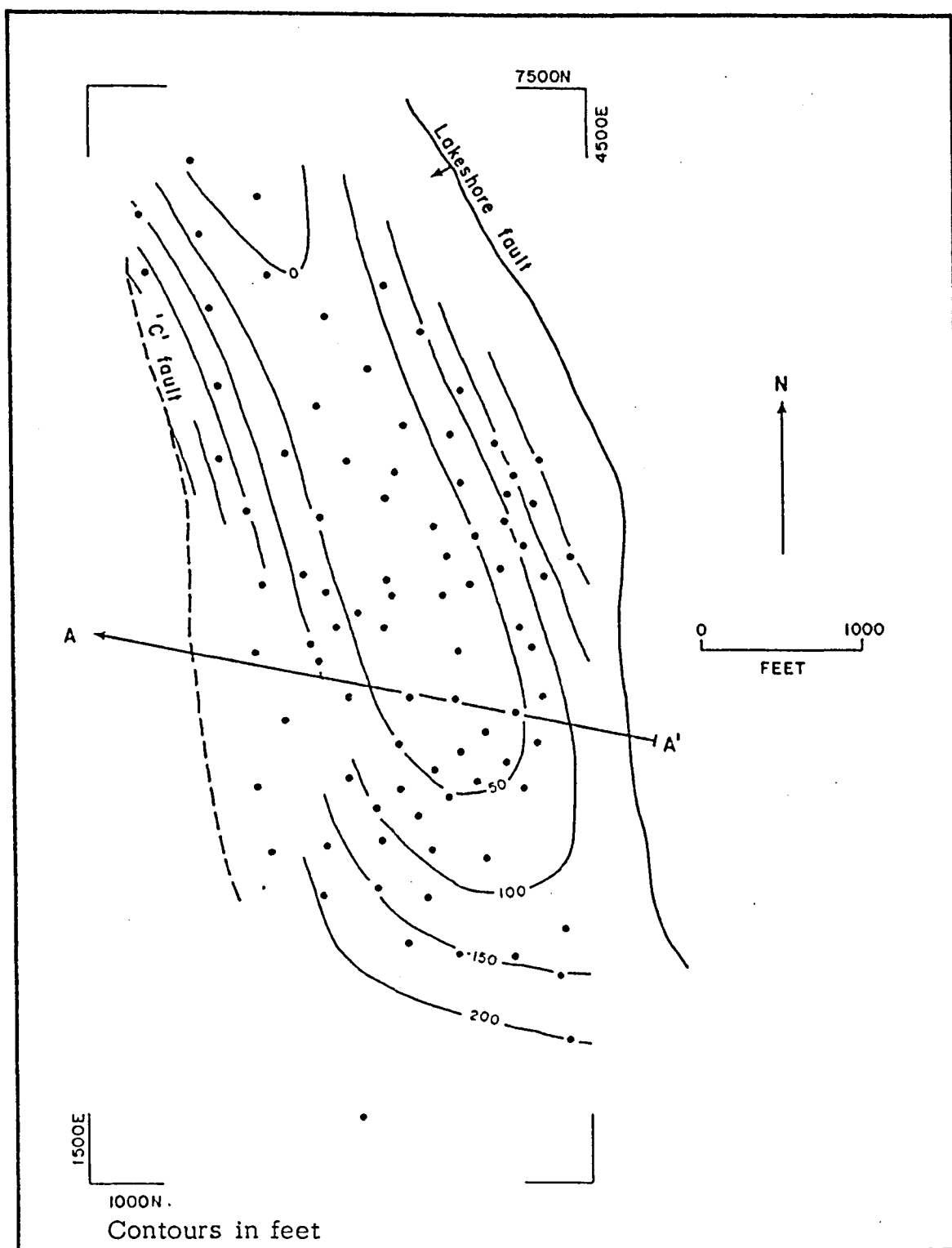


Figure 18. Isopach Map of the Cretaceous Volcanic and Sedimentary Rocks within the Sulfide Zone, Lakeshore Mine

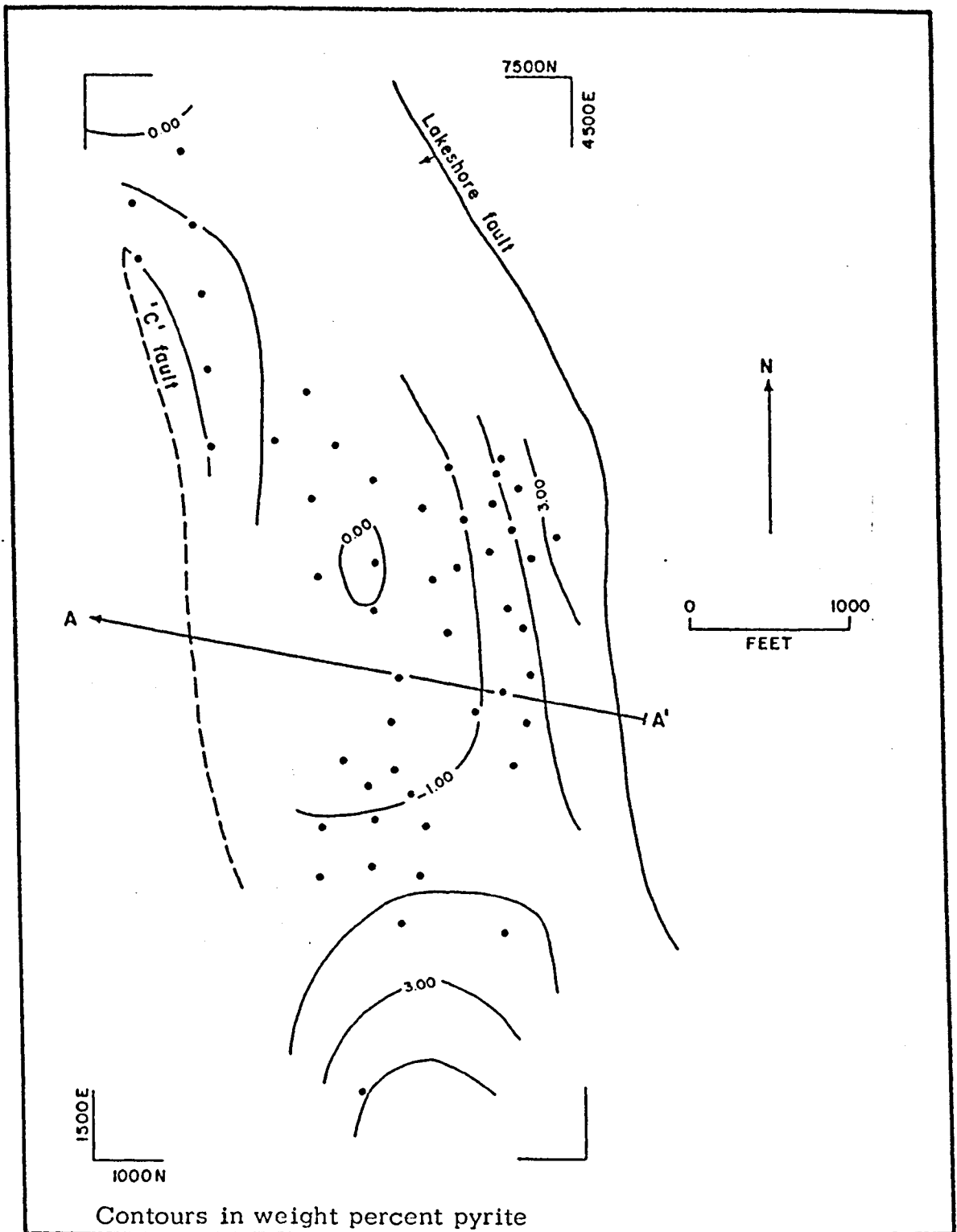


Figure 19. Zoning Pattern of Pyrite in Cretaceous Volcanic and Sedimentary Rocks, Lakeshore Mine

Percent SS contribution: 26.32; significance level: +90%.

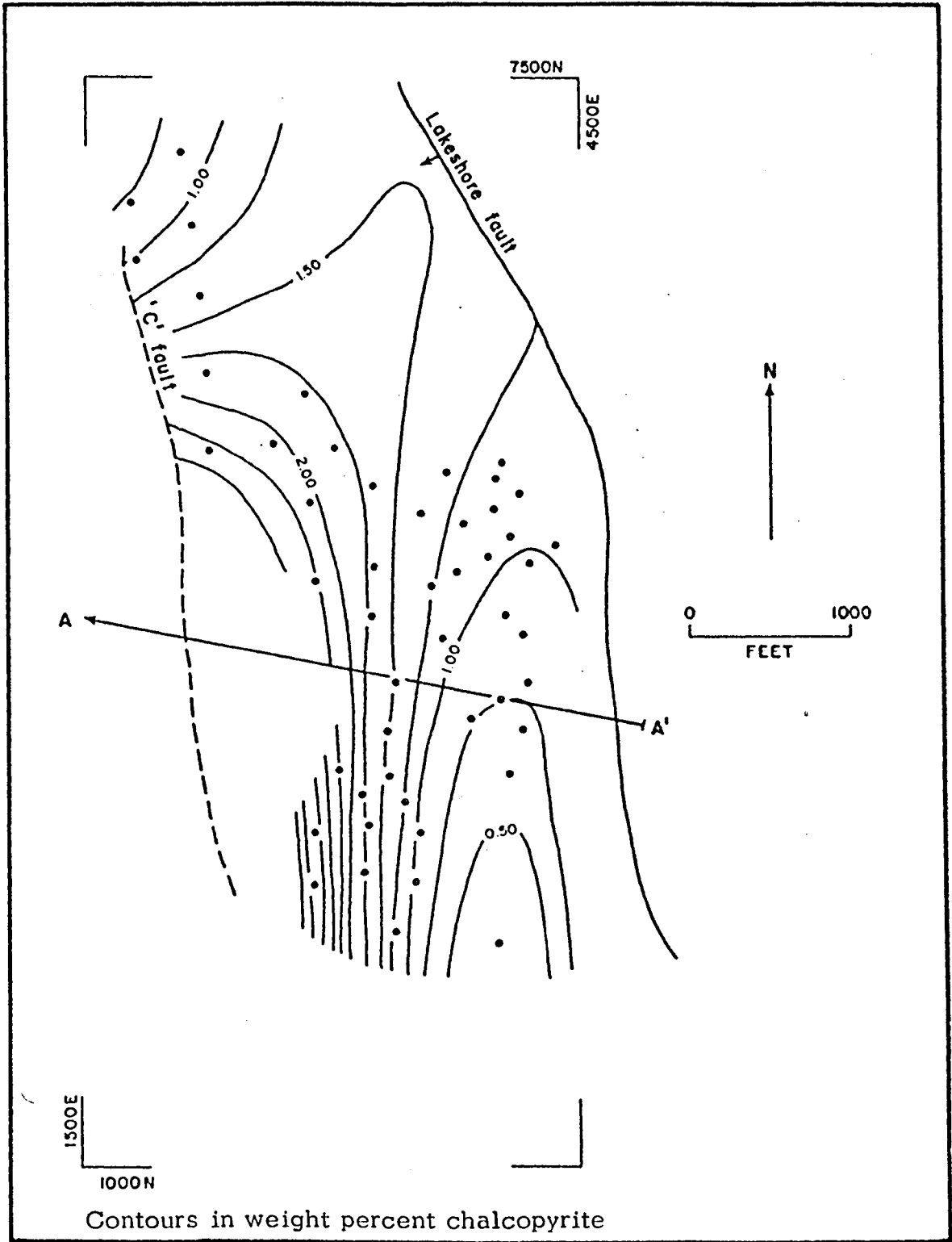


Figure 20. Zoning Pattern of Chalcopyrite in Cretaceous Volcanic and Sedimentary Rocks, Lakeshore Mine

Percent SS contribution: 54.51; significance level: +90%.

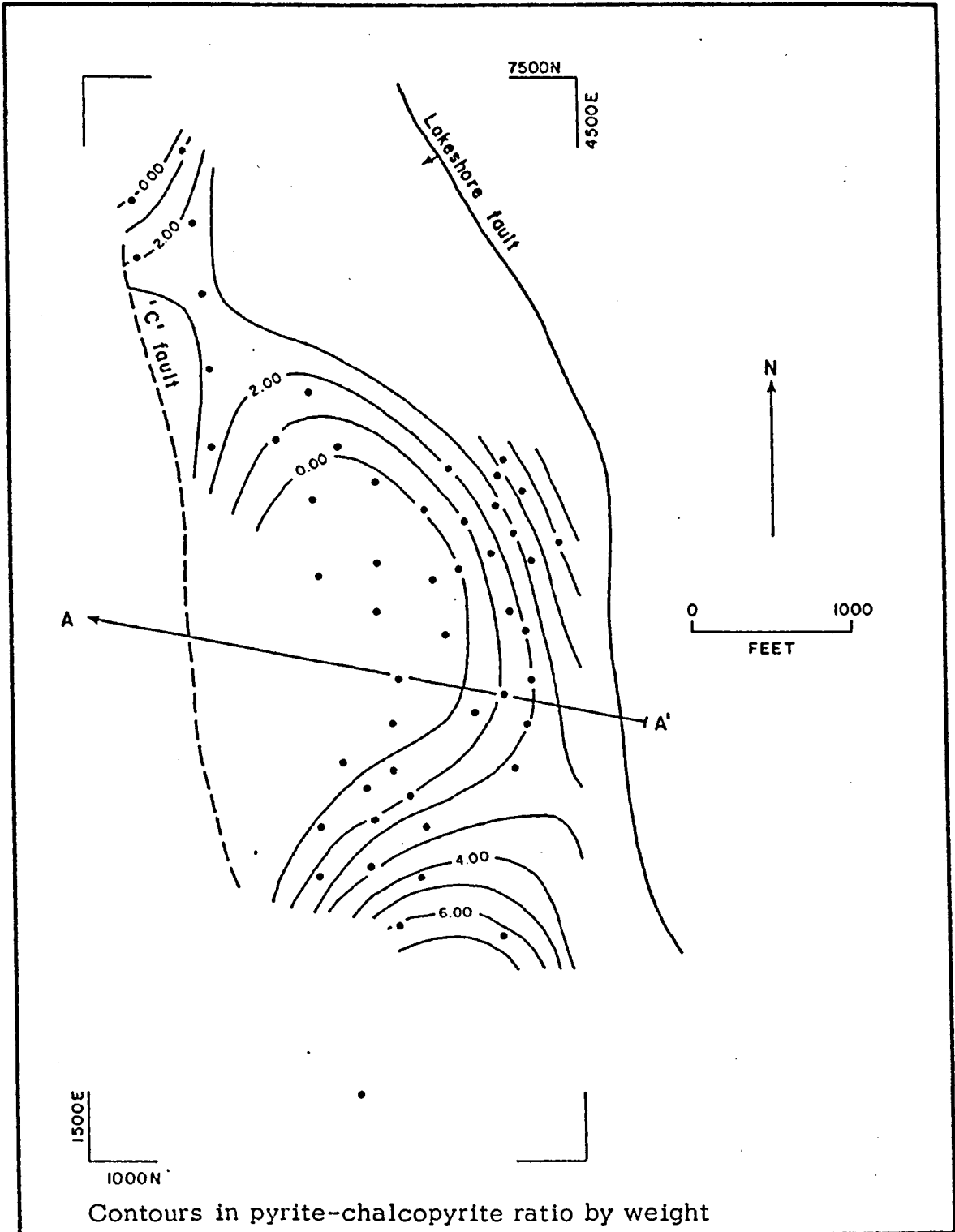


Figure 21. Zoning Pattern of Pyrite-chalcopyrite Ratio in Cretaceous Volcanic and Sedimentary Rocks, Lakeshore Mine

The pyrite-chalcopyrite ratio map also reflects the chalcopyrite high in the southwest, as evidenced by the low ratio. High ratios away from the upper porphyry represent a pyrite halo, with a gap in the halo to the northwest.

Tactite. The isopach map for the tactite horizon (Mescal Limestone) is shown in Figure 22, and Figures 23, 24, and 25 show the zoning pattern. The isopach map shows that the tactite is thickest in the south.

The pyrite map (Fig. 23) shows a saddle in the south-central portion of the map, with pyrite highs to the east and west. The northwest trend is shown by a decrease in pyrite values to the north and south of the saddle. The pyrite saddle is to the northwest of the thickest part of the tactite section. However, a chalcopyrite high and a pyrite-chalcopyrite ratio low both coincide with the thickest section of the tactite in the south part of the area. Farther south the tactite has been cut out by faulting. In addition, there is an indication of a chalcopyrite high on the north end of the 'C' fault on the chalcopyrite map (Fig. 24), truncated by the 'C' fault. Once again, an area of mineralization on the west side of the 'C' fault is a possible exploration target.

The thickness of the tactite horizon is apparently the main control for the tactite mineralization. However, in the thinner areas of the horizon, tactite may have been cut out by the upper porphyry and mineralization is occurring in thicker sections of tactite immediately adjacent to the upper porphyry. In this rather unlikely condition, both the thickness of the tactite and the sulfide zoning pattern are related to the upper porphyry.

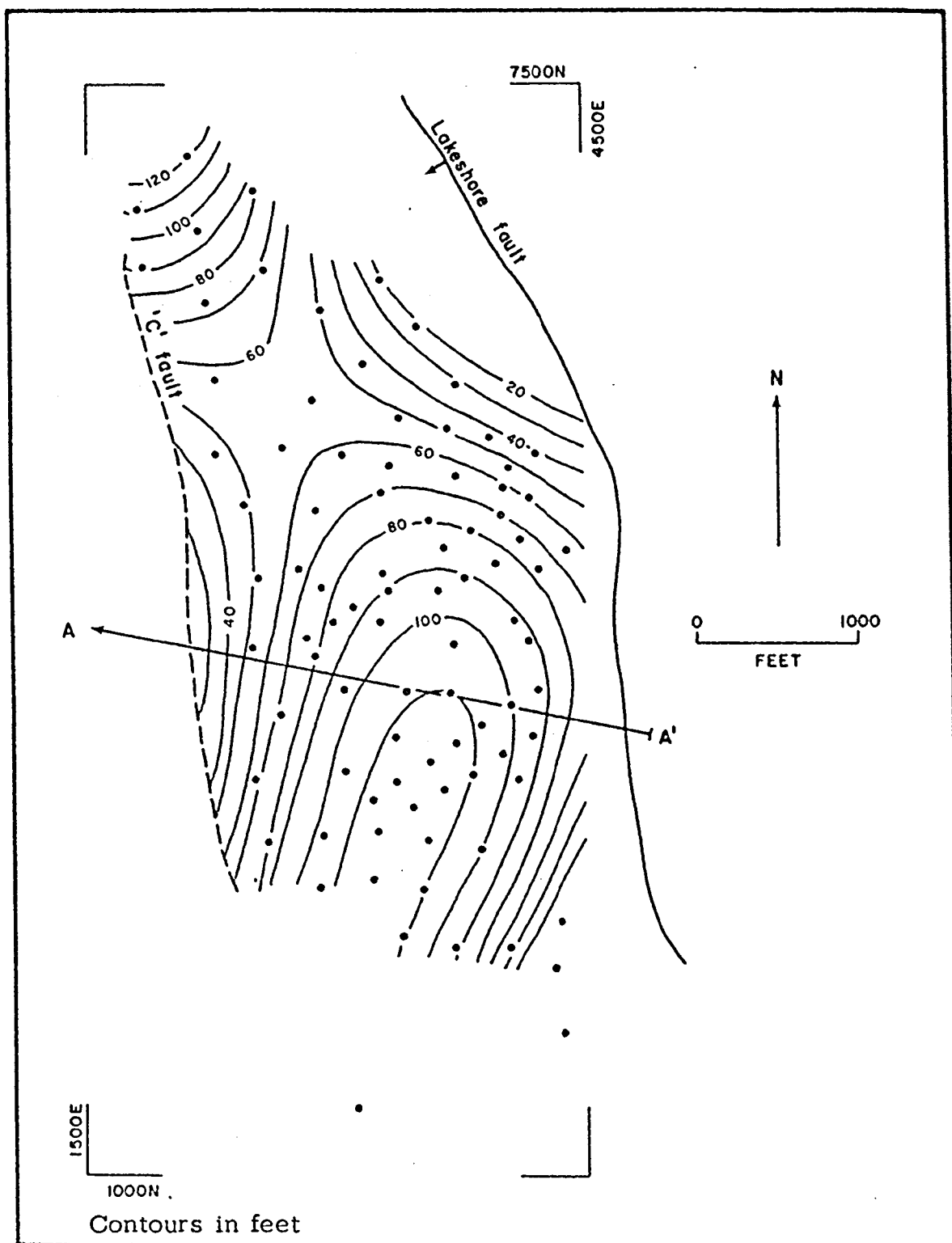


Figure 22. Isopach Map of the Tactite within the Sulfide Zone, Lakeshore Mine



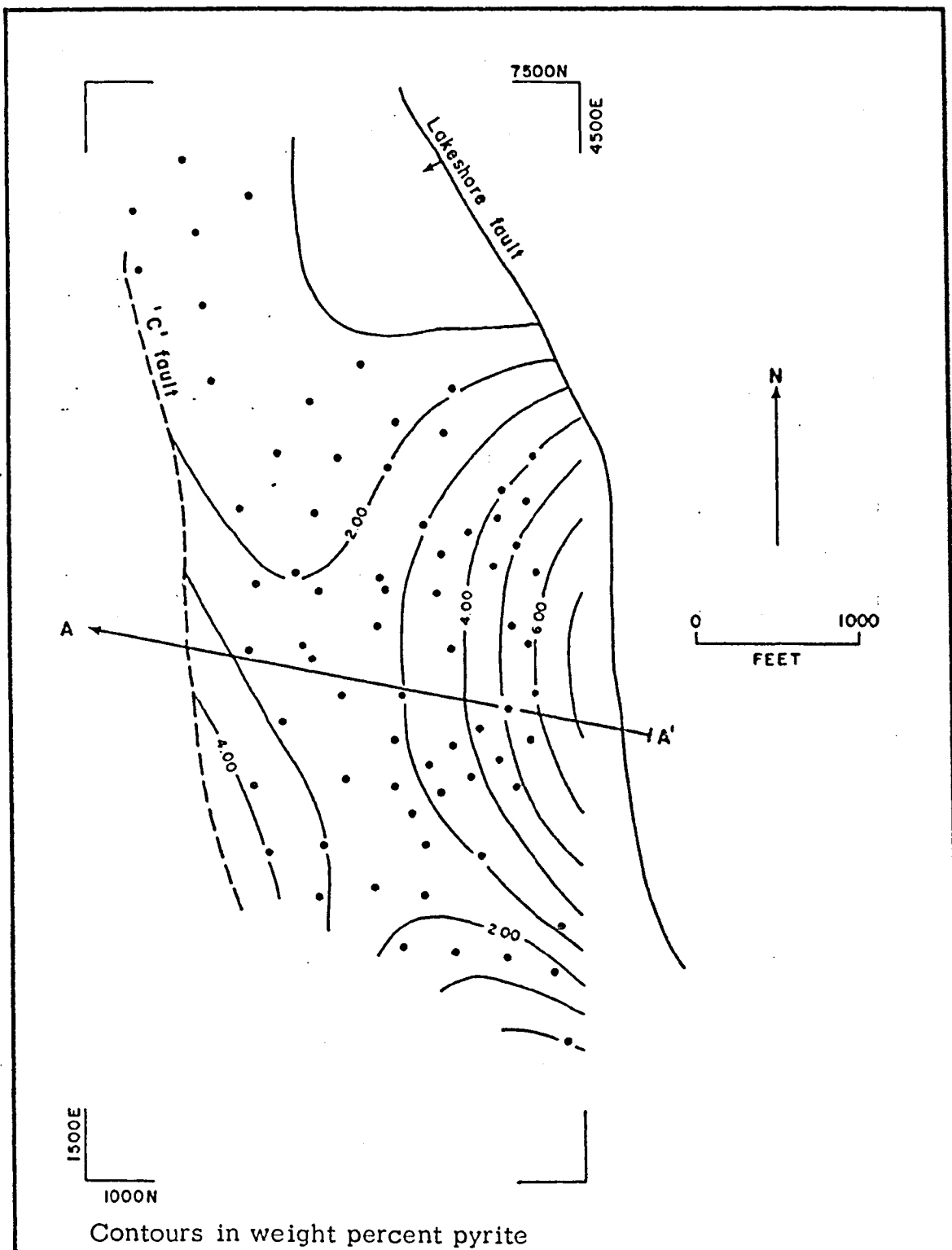


Figure 23. Zoning Pattern of Pyrite in Tactite, Lakeshore Mine  
 Percent SS contribution: 22.29; significance level: +90%.

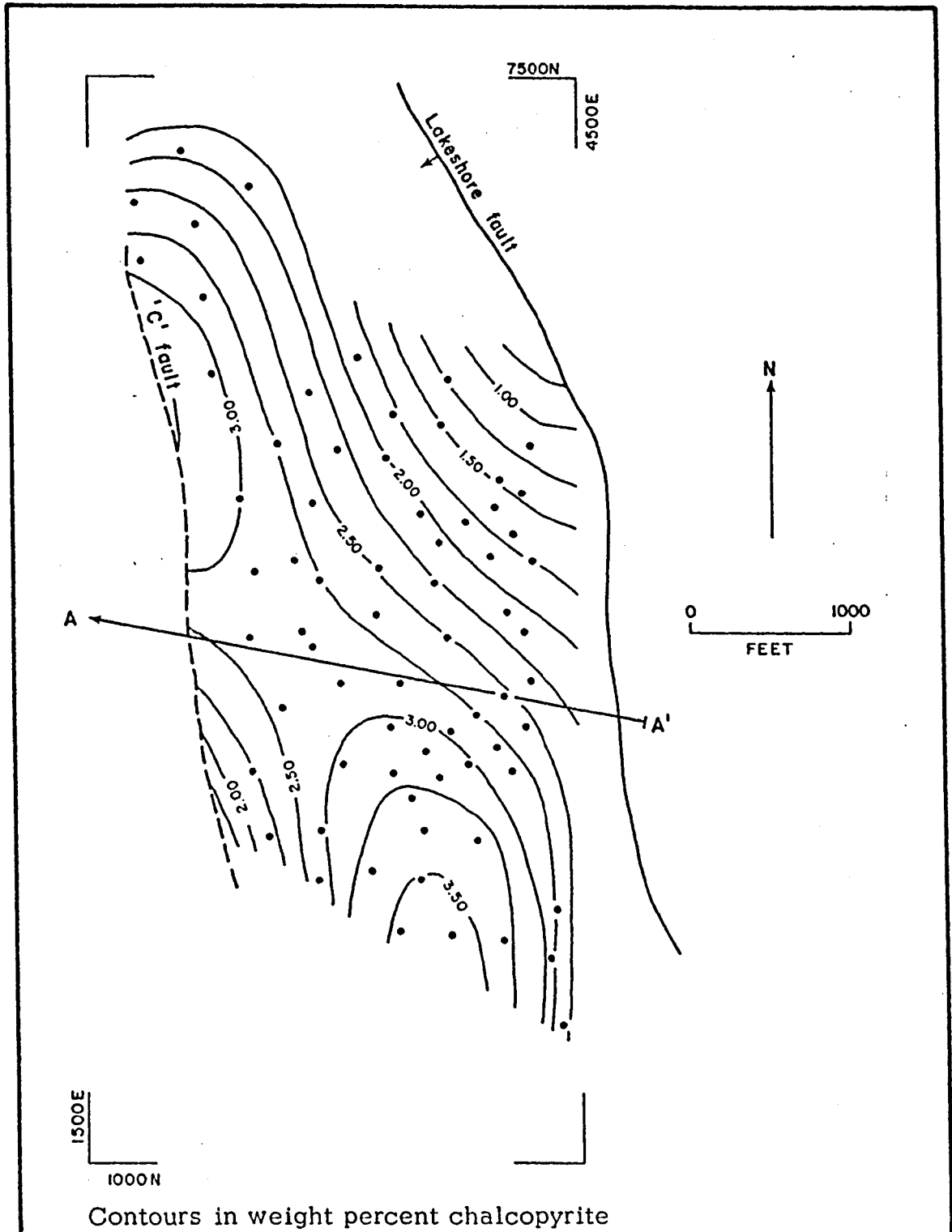


Figure 24. Zoning Pattern of Chalcopyrite in Tactite, Lakeshore Mine

Percent SS contribution: 14.70; significance level: +75%.

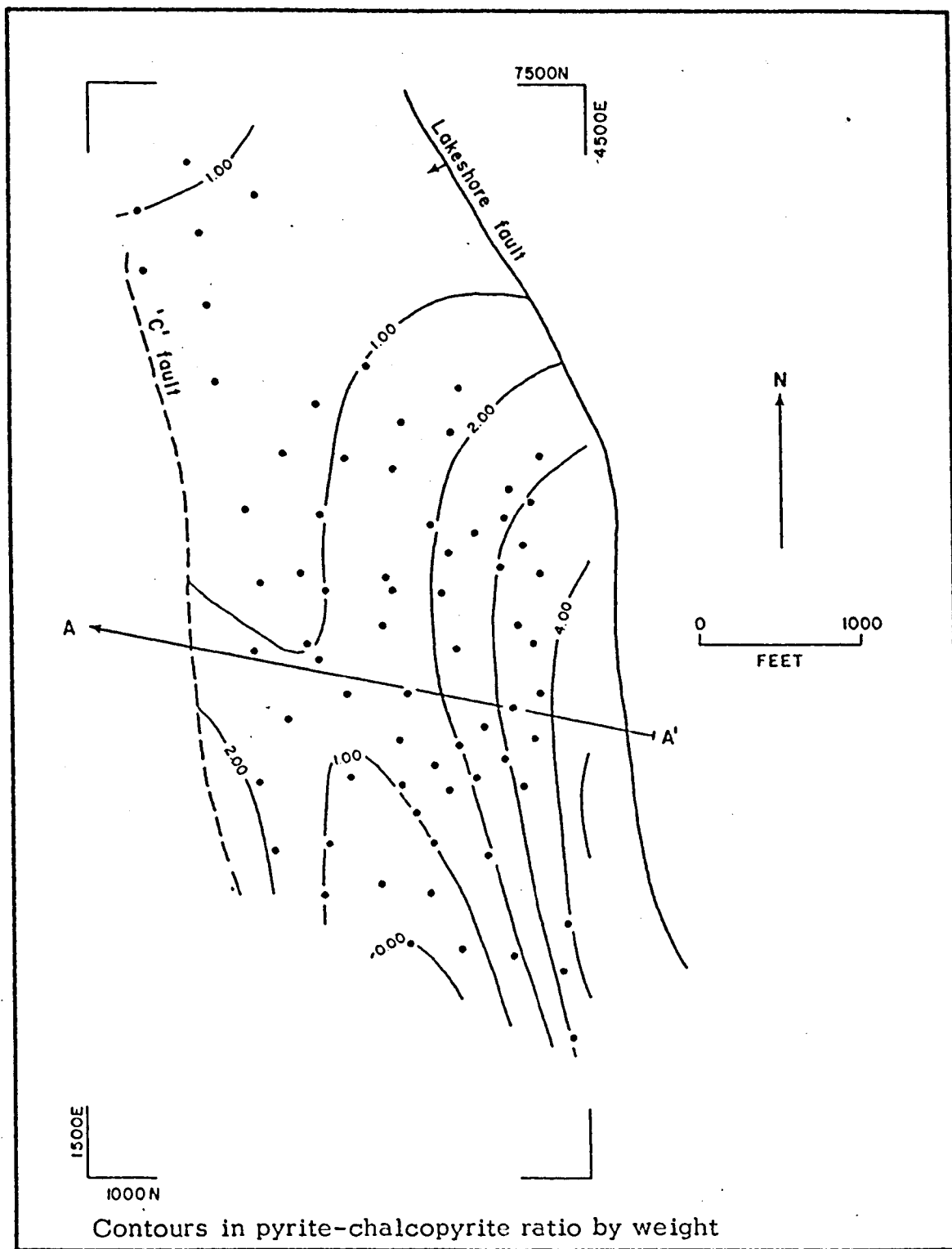


Figure 25. Zoning Pattern of Pyrite-chalcopyrite Ratio in Tactite, Lakeshore Mine

Percent SS contribution: 20.45; significance level: +90%.

Dripping Spring Quartzite. The isopach map for the Dripping Spring Quartzite is shown in Figure 26, and the zoning pattern in Figures 27, 28, and 29. The Dripping Spring Quartzite is composed of nonreactive quartzites, sandstones, and siltstones and is relatively unmineralized. Nonetheless, a pyrite low is centered in the north-central part of the map, and the chalcopryrite map (Fig. 27) shows a vague chalcopryrite high in the central portion of the map and to the northwest and southeast, dropping off in the surrounding area. The significance level of the chalcopryrite map is low, only 65 percent, and the drill holes used to make the map are scattered, so this map is probably not as valid as the pyrite and pyrite-chalcopryrite ratio maps, both of which have significance levels in excess of 90 percent.

The pyrite-chalcopryrite ratio map (Fig. 28) shows a low in the center of the map with a surrounding high which reflects the pyrite halo. Low ratios to the northwest and southeast reflect gaps in the halo along the northwest trend.

Diabase. The diabase isopach map is shown in Figure 30, and the zoning patterns in Figures 31, 32, and 33. The diabase occurs as sills and dikes within the Dripping Spring Quartzite and the Mescal Limestone (tactite horizon).

The pyrite map (Fig. 31) shows a saddle in the central part of the area, with pyrite increasing to the east and west and decreasing to the north and south. The chalcopryrite map (Fig. 32) also shows a saddle area in the central part of the map, increasing to the west, northeast, and south and decreasing to the northwest, southwest, and east. The pyrite-chalcopryrite ratio map (Fig. 33) shows the northwest trend, with

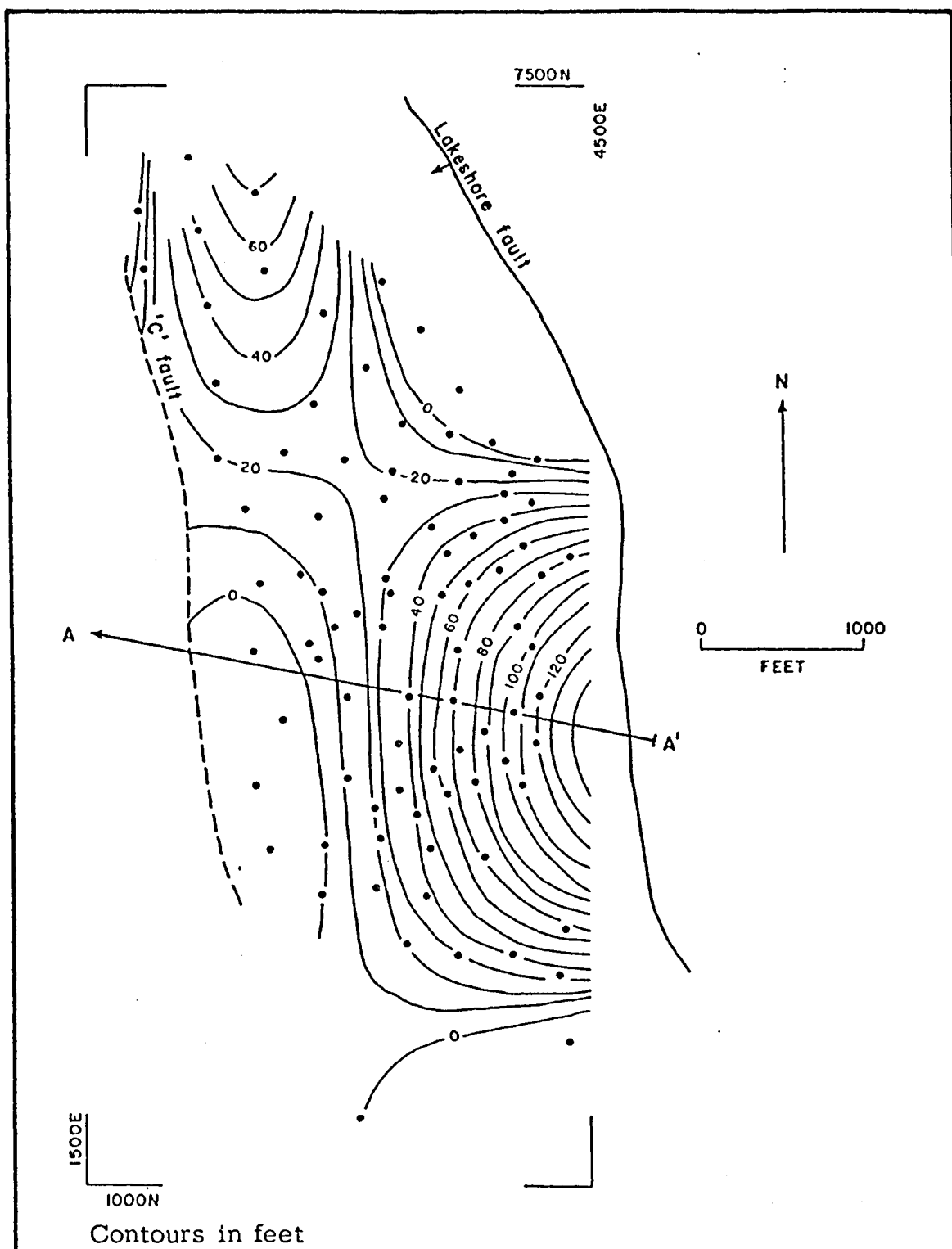


Figure 26. Isopach Map of the Dripping Spring Quartzite with-  
in the Sulfide Zone, Lakeshore Mine

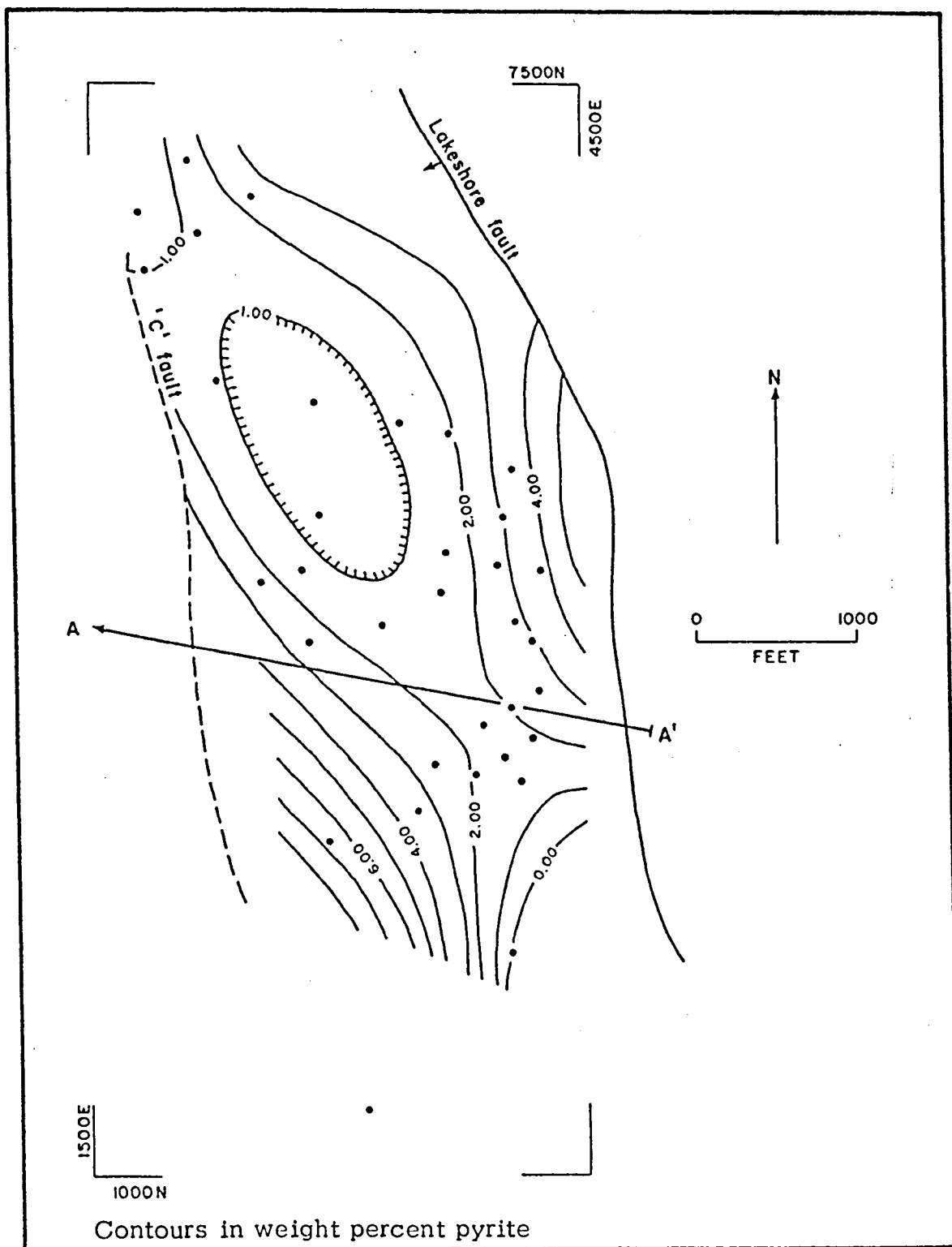


Figure 27. Zoning Pattern of Pyrite in Drizzling Spring Quartzite, Lakeshore Mine

Percent SS contribution: 56.88; significance level: +90%.

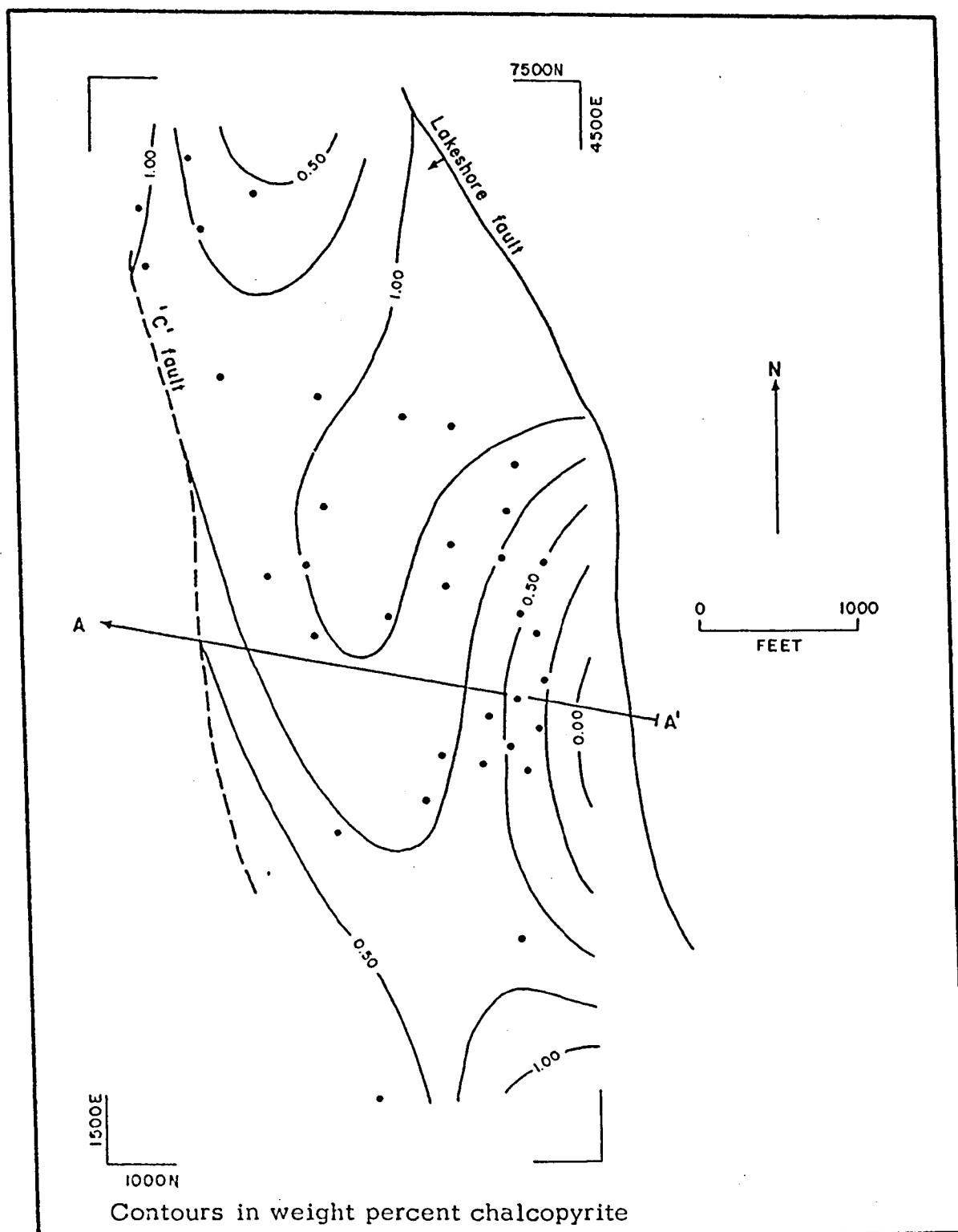


Figure 28. Zoning Pattern of Chalcopyrite in Dripping Spring Quartzite, Lakeshore Mine

Percent SS contribution: 29.25; significance level: +65%.

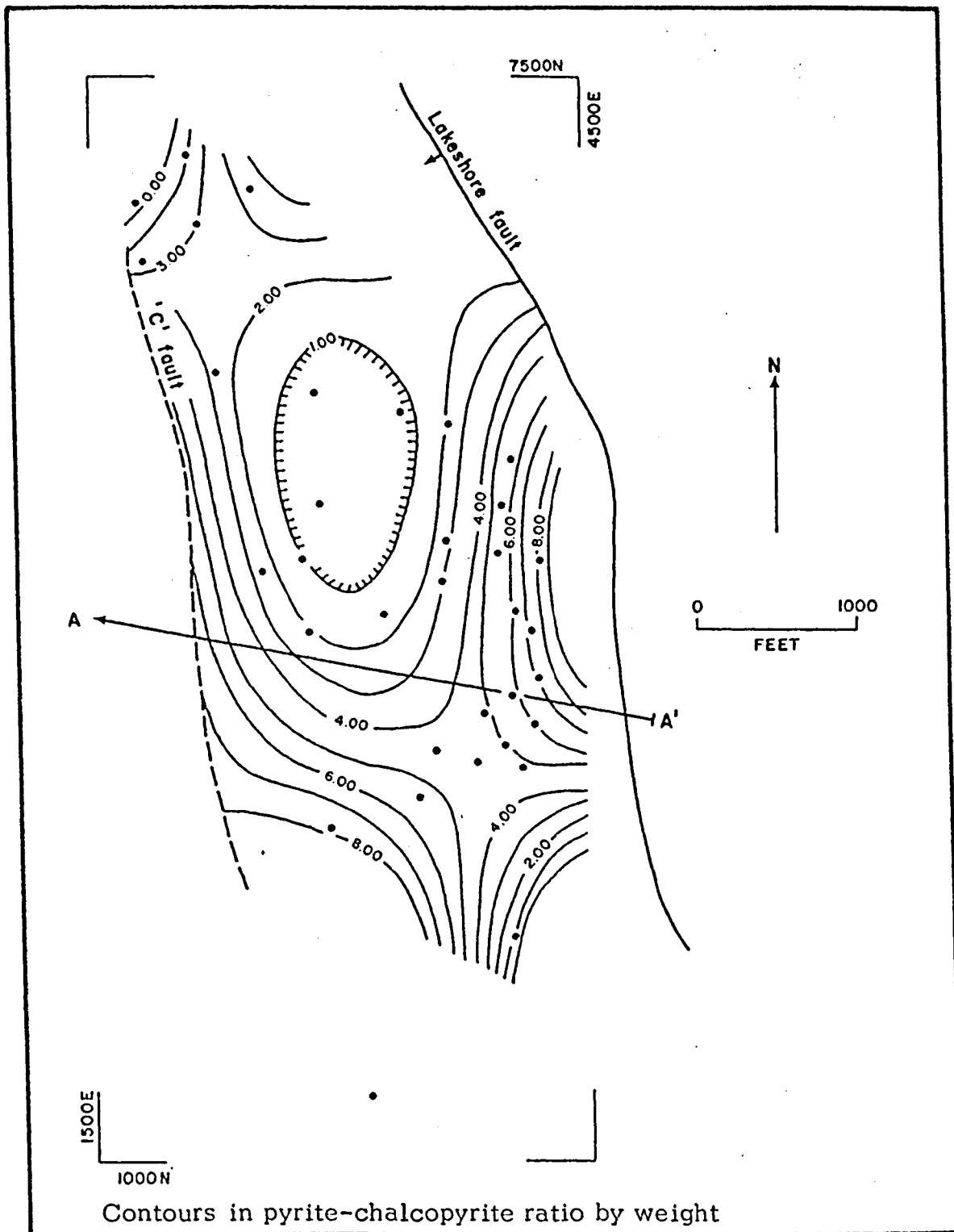


Figure 29. Zoning Pattern of Pyrite-chalcopyrite Ratio in Dripping Spring Quartzite, Lakeshore Mine

Percent SS contribution: 63.93; significance level: +90%.



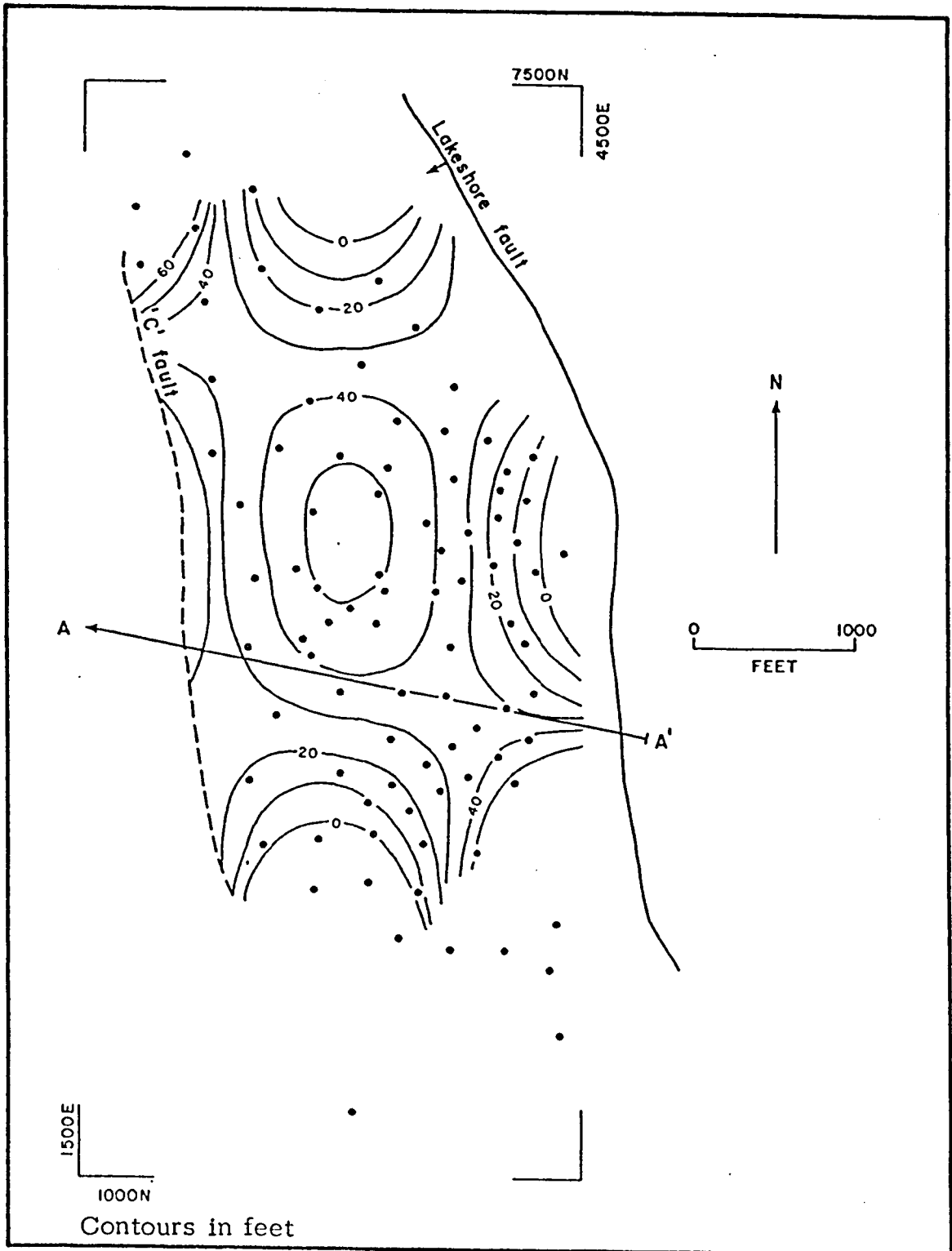


Figure 30. Isopach Map of the Diabase within the Sulfide Zone, Lakeshore Mine

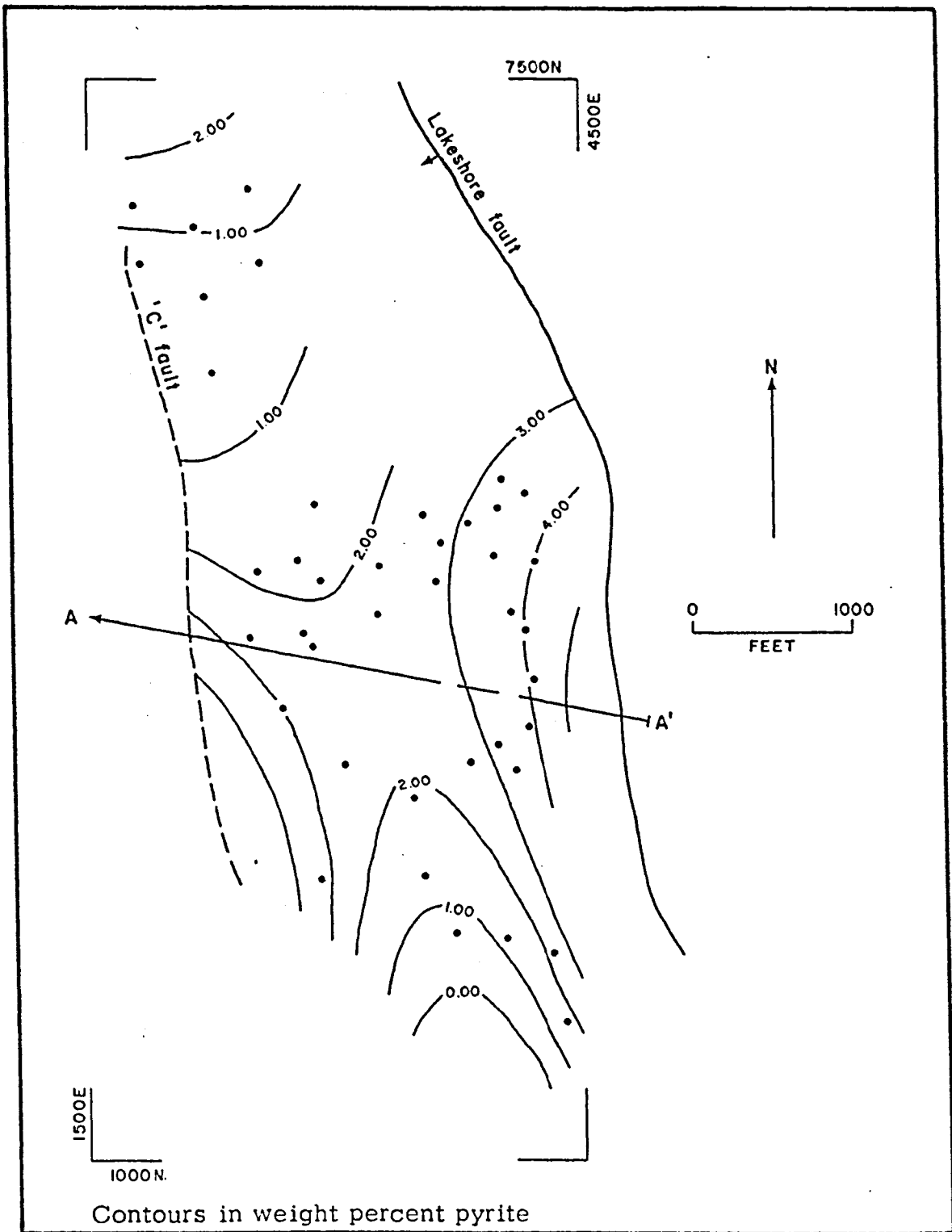


Figure 31. Zoning Pattern of Pyrite in Diabase, Lakeshore Mine  
 Percent SS contribution: 62.45; significance level: +90%.

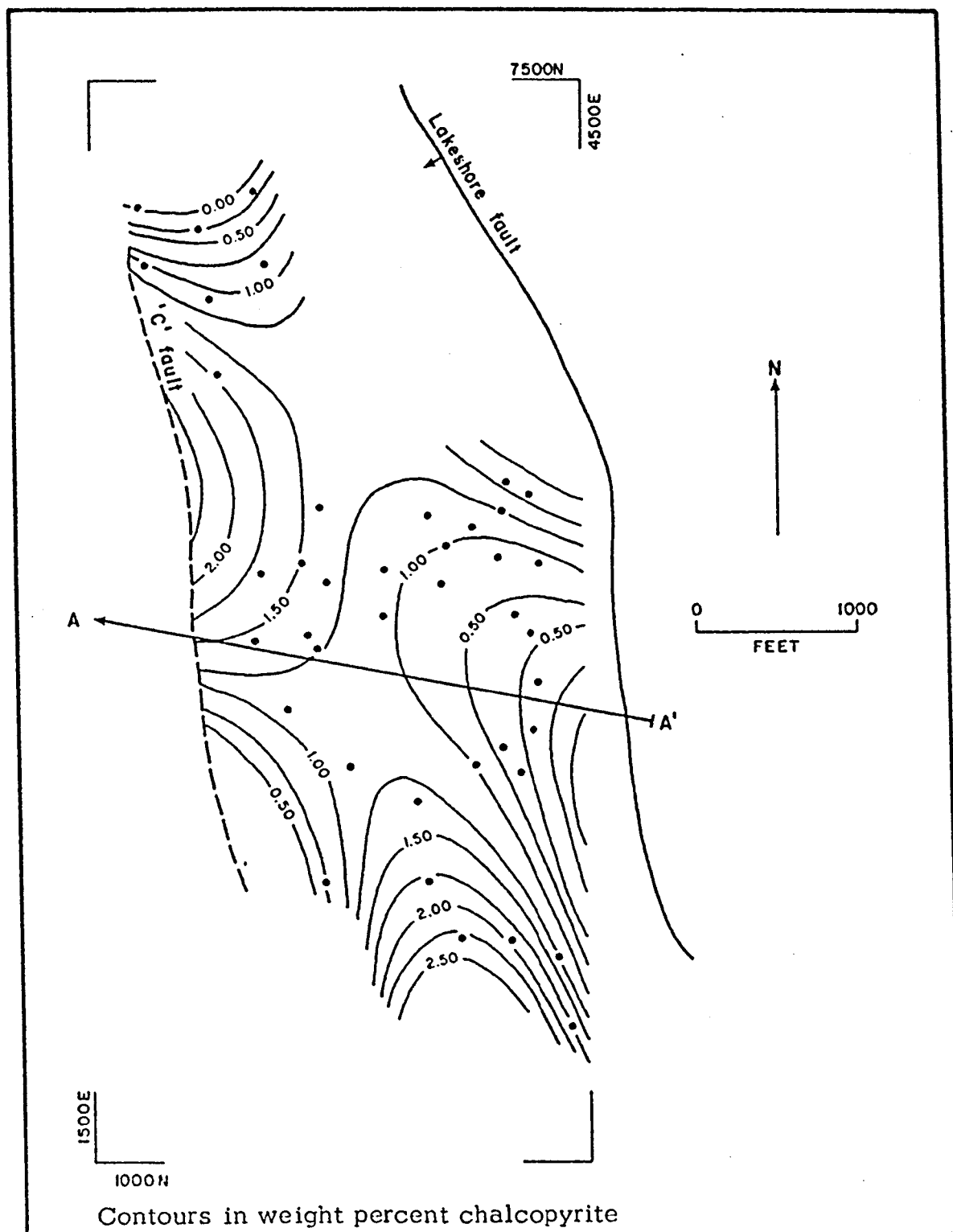


Figure 32. Zoning Pattern of Chalcopyrite in Diabase, Lakeshore Mine

Percent SS contribution: 44.77; significance level: +90%.

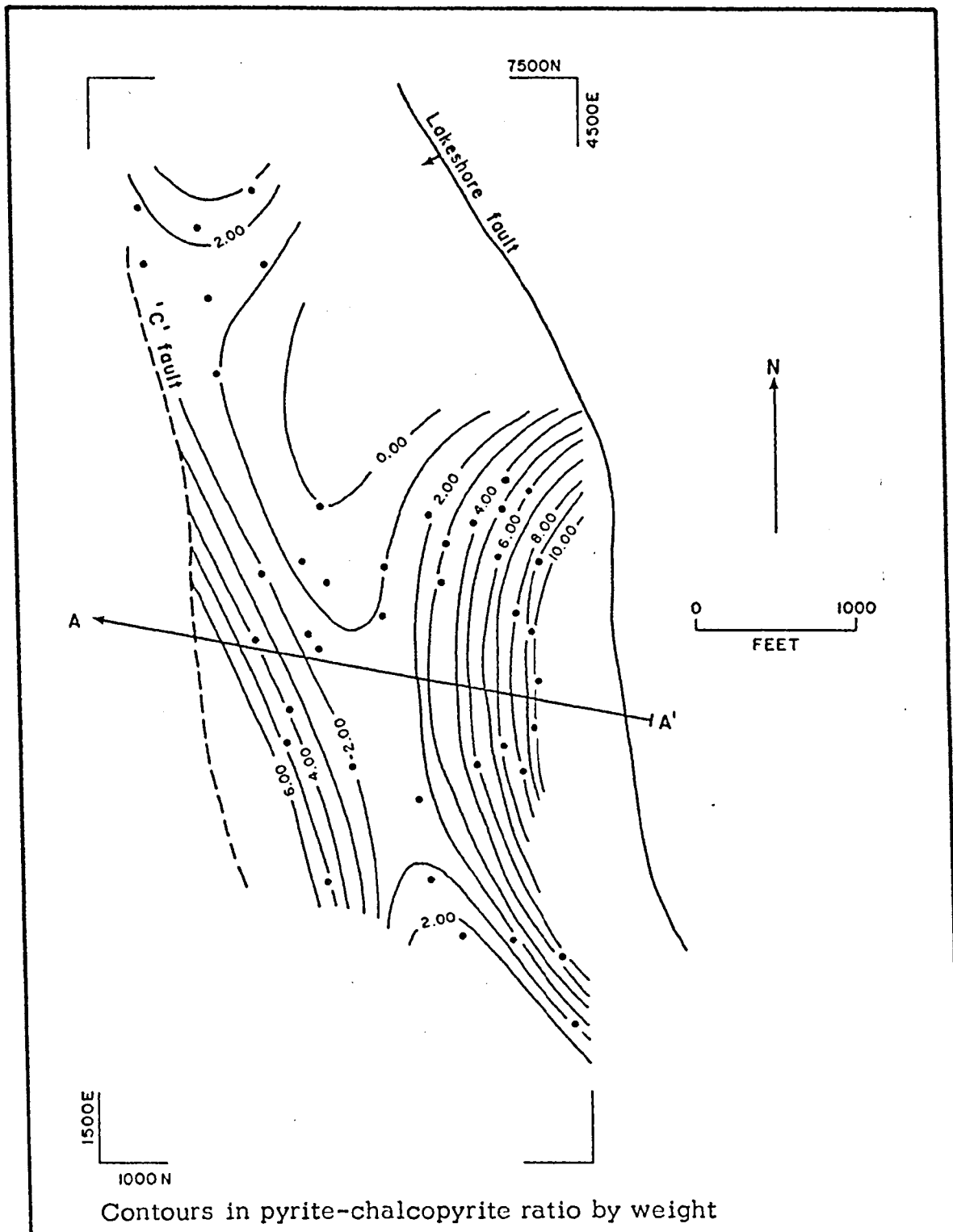


Figure 33. Zoning Pattern of Pyrite-chalcopyrite Ratio in Diabase, Lakeshore Mine

Percent SS contribution: 41.56; significance level: +90%.

a north-south elongate low flanked by high pyrite-chalcopyrite ratios to the east and west.

From the maps, the zoning pattern is apparently not too well defined in the diabase, possibly because of the discontinuous nature of the sills and dikes.

#### Sulfide Zoning by Level

The geology of the 100, 200, 300, and 400 levels of the deposit is shown in Figures 34, 35, 36, and 37, respectively. It can be seen that the Lakeshore fault and the 'C' fault form a wedge, opening upward. Within this wedge, the tactite horizon and the Dripping Spring Quartzite dip westward (Fig. 3), appearing on the level maps progressively farther east as elevation increases. The upper porphyry in the central part of the deposit has been intruded upward and to the east and occurs as a thin sliver adjacent to the 'C' fault on the 100 level and engulfs more sedimentary rocks as elevation increases occupying a considerable area in the west-central part of the map on higher levels. A large volume of upper porphyry is also in the northern part of the area. The lower porphyry is below the tactite horizon, occupying a large area in the eastern part of the deposit along the Lakeshore fault on the 100 level (Fig. 34) and occupying progressively smaller areas on higher levels as the sedimentary rocks are encountered. On the 400 level, the lower porphyry occurs only in small areas adjacent to the Lakeshore fault (Fig. 37).

The maps show a dominant northerly trend, both in the strike of the tactite horizon and the Dripping Spring Quartzite and in the strike of the Lakeshore fault and the 'C' fault.

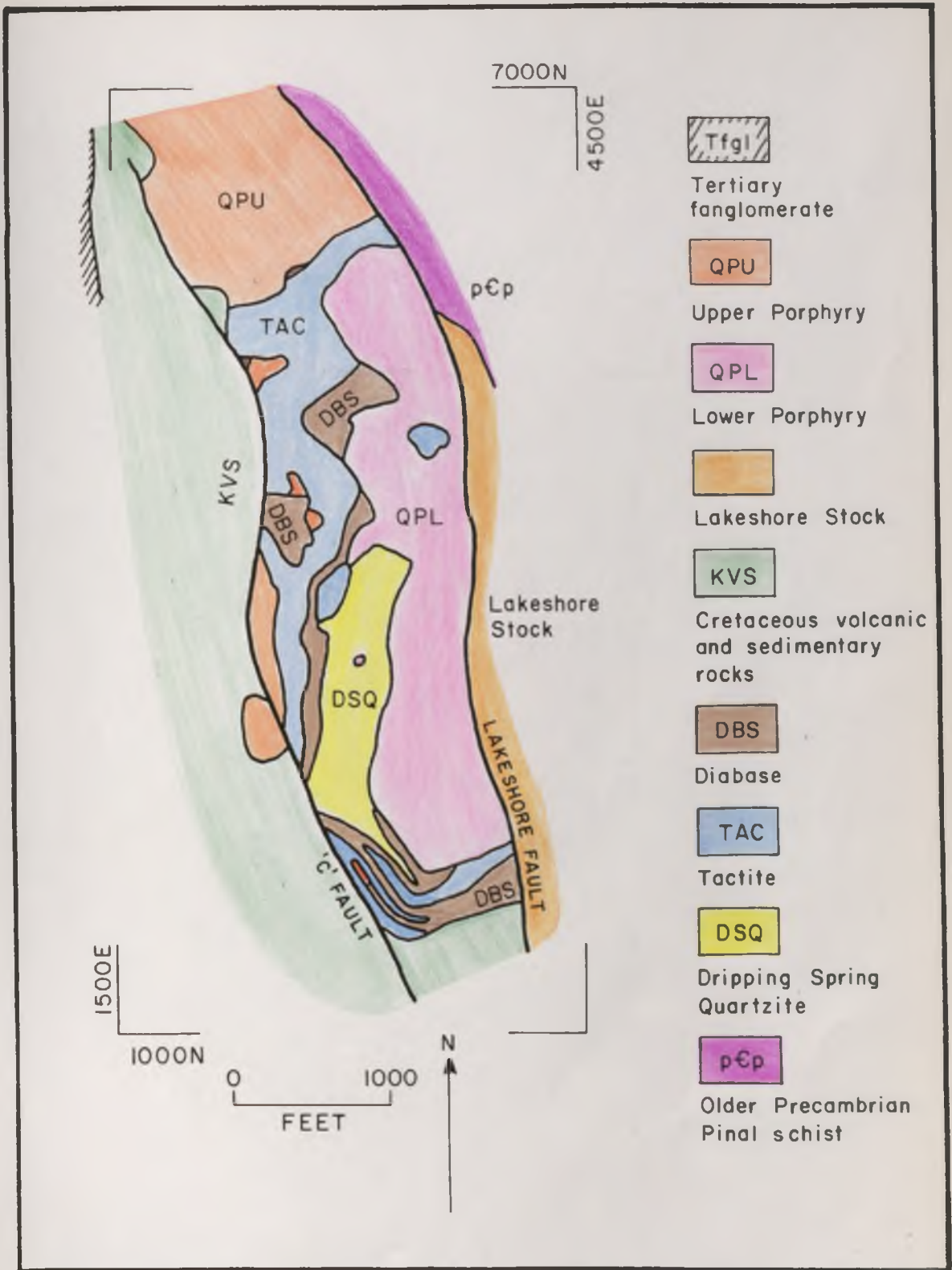


Figure 34. Geologic Map of the 100 Level, Lakeshore Mine

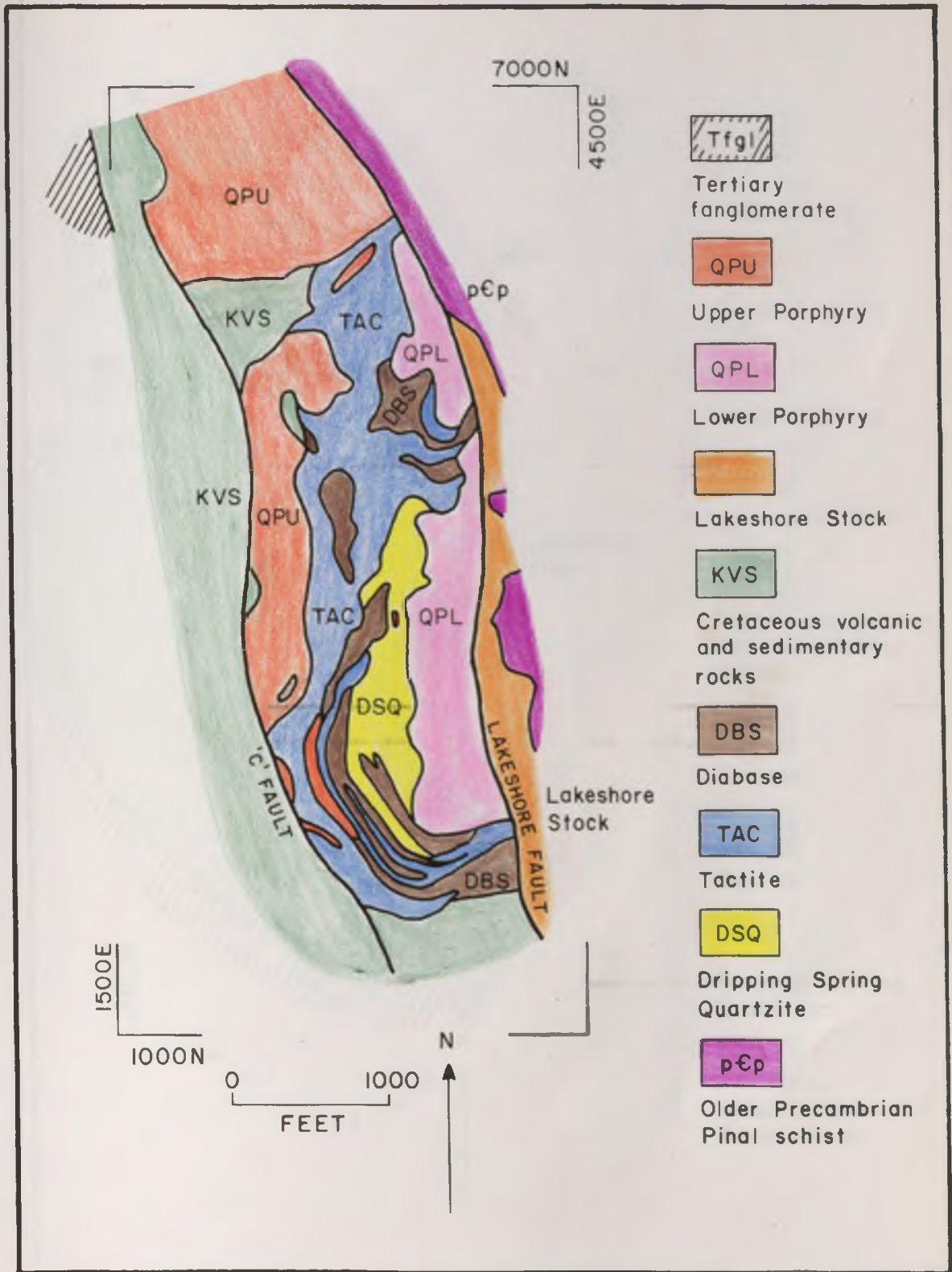


Figure 35. Geologic Map of the 200 Level, Lakeshore Mine

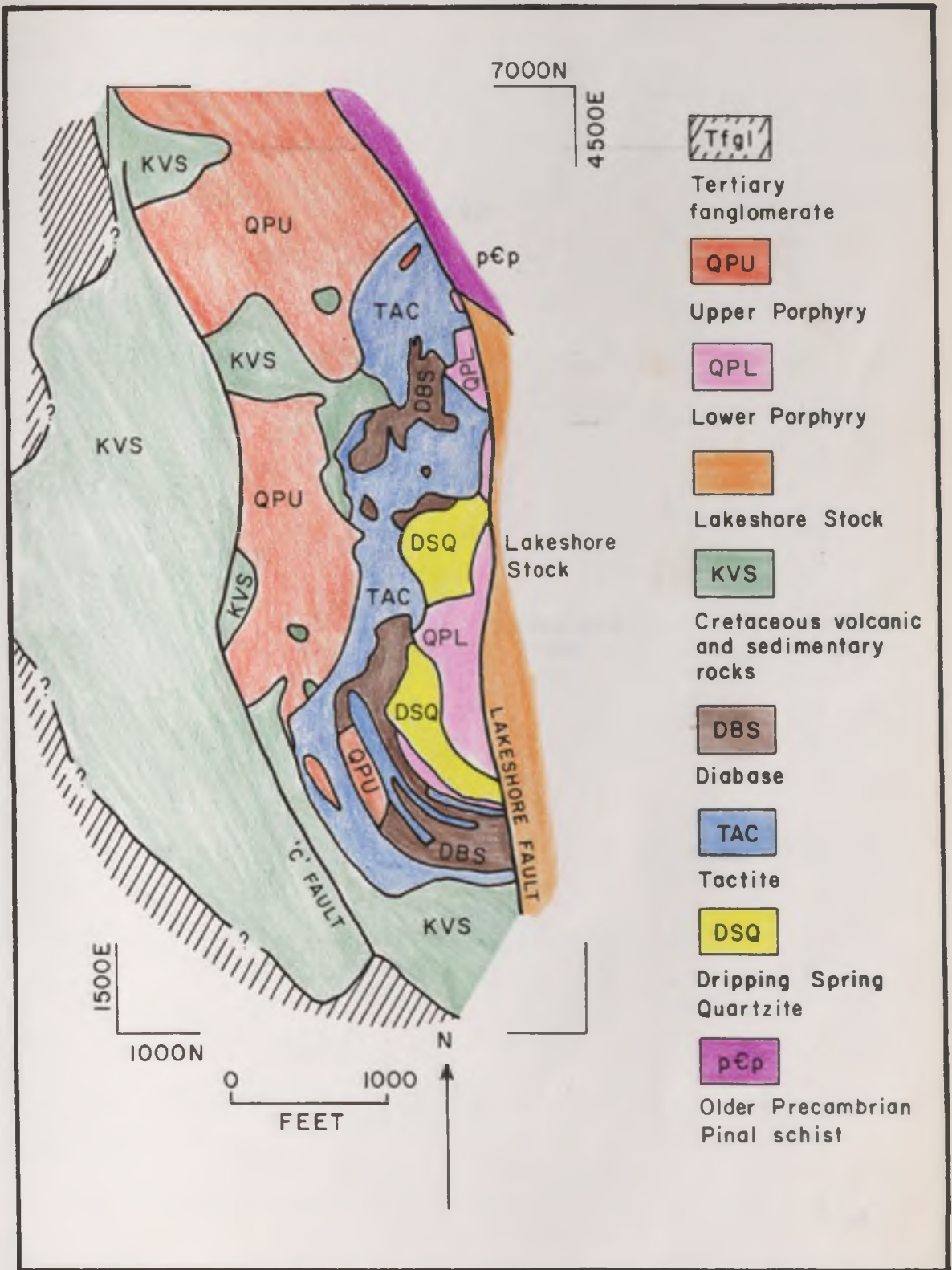


Figure 36. Geologic Map of the 300 Level, Lakeshore Mine



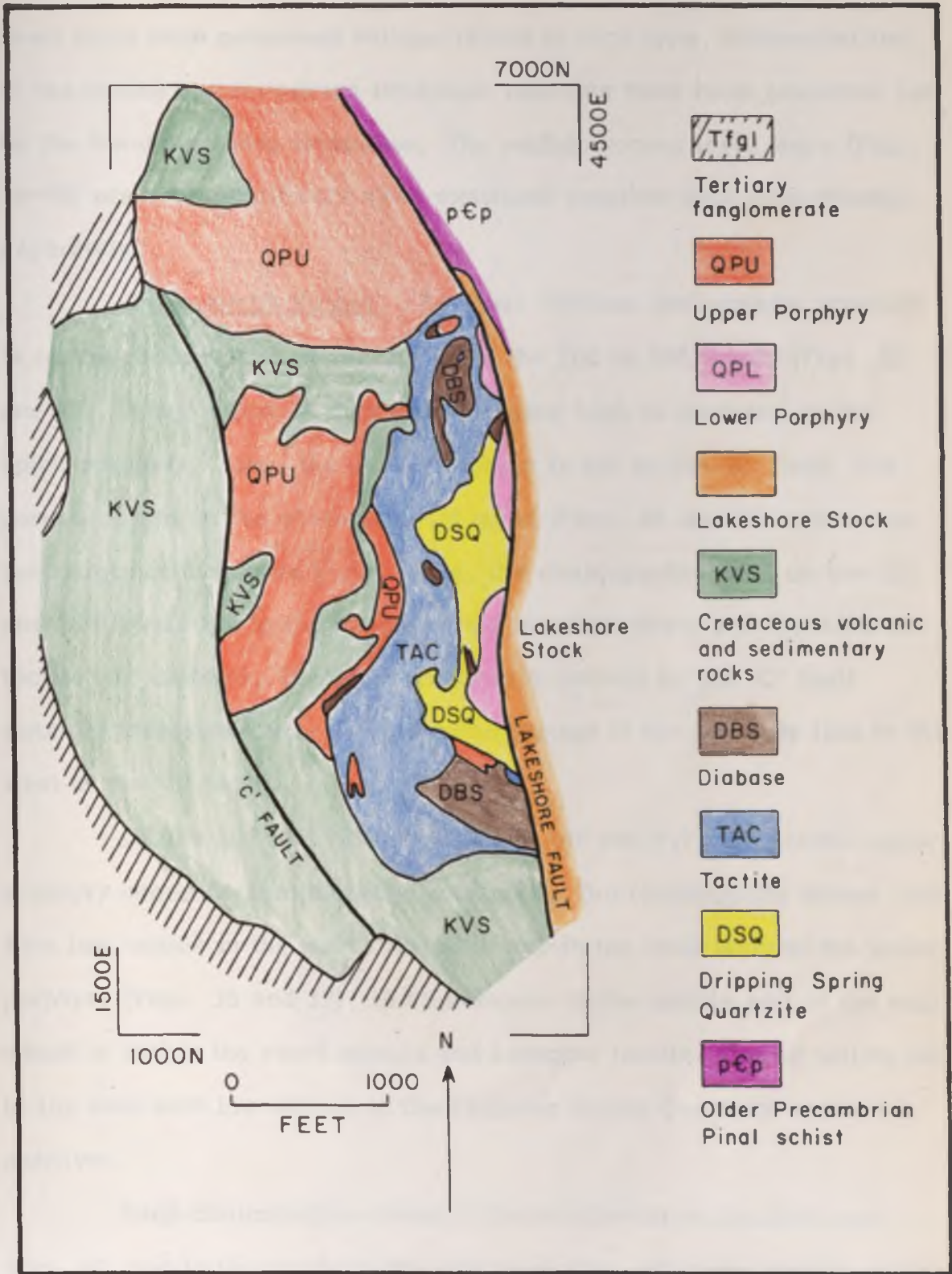


Figure 37. Geologic Map of the 400 Level, Lakeshore Mine

The rock types on any given level are quite varied. Since the level maps were generated without regard to rock type, discontinuities in the zoning pattern across lithologic contacts have been smoothed out by the trend surfacing technique. The sulfide zoning level maps (Figs. 38-49) are more significant when examined together than when treated separately.

Chalcopyrite Zoning. The most striking chalcopyrite zonation is on the chalcopyrite zoning maps for the 100 to 200 levels (Figs. 38 and 39). A concentric pattern with a copper high is centered on the upper porphyry. Since the upper porphyry is cut by the 'C' fault, the portion shown on the geologic level maps (Figs. 34 and 35) represents the margin of the entire body. Thus, the chalcopyrite highs on the 100 and 200 levels are in the margin of the upper porphyry and the adjacent tactite and diabase. The truncation of the pattern by the 'C' fault strongly indicates that a down-faulted portion of the ore body lies to the west of the 'C' fault.

On the 300 and 400 levels (Figs. 40 and 41), the central upper porphyry occupies considerably more area. The chalcopyrite values rise from low values in the west, which is within the main body of the upper porphyry (Figs. 36 and 37), to high values in the middle part of the map, which is within the stock margin and adjacent tactite, finally tailing off to the east with low values in the Dripping Spring Quartzite and lower porphyry.

High chalcopyrite values in the southwest on the 300 level (Fig. 40) and in the south on the 400 level (Fig. 41) represent the main part of the tactite horizon. On the northern part of the 400 level is a

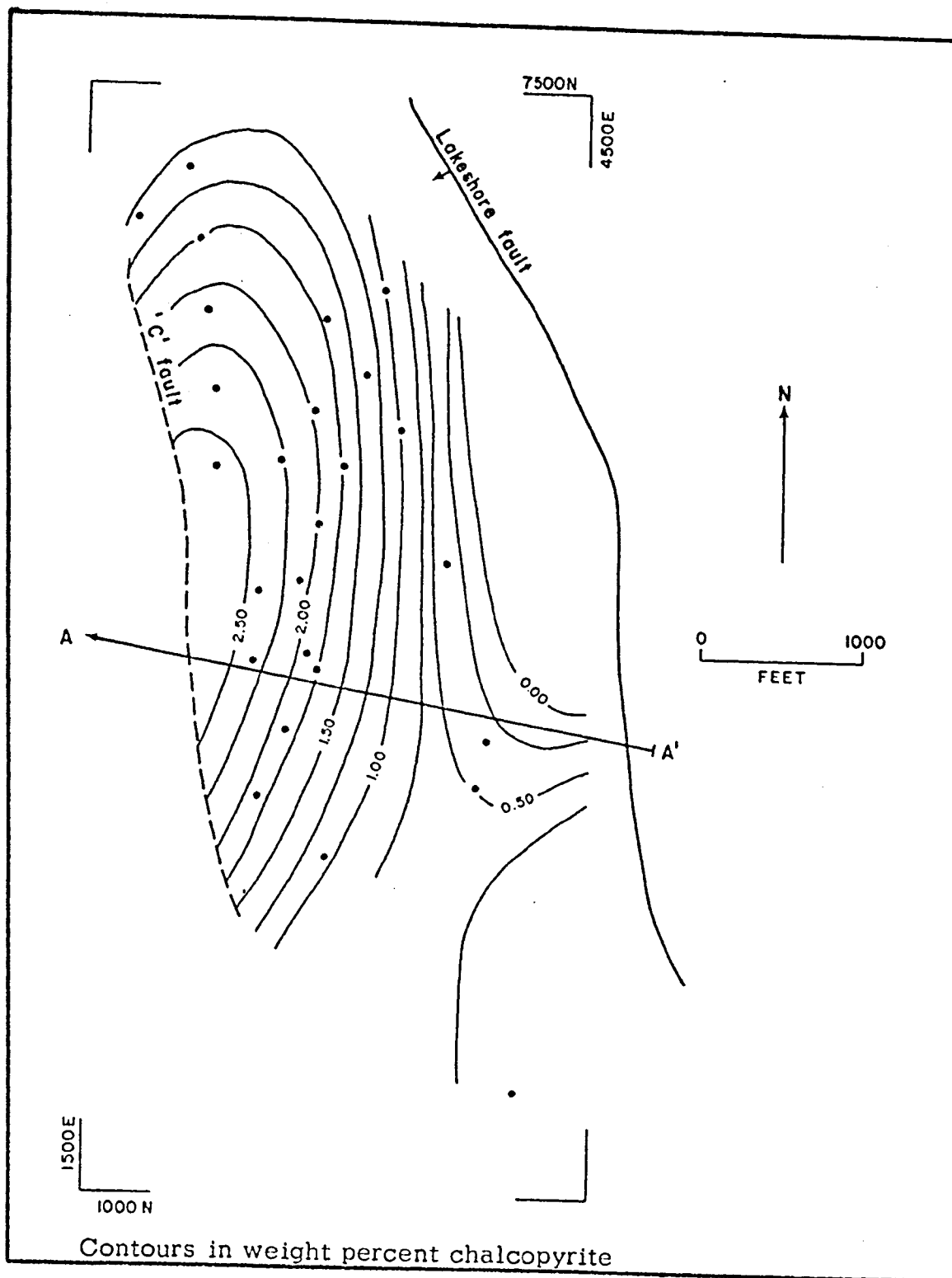


Figure 38. Zoning Pattern of Chalcopyrite in the 100 Level, Lakeshore Mine

Percent SS contribution: 52.6; significance level: +90%.

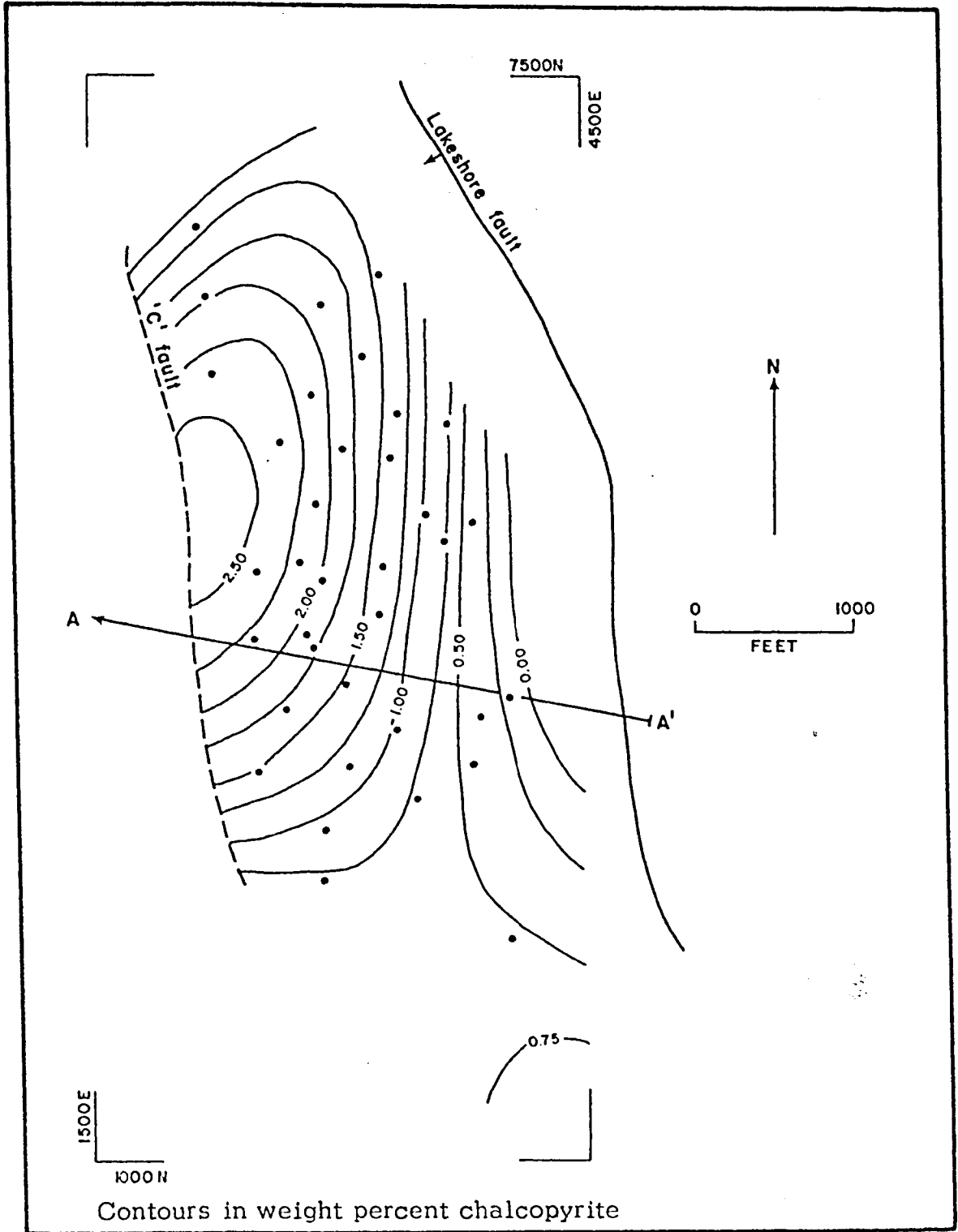


Figure 39. Zoning Pattern of Chalcopyrite in the 200 Level, Lakeshore Mine

Percent SS contribution: 34; significance level: +90%.

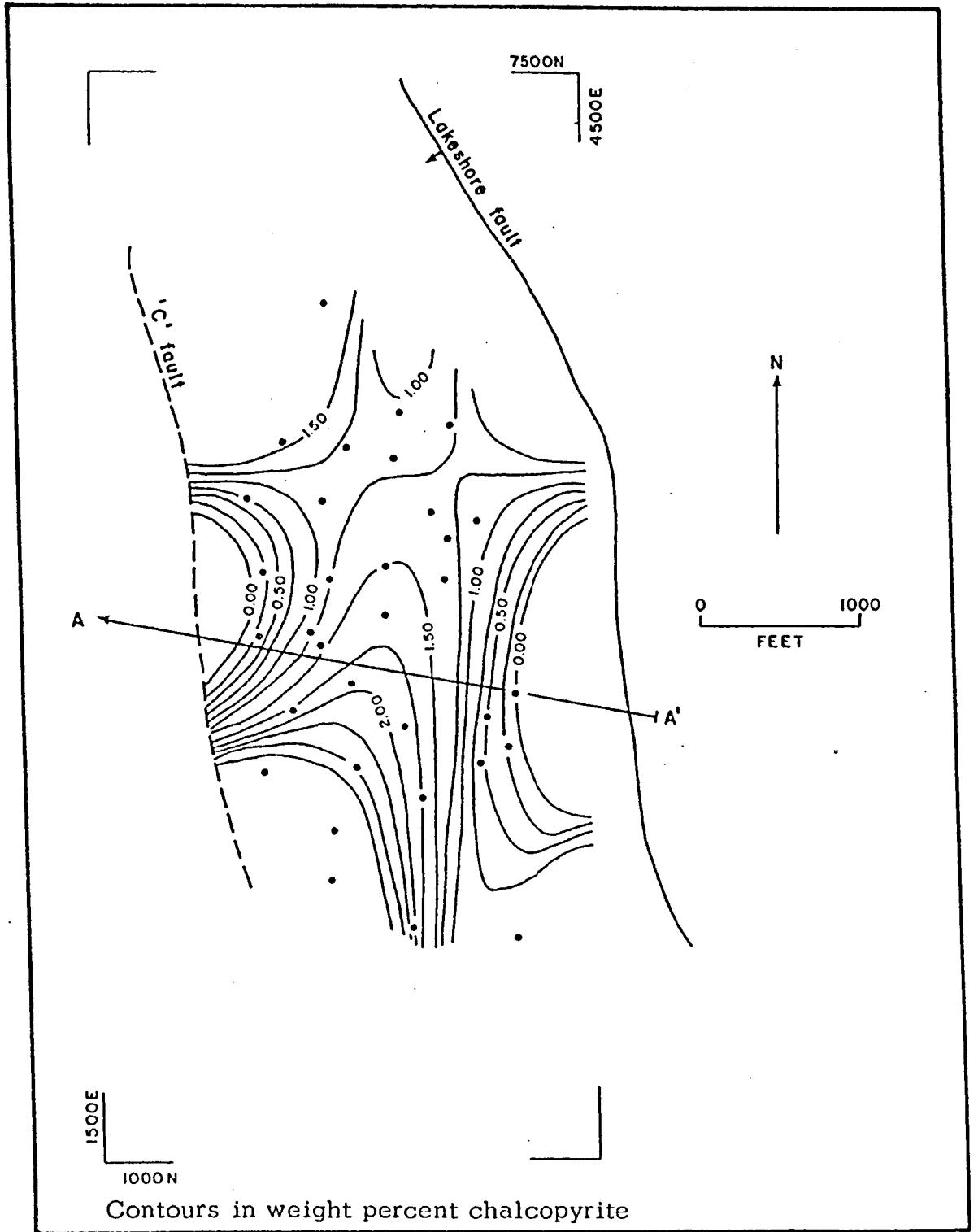


Figure 40. Zoning Pattern of Chalcopyrite in the 300 Level, Lakeshore Mine

Percent SS contribution: 38.2; significance level: +90%.

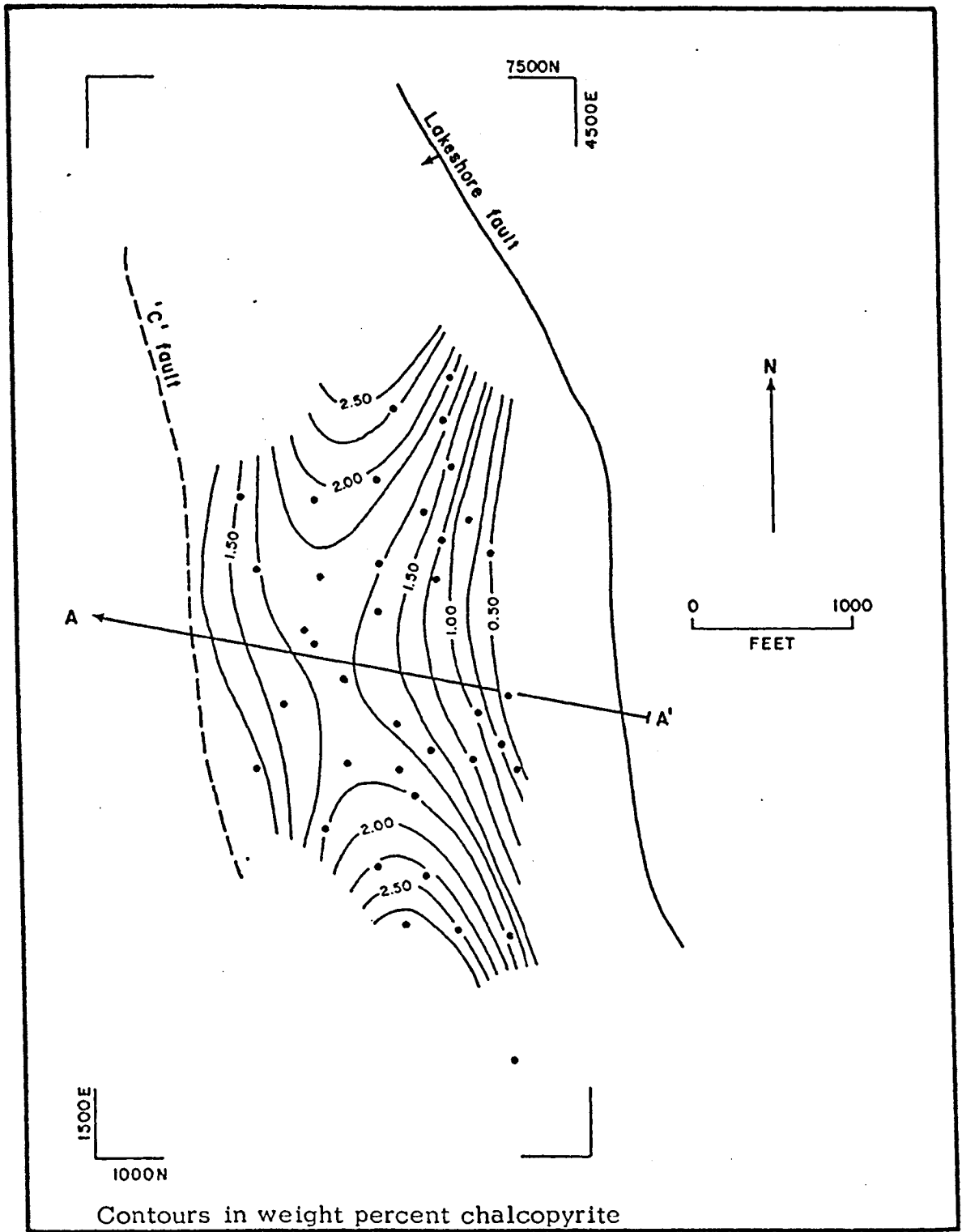


Figure 41. Zoning Pattern of Chalcopyrite in the 400 Level, Lakeshore Mine

Percent SS contribution: 99.3; significance level: +90%.

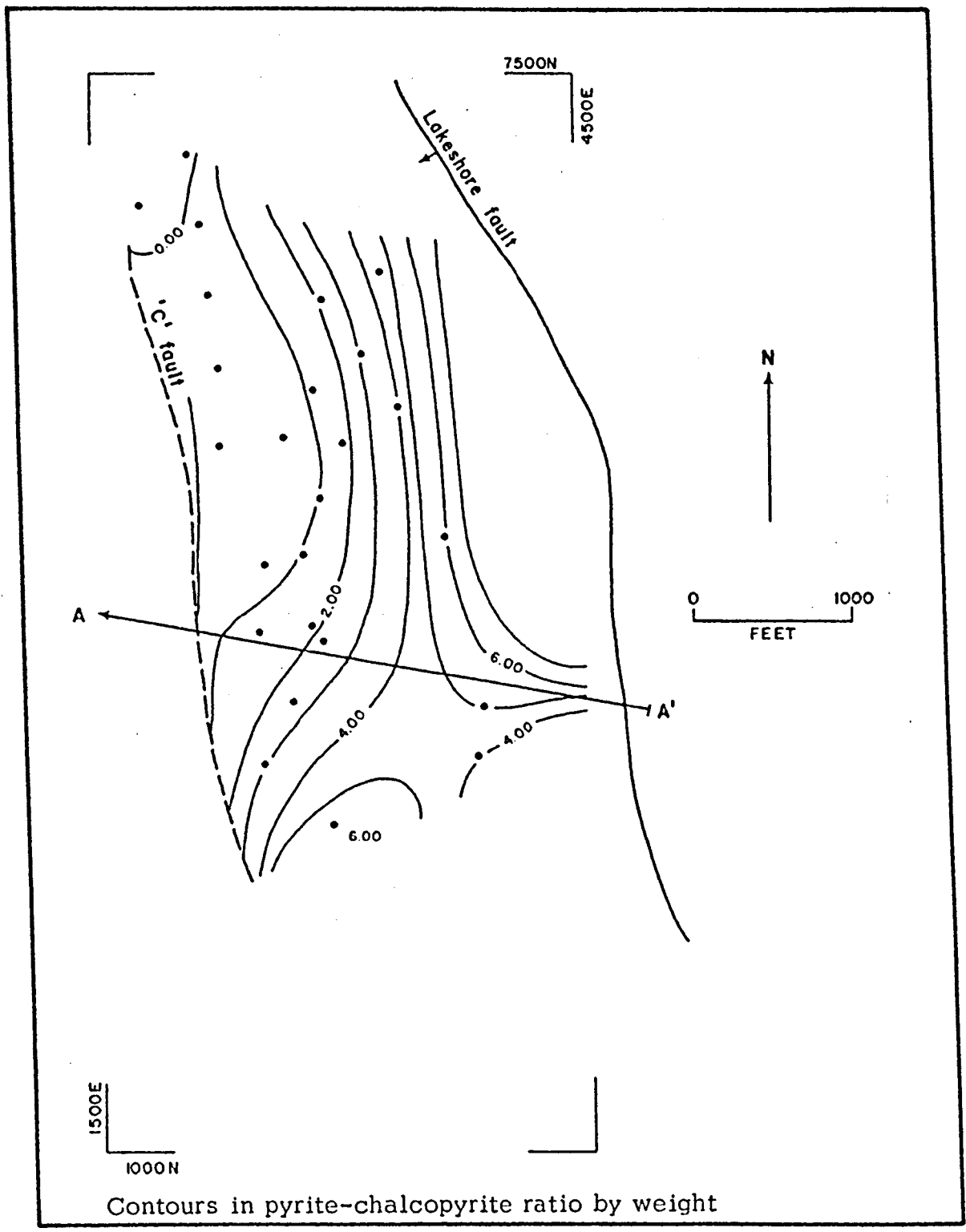
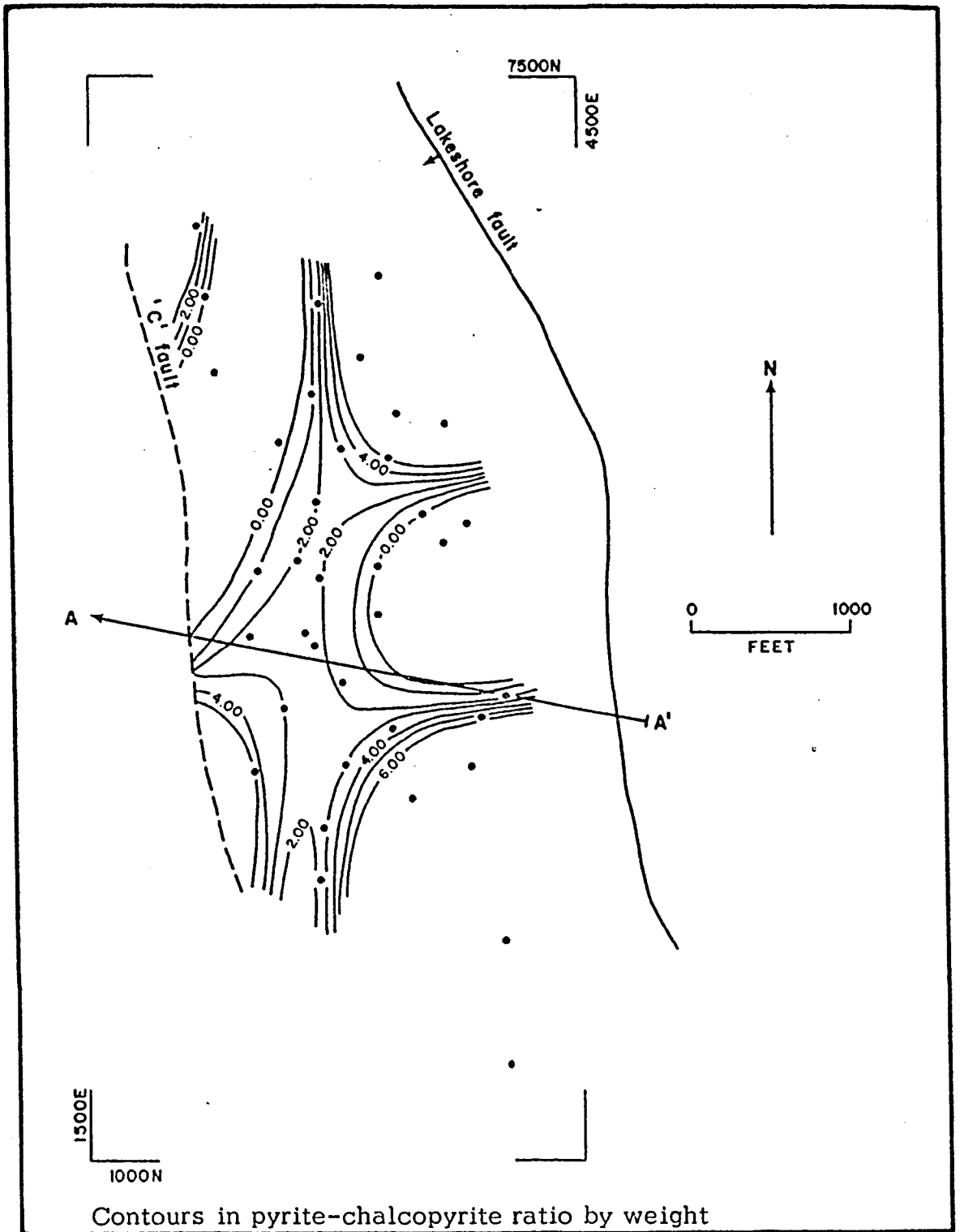


Figure 42. Zoning Pattern of Pyrite-chalcopyrite Ratio in the 100 Level, Lakeshore Mine

Percent SS contribution: 54.66; significance level: +90%.



Contours in pyrite-chalcopyrite ratio by weight

Figure 43. Zoning Pattern of Pyrite-chalcopyrite Ratio in the 200 Level, Lakeshore Mine

Percent SS contribution: 94.0; significance level: +90%.



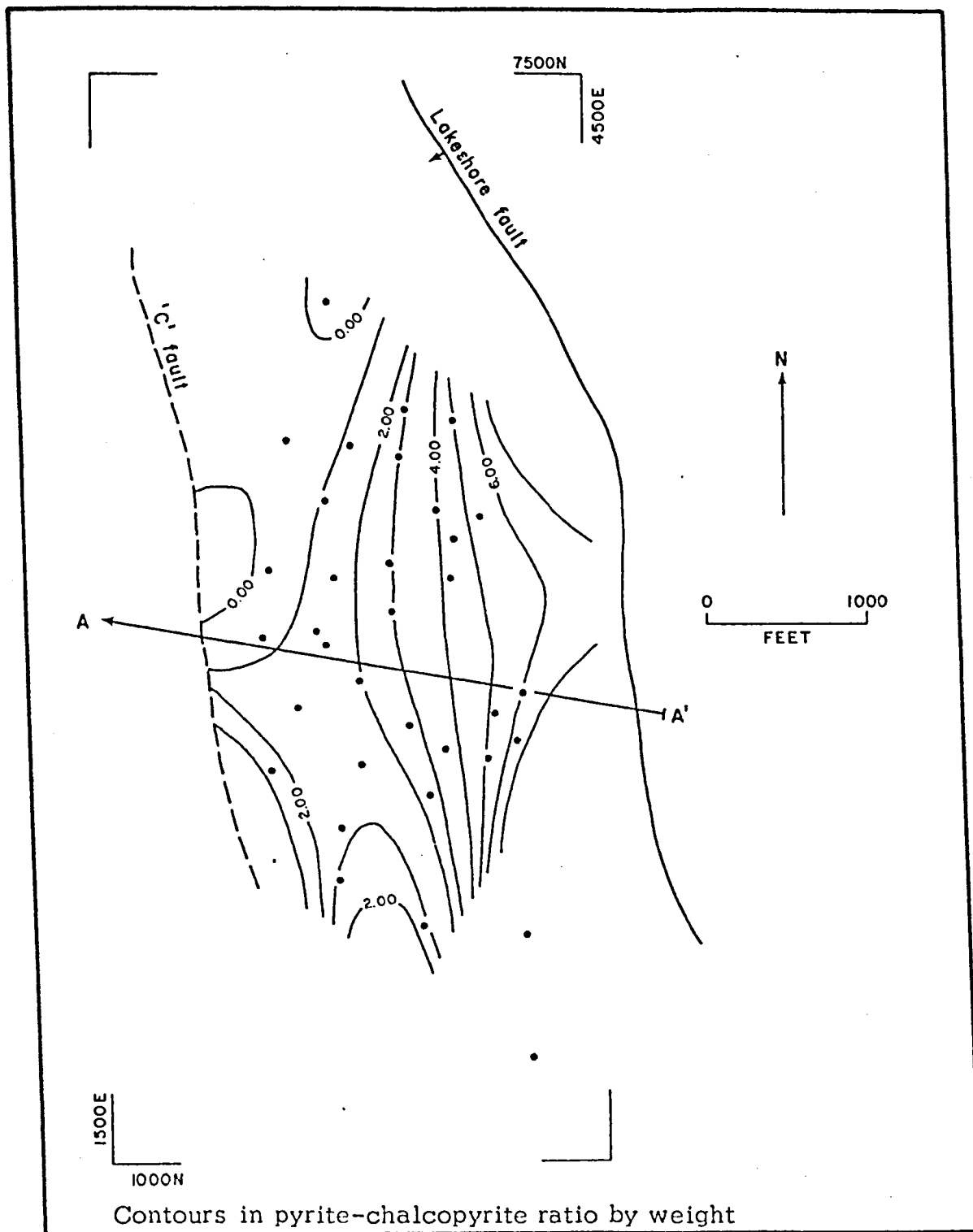


Figure 44. Zoning Pattern of Pyrite-chalcopyrite Ratio in the 300 Level, Lakeshore Mine

Percent SS contribution: 41.9; significance level: +90%.

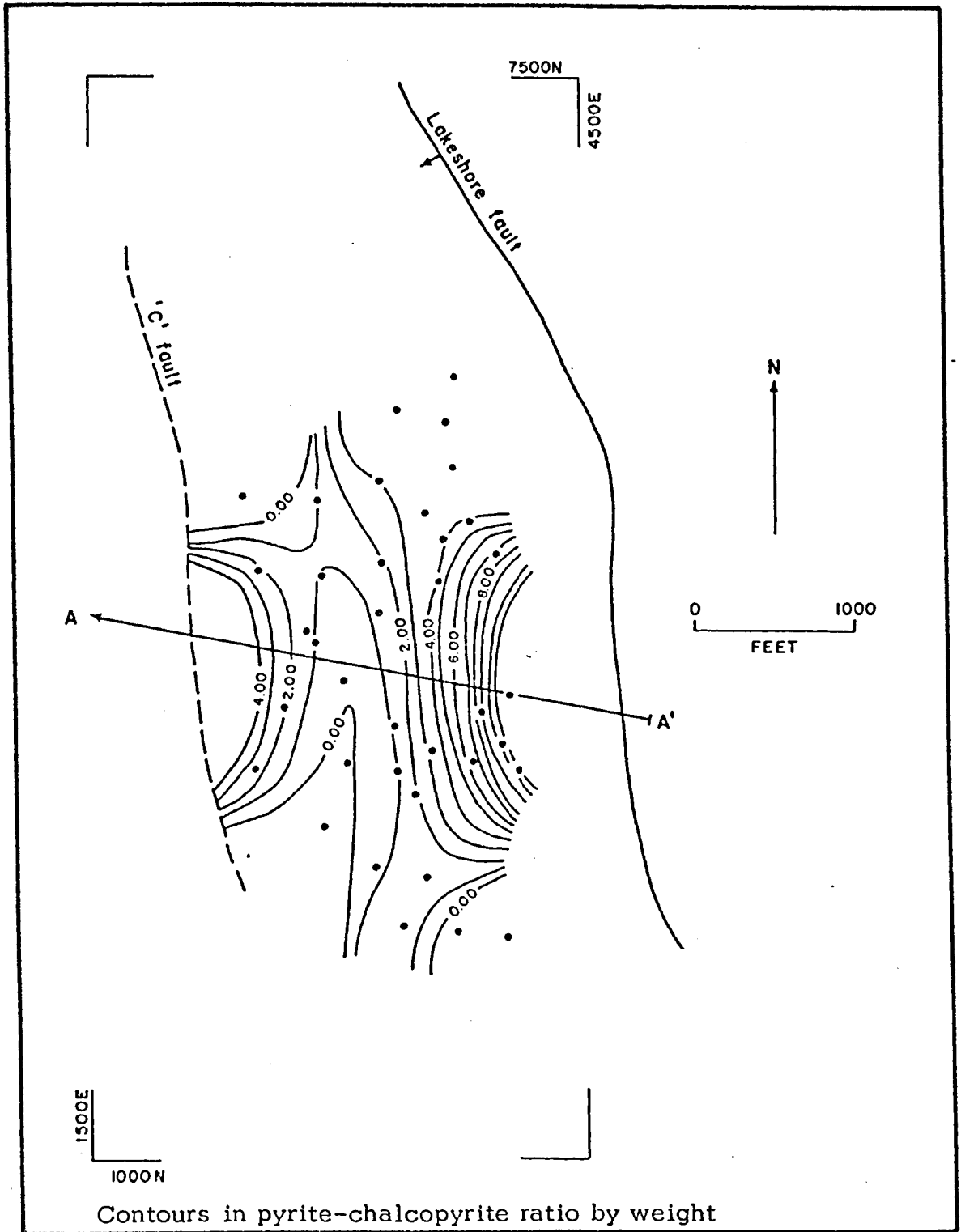


Figure 45. Zoning Pattern in Pyrite-chalcopyrite Ratio in the 400 Level, Lakeshore Mine

Percent SS contribution: 30.5; significance level: +90%.

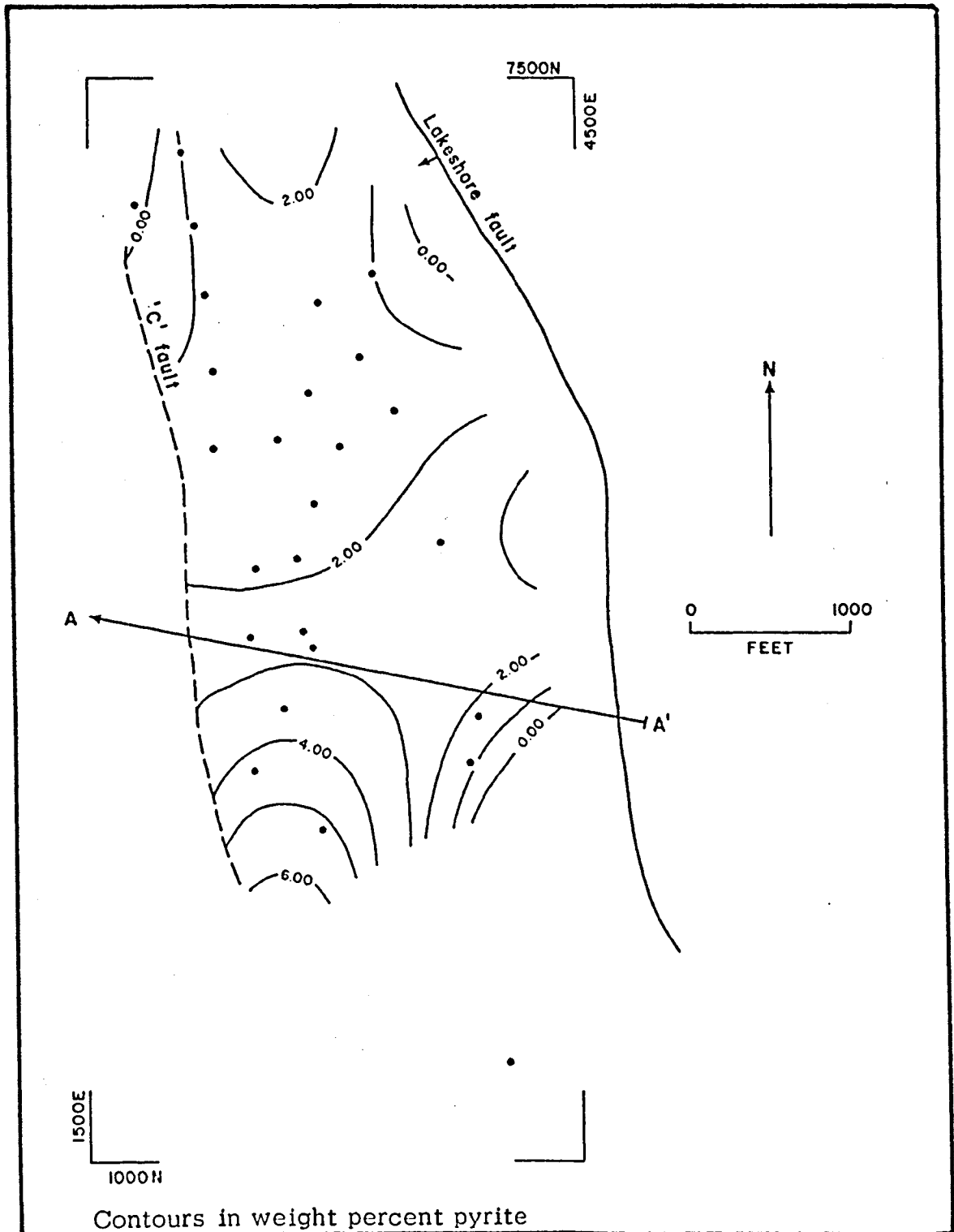


Figure 46. Zoning Pattern of Pyrite in the 100 Level, Lakeshore Mine

Percent SS contribution: 59.6; significance level: +90%.

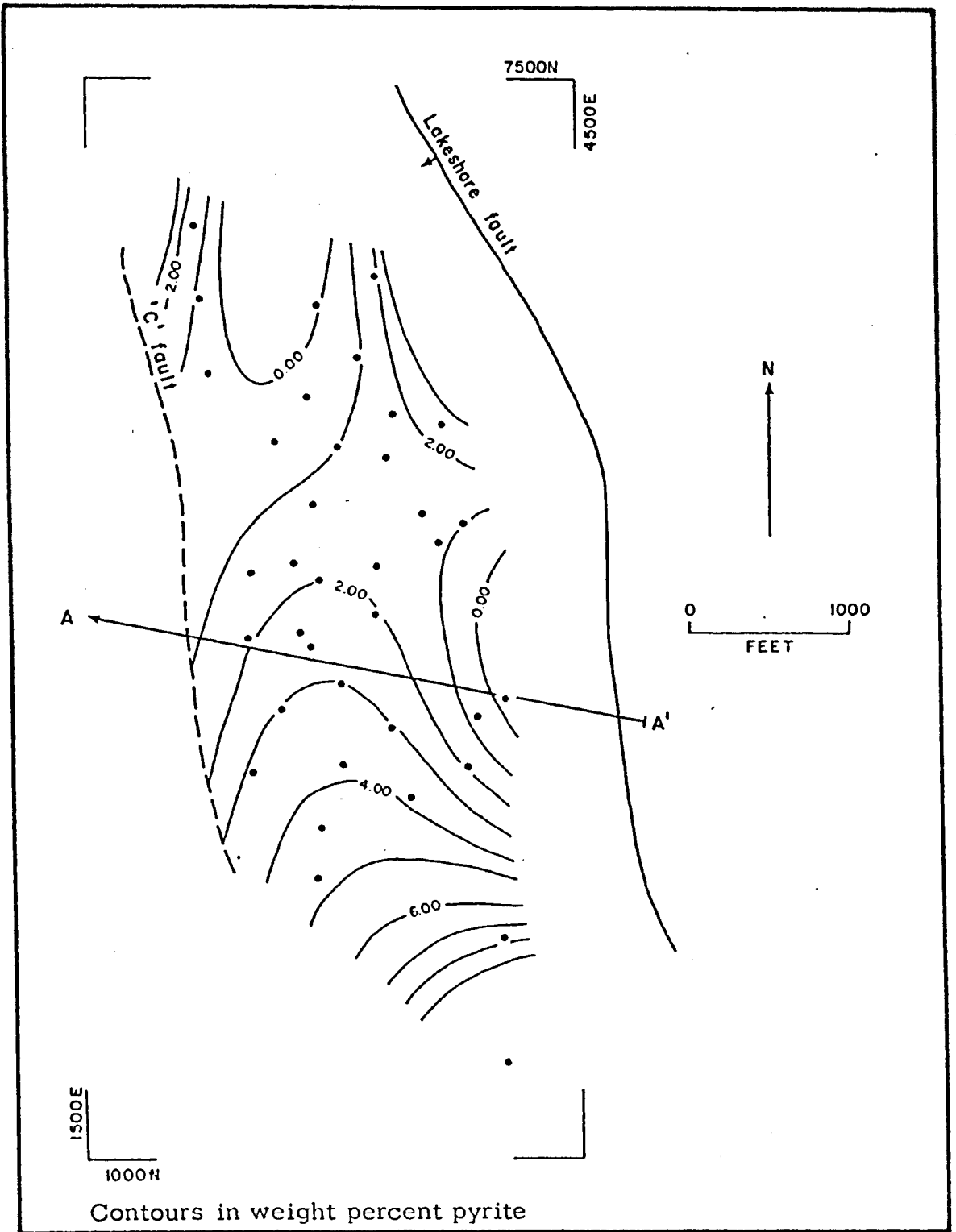


Figure 47. Zoning Pattern of Pyrite in the 200 Level, Lakeshore Mine

Percent SS contribution: 48.5; significance level: +90%.

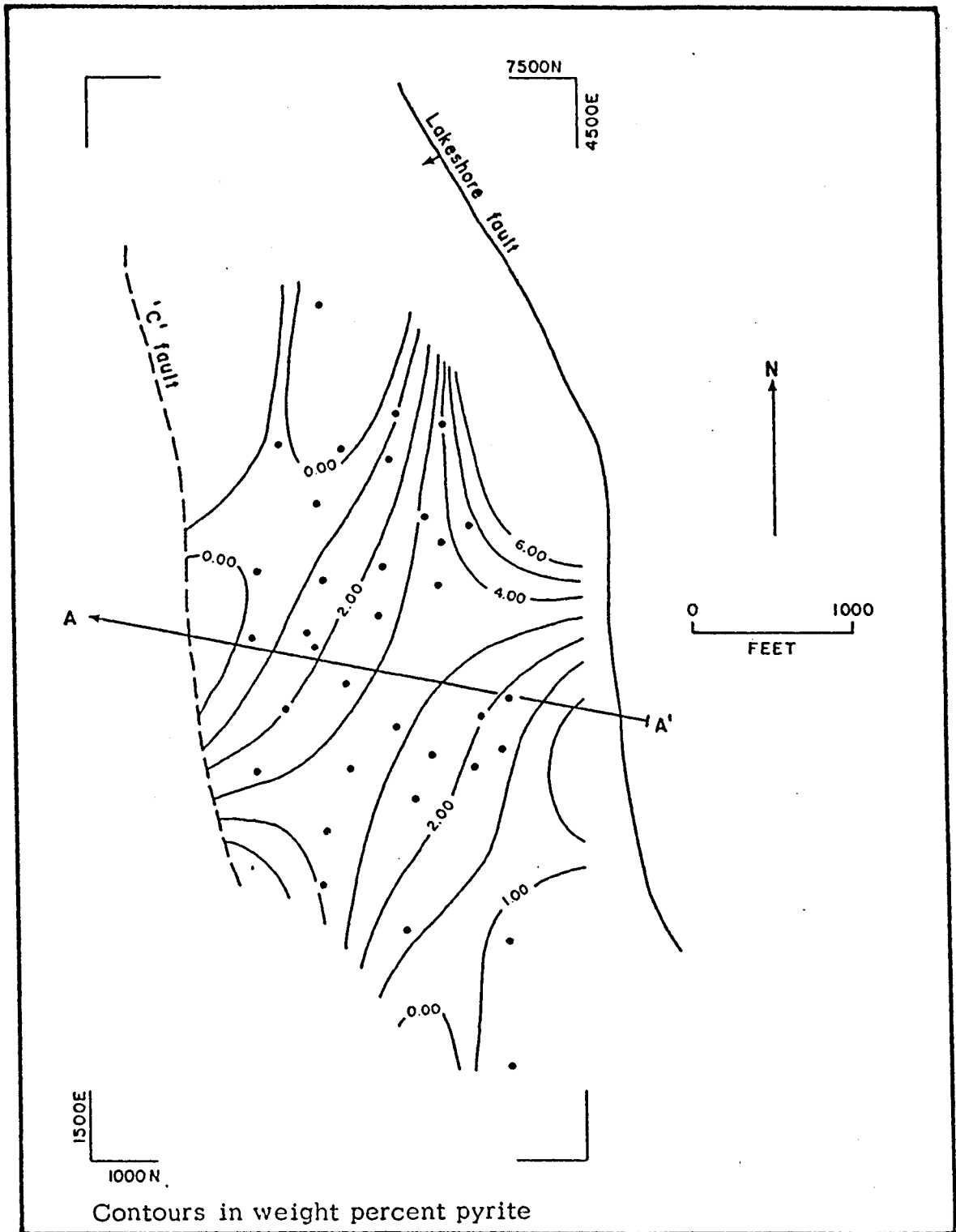


Figure 48. Zoning Pattern of Pyrite in the 300 Level, Lakeshore Mine

Percent SS contribution: 37.8; significance level: +90%.

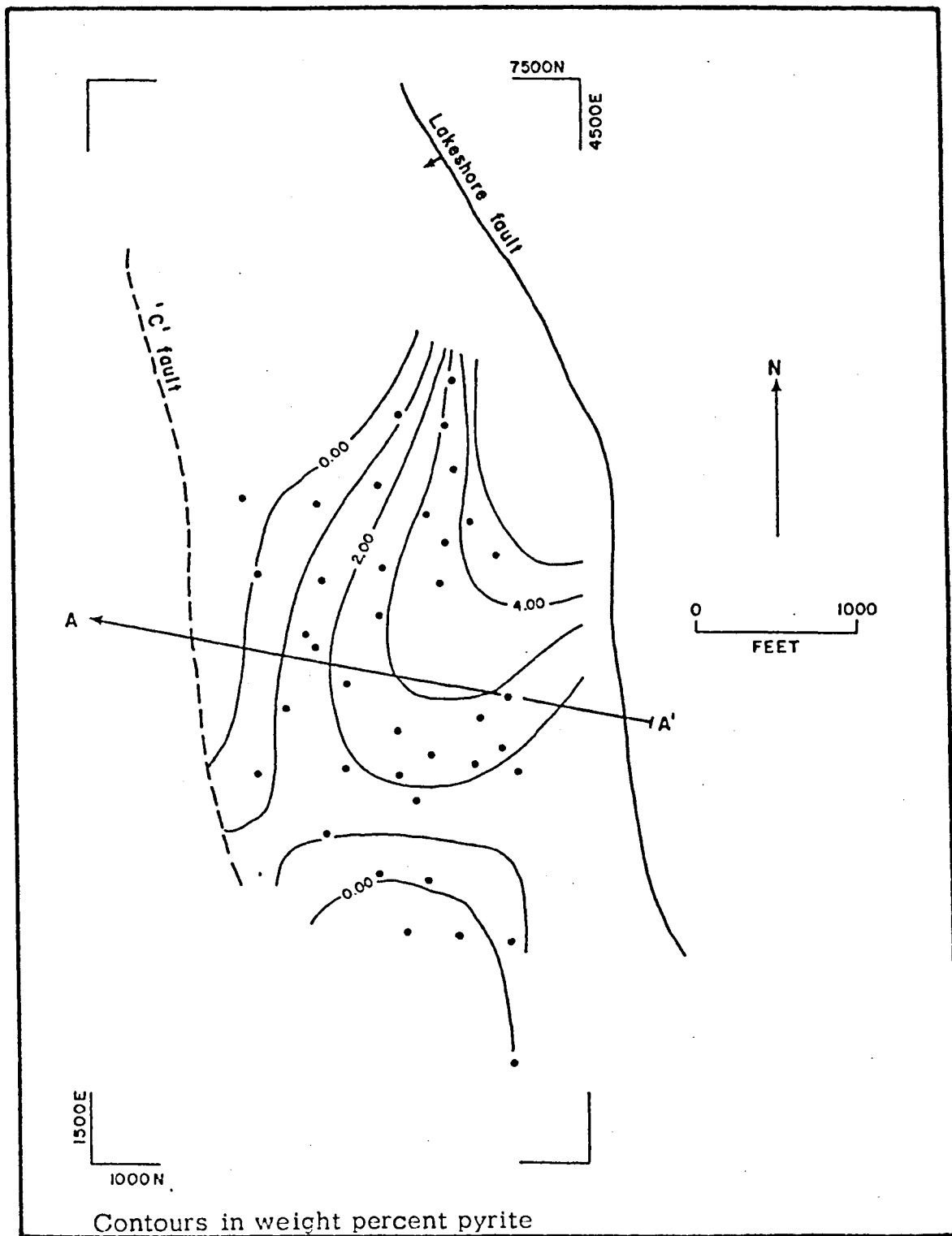


Figure 49. Zoning Pattern of Pyrite in the 400 Level, Lakeshore Mine

Percent SS contribution: 36.0; significance level: +90%.

chalcopyrite high which is probably related to the margin of the north upper porphyry body and the adjacent tactite (Fig. 37).

Pyrite-chalcopyrite Ratio Zoning. On the 100 level, the pyrite-chalcopyrite ratio is relatively uniform in the west part of the map (Fig. 42), with low values prevailing; to the east, the ratio increases.

A similar situation exists on the 200 level (Fig. 43), with a low pyrite-chalcopyrite ratio extending northward from the 'C' fault along the upper porphyry and increasing outward from the upper porphyry and the adjacent sedimentary rocks. There is a low ratio area in the east-central part of the map, but its cause is unknown.

On the 300 level (Fig. 44), there are three distinct centers of low pyrite-chalcopyrite ratios. One is to the north, centered on the body of upper porphyry in that area (Fig. 36). Another is centered on the central body of upper porphyry, and the third, to the south, is in the tactite horizon.

On the 400 level (Fig. 45), there is a saddle area of low pyrite-chalcopyrite ratios in the center of the map along the margin of the upper porphyry. To the west, in the main body of the upper porphyry (Fig. 37), the ratios rise, and the ratios also rise to the east as the Dripping Spring Quartzite and the lower porphyry are encountered.

Pyrite Zoning. The pyrite zoning pattern is not as well developed as either the chalcopyrite or the pyrite-chalcopyrite ratio zoning patterns. However, several persistent trends show up on the different levels.

The pyrite zoning pattern in the upper porphyry shows up as a persistent northeast-trending area of low pyrite values in the northwest

corners of the 200, 300, and 400 levels (Figs. 47, 48, and 49). Away from the upper porphyry (Figs. 35, 36, and 37), pyrite values increase. On the southern part of the 300 and 400 levels, low pyrite values reflect the main tactite horizon.

High pyrite values on the eastern side of the 100 level (Fig. 46) are within the main body of the lower porphyry (Fig. 34). On the 200 and 300 levels, low pyrite values prevail in the same area as the high pyrite values on the 100 level where the margin of the lower porphyry is approached, and the values rise on the 400 level as the Apache Group rocks, notably the Dripping Spring Quartzite, are encountered.

#### Summary of Sulfide Zoning Patterns at the Lakeshore Mine

The sulfide zoning at Lakeshore is related to the quartz monzonite porphyry, being centered on that body and extending into the adjacent Cretaceous volcanic and sedimentary rocks and the tactite horizon. The zoning pattern in the diabase is irregular, due to the discontinuous nature of the sills and dikes. Although the Dripping Spring Quartzite and the lower porphyry are only weakly mineralized, they still exhibit fair zoning patterns.

Because the pyrite-chalcopyrite ratio apparently is the most sensitive indicator of sulfide zoning, the zoning patterns of the pyrite-chalcopyrite ratios for the different rock types and for the different levels are briefly summarized. In all the maps, the significance level of the pyrite-chalcopyrite ratio zoning pattern is greater than 90 percent, whereas the significance level is considerably less than 90 percent for some of the individual pyrite and chalcopyrite maps.



Overall Zoning Pattern. A pyrite-chalcopyrite ratio low is centered on the upper porphyry, with rising values outward indicating a pyrite halo.

Upper Porphyry. The pyrite-chalcopyrite ratio is low in the central part of the upper porphyry and increases to the north and south. The ratio is lowest in the east-central margin of the upper porphyry.

Lower Porphyry. The pyrite-chalcopyrite ratios are low to the north, southeast, and southwest and are high to the south, northeast, and northwest. This pattern is difficult to interpret, but it may be explained if the lower porphyry were the root zone of the deposit in which ore-forming solutions were dominantly ascending rather than moving laterally. The areas of low ratios could represent main areas of solution ascension in which pressures and temperatures were relatively high, preventing pyrite deposition but allowing chalcopyrite deposition.

Cretaceous Volcanic and Sedimentary Rocks. The pyrite-chalcopyrite ratio is low in the Cretaceous volcanic rocks in the central part of the deposit in the area adjacent to the upper porphyry. In the western part of the map area, the upper porphyry has cut out the Cretaceous rocks. The zoning pattern is controlled by the contact between the upper porphyry and the Cretaceous volcanic and sedimentary rocks, being centered on the upper porphyry and rising from low ratios in the Cretaceous volcanic and sedimentary rocks adjacent to the upper porphyry to high values away from the upper porphyry.

Tactite. The pyrite-chalcopyrite ratios are lowest in the southern part of the map area in the main area of chalcopyrite mineralization of the tactite horizon. To the north, the pyrite-chalcopyrite

ratios remain fairly uniform but rise to the east and west away from the area in which the upper porphyry has intruded.

Dripping Spring Quartzite. Although the Dripping Spring Quartzite is a relatively nonreactive unit, a well-formed pyrite-chalcopyrite ratio low is centered between the Lakeshore fault and the 'C' fault. This low is below the upper porphyry and may be due to a lateral spreading of ascending ore solutions from the lower porphyry.

Diabase. A north-northwest-trending pyrite-chalcopyrite ratio low runs through the map area, with rising values to the east and west. The diabase occurs mainly in the tactite horizon, and sulfide deposition within the tactite horizon may control sulfide deposition within the diabase. The lows to the south and northeast in the diabase roughly correspond to lows in the tactite horizon.

Level Maps. The level maps show low pyrite-chalcopyrite ratios prevailing on the west side of the map area and increasing eastward. The central body of the upper porphyry moves eastward as higher levels are encountered, occupying only a small area adjacent to the 'C' fault on the 100 level but occupying a considerable area in the central part of the deposit on the 400 level. The pyrite-chalcopyrite ratio pattern is similarly shifted to the east at higher elevations. This shift indicates that the low ratios are in the upper porphyry and adjacent rocks and that the ratio increases outward away from the margin of the upper porphyry. With the exception of the 300 level, the northern body of upper porphyry does not seem to have much effect on the ratios, and it is inferred that the main mineralization is related to the central body of the upper porphyry.

## COMPARISON OF ZONING AT LAKESHORE WITH HYPOTHETICAL ZONING IN PORPHYRY COPPER DEPOSITS

As mentioned previously, idealized zoning patterns have been determined for the porphyry copper deposits as a class. Lowell and Guilbert (1970) have done extensive work at the San Manuel-Kalamazoo deposit. At this deposit, a Laramide monzonite porphyry has intruded the Precambrian Oracle Granite. Copper mineralization is associated with the Laramide monzonite porphyry.

The uniform lithology of the Oracle Granite host rock, which is really a quartz monzonite, allowed the Laramide porphyry to establish pressure and temperature gradients and to develop excellent zoning exemplary among the porphyry ore deposits. By examining the San Manuel-Kalamazoo deposit and comparing it with twenty-six other major porphyry ore deposits, Lowell and Guilbert have arrived at a consistent picture of zoning in porphyry ore deposits.

Porphyry ore deposits form from granitic intrusions which have been emplaced at shallow depths, 5,000 to 10,000 feet. The intrusions, which are generally stock-like, begin to cool from the surface, establishing pressure-temperature gradients as standing forms, rather than as advancing fronts (Lowell and Guilbert, 1970).

The mineral zoning pattern at the San Manuel-Kalamazoo deposit is shown in Figure 50. This pattern is typical of the porphyry copper deposits. As can be seen, a low-grade core occurs in the mineralizing porphyry. In the margin of the porphyry and the adjacent wall

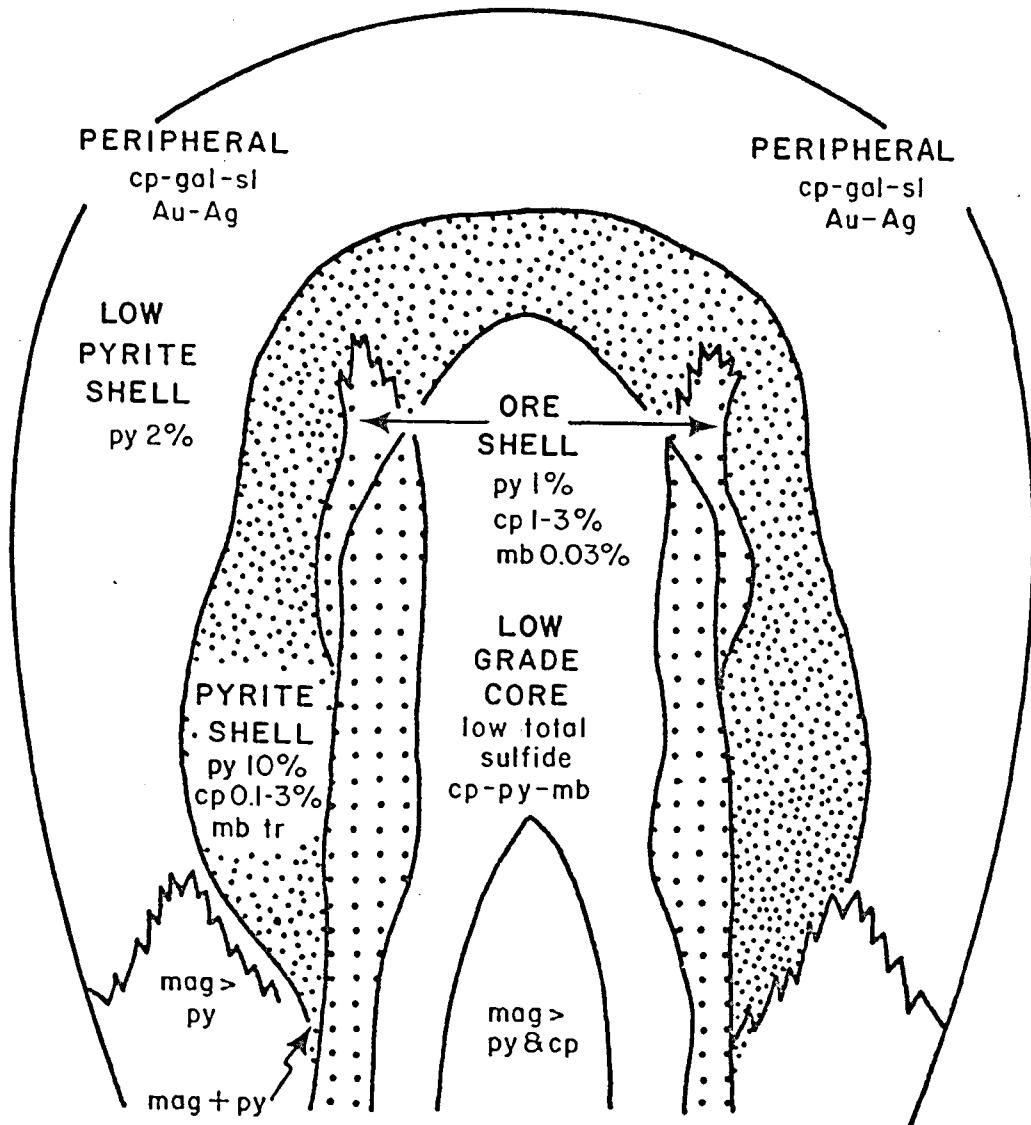


Figure 50. Sulfide Zoning at the San Manuel-Kalamazoo Deposit. --From Lowell and Guilbert (1970, p. 379)

rocks is an ore shell, and surrounding the ore shell is a pyrite halo. This agrees with Rose's (1970, p. 920) description of sulfide zoning in porphyry copper deposits: "The hypogene sulfides are also zoned, from a central zone with low pyrite/chalcopyrite ratio and generally low sulfides, through a zone of moderate sulfides with dominant chalcopyrite, then to a halo of high pyrite/chalcopyrite and high total sulfides which grades outward to lower total sulfides."

A. H. James (1971) has described the geology of several porphyry copper deposits and has inferred that hypogene sulfide mineralization occurs as an inverted cup, crosscutting the regional host rock and the upper consolidated portions of the source intrusion, extending downward around a deeper barren core.

The zoning pattern at Lakeshore agrees well with the hypothetical patterns described by Rose (1970), A. H. James (1971), and Lowell and Guilbert (1970). The upper porphyry has a low-grade core, with increasing chalcopyrite occurring on the margin of the upper porphyry. Figure 12, the chalcopyrite map within the upper porphyry, shows the chalcopyrite as being highest on the southeast margin of the body. Chalcopyrite is also high in the Cretaceous volcanic and sedimentary rocks and the tactite horizon immediately adjacent to the upper porphyry. A pyrite halo surrounds the upper porphyry, and mineralization drops off away from the upper porphyry and in the nonreactive Dripping Spring Quartzite.

Although the core of the upper porphyry at Lakeshore is low grade, it does have some copper mineralization, whereas the lower porphyry is essentially barren throughout. Therefore, the upper porphyry

may represent the mineralized upper consolidated cupola of the source intrusion, as inferred by A. H. James (1971). Ore fluids originated in the lower porphyry and moved upward and outward, establishing pressure-temperature gradients about the porphyry mass as a whole and deposited sulfides in the margin of the porphyry and the surrounding rocks. The concentric zoning indicates that fluids migrated outward from the upper porphyry in response to the pressure-temperature gradients and that the influence of the wall-rock lithology in controlling zoning was secondary, except for the highly reactive Mescal Limestone, which formed the tac-tite horizon. The north-northwest trend is probably due to structural control, but the exact cause is unknown.

## APPENDIX

### TREND SURFACE ANALYSIS

The chalcopyrite, pyrite, and pyrite-chalcopyrite ratio maps presented in this thesis were generated by applying a double-Fourier trend surface analysis to the assay data. This appendix discusses this method of analysis in detail and is provided for those readers who want to gain a deeper understanding of how the zoning maps were developed. It is also hoped that this discussion will provide a clear explanation of the trend surface technique for those who may have problems to which the technique may apply. Double-Fourier trend surface analysis may be used to generate contour maps of any set of irregularly spaced data.

The double-Fourier trend surface analysis, which was done with the University of Arizona CDC 6400 computer, is a mathematical surface-fitting technique which uses the least-squares criterion to fit a surface to a set of data points. In this study, three different sets of data points were generated, one each for observed values of chalcopyrite, pyrite, and pyrite-chalcopyrite ratio, and maps were generated using these three sets of data.

A double-Fourier series is an equation for a surface. The observed value of, say, chalcopyrite at a given point is used along with all the observed values at other points to calculate coefficients to the Fourier series. The north and east coordinates of a particular point may then be used as independent variables and be substituted into the Fourier

series with the coefficients obtained from the observed values. This substitution will yield a trend value of chalcopyrite at those coordinates. A map is generated by doing this for successive coordinate points.

A double-Fourier series is only one of many equations which may be used. Any equation involving two independent variables may be used to generate a surface, the two independent variables being the coordinates of a point on the surface and the dependent variable being the data value at that point. Surface fitting is often performed with polynomial equations rather than Fourier series. The fitting technique involves finding the coefficients to whatever equation is used. To do this, the least-squares criterion is used. Using this criterion, the computed surface passes through, above, or below a given observed value. There is thus a difference between the observed value and the trend value. This difference is termed the deviation and may be expressed mathematically as:

$$\text{deviation} = Z_o - Z_{tr} \quad (1)$$

where  $Z_o$  is the observed value and  $Z_{tr}$  is the trend value. For the least-squares criterion to be met, the sum of the squares of the deviations for all points must be minimized, such that:

$$\sum (Z_o - Z_{tr})^2 = \text{minimum}. \quad (2)$$

This minimizing will result in a unique surface based on the available data. Figure 51 shows a least-squares fit of a plane to a set of data points.

As mentioned, either Fourier series or polynomial equations may be used for surface fitting. Equation coefficients are calculated so as to minimize the deviation values of the data points. In order to describe



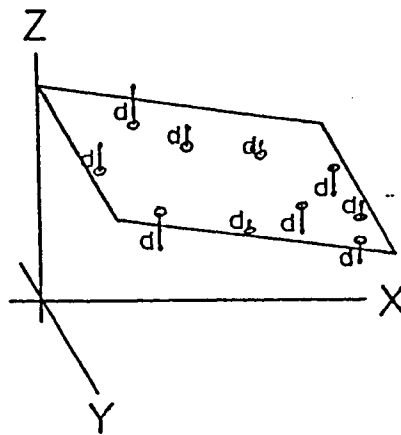


Figure 51. Least-squares Fit of Plane to Points

Plane has been fitted so that the sum of squared deviations (marked with d's) is minimized. After Harbaugh and Merriam (1968, p. 63).

the process a first-degree trend surface involving polynomial equations will be considered. A first-degree trend surface is simply a plane and is used because it is simpler than a higher order polynomial or Fourier surface. The process for higher order surface fitting is the same but more complex, and nonplanar surfaces may be generated.

The basic equation for a plane is:

$$Z_{tr} = A + Bx + Cy \quad (3)$$

where,  $x$  = coordinate value in  $x$  direction,

$y$  = coordinate value in  $y$  direction, and

$A, B, C$  = equation coefficients.

In order to fit this plane to a set of data points, the equation coefficients  $A, B,$  and  $C$  must be calculated such that the deviation is at a minimum.

For a particular point:

$$\text{deviation} = Z_o - Z_{tr}.$$

Since  $Z_{tr}$  is given by equation (3), then

$$\text{deviation} = Z_o - (A + Bx + Cy) \quad (4)$$

$$= Z_o - A - Bx - Cy. \quad (5)$$

Thus, the sum of the squared deviations is a function of the equation coefficients:

$$\text{sum of squared deviations} = F(A, B, C). \quad (6)$$

Combining equation (5) and equation (6):

$$F(A, B, C) = (Z_o - A - Bx - Cy)^2. \quad (7)$$

For  $F(A, B, C)$  to be at a minimum, it is necessary that:

$$\frac{dF}{dA} = \frac{dF}{dB} = \frac{dF}{dC} = 0. \quad (8)$$

The partial derivatives are:

$$\frac{dF}{dA} = \sum 2(Z_0 - A - Bx - Cy)(-1) = 0 \quad (9)$$

$$\frac{dF}{dB} = \sum 2(Z_0 - A - Bx - Cy)(-x) = 0 \quad (10)$$

$$\frac{dF}{dC} = \sum 2(Z_0 - A - Bx - Cy)(-y) = 0. \quad (11)$$

Multiplication of each expression and summation of the individual terms yields:

$$-\sum Z_0 + An + B\sum x + C\sum y = 0. \quad (12)$$

$$-\sum Z_0 + A\sum x + B\sum x^2 + C\sum xy = 0 \quad (13)$$

$$-\sum Z_0 y + A\sum y + B\sum xy + C\sum y^2 = 0 \quad (14)$$

where  $n$  = number of data points.

Rearranging:

$$An + B\sum x + C\sum y = \sum Z_0 \quad (15)$$

$$A\sum x + B\sum x^2 + C\sum xy = \sum Z_0 x \quad (16)$$

$$A\sum y + B\sum xy + C\sum y^2 = \sum Z_0 y. \quad (17)$$

If a solution exists for these three linear equations, it may be found by matrix algebra methods. We may restate the normal equations with a single matrix equation:

$$\begin{bmatrix} n & \sum x & \sum y \\ \sum x & \sum x^2 & \sum xy \\ \sum y & \sum xy & \sum y^2 \end{bmatrix} \times \begin{bmatrix} A \\ B \\ C \end{bmatrix} = \begin{bmatrix} \sum Z_0 \\ \sum Z_0 x \\ \sum Z_0 y \end{bmatrix} \quad (18)$$

Since  $x$ ,  $y$ , and  $Z_0$  are known, the ABC vector may be determined:

$$\begin{bmatrix} A \\ B \\ C \end{bmatrix} = \frac{\begin{bmatrix} \sum Z_o \\ \sum Z_o x \\ \sum Z_o y \end{bmatrix}}{\begin{bmatrix} n & \sum x & \sum y \\ \sum x & \sum x^2 & \sum xy \\ \sum y & \sum xy & \sum y^2 \end{bmatrix}} \quad (19)$$

With the coefficients A, B, and C thus known, values for  $Z_{tr}$  can be computed and plotted on the coordinate system to produce the trend surface.

The above example was used because the mathematics are simpler than for a double-Fourier series. However, the method of calculating the coefficients for a double-Fourier series is the same, inasmuch as a double Fourier series is a form of polynomial based on sine and cosine functions. The general form of the Fourier series is:

$$\begin{aligned} Z_{tr} = F(x, y) = & \sum_{m=0}^M \sum_{n=0}^N \lambda_{mn} \left( a_{mn} \cos \frac{(m\pi x)}{L} \cos \frac{(n\pi y)}{H} \right. \\ & + b_{mn} \sin \frac{(m\pi x)}{L} \cos \frac{(n\pi y)}{H} + c_{mn} \cos \frac{(m\pi x)}{L} \sin \frac{(n\pi y)}{H} \\ & \left. + d_{mn} \sin \frac{(m\pi x)}{L} \sin \frac{(n\pi y)}{H} \right) \quad (20) \end{aligned}$$

where,  $Z_{tr}$  = dependent variable (trend value),

$F(x, y)$  = Fourier approximation at coordinate point  $x, y$ ,

$m$  = index of degree of terms pertaining to  $x$  direction

$$(m = 0, 1, \dots, M),$$

$n$  = index of degree of terms pertaining to  $y$  direction

$$(n = 0, 1, \dots, N),$$

$a_{mn}$  = coefficient of cosine-cosine term of degree mn,

$b_{mn}$  = coefficient of sine-cosine term of degree mn,

$c_{mn}$  = coefficient of cosine-sine term of degree mn,

$d_{mn}$  = coefficient of sine-sine term of degree mn,

M = specified maximum degree of terms pertaining to  
x direction,

N = specified maximum degree of terms pertaining to  
y direction,

L = fundamental wavelength in x direction,

H = fundamental wavelength in y direction,

x = coordinate value in x direction,

y = coordinate value in y direction,

and,

$$\lambda_{mn} = 1/4, m = n = 0$$

$$\lambda_{mn} = 1/2, m = 0, n > 0, \text{ or } m > 0, n = 0$$

$$\lambda_{mn} = 1, m > 0, n > 0.$$

The coefficients may be found with a matrix equation similar to equation (18). To simplify the equation the following notation will be used:

$$Q_n = \cos \frac{(n\pi y)}{H}$$

$$R_n = \sin \frac{(n\pi y)}{H}$$

$$S_m = \cos \frac{(m\pi x)}{L}$$

$$T_m = \sin \frac{(m\pi x)}{L} .$$

The matrix equation is:

$$\begin{bmatrix}
 \sum(Q_0 S_0)^2 & \sum Q_1 S_0 Q_0 S_0 & \dots & \sum R_N^{TM} Q_0 S_0 \\
 \sum Q_0 S_0 Q_1 S_0 & \sum(Q_1 S_0)^2 & \dots & \sum R_N^{TM} Q_1 S_1 \\
 \cdot & \cdot & \dots & \cdot \\
 \cdot & \cdot & \dots & \cdot \\
 \cdot & \cdot & \dots & \cdot \\
 \sum Q_0 S_0 Q_3 T_1 & \sum Q_1 S_0 Q_3 T_1 & \dots & \sum R_N^{TM} Q_3 T_1 \\
 \cdot & \cdot & \dots & \cdot \\
 \cdot & \cdot & \dots & \cdot \\
 \sum Q_0 S_0 R_N^{TM} & \sum Q_1 S_0 R_N^{TM} & \dots & \sum (R_N^{TM})^2
 \end{bmatrix}
 \times
 \begin{bmatrix}
 a_{0,0} \\
 a_{1,0} \\
 \cdot \\
 \cdot \\
 \cdot \\
 \cdot \\
 \cdot \\
 d_{N,M}
 \end{bmatrix}$$

$$=
 \begin{bmatrix}
 \sum Z(x,y) Q_0 S_0 \\
 \sum Z(x,y) Q_1 S_0 \\
 \cdot \\
 \cdot \\
 \cdot \\
 \sum Z(x,y) Q_3 T_1 \\
 \cdot \\
 \cdot \\
 \sum Z(x,y) Q_N^{TM}
 \end{bmatrix}
 \tag{21}$$

The above description is modified from Harbaugh and Merriam (1968, p. 64-66 and 148-151).

There is no simple way to decide whether Fourier series or polynomial equations should be used for a particular application. Since

a Fourier series is based on trigonometric wave functions, it is generally used to best advantage where some sort of periodicity in the data is suspected. By using judgement when picking the fundamental wavelengths, the periodicity may be emphasized. Another advantage is that the orthogonal nature of the Fourier series permits the extrapolation of trend surfaces beyond the area of control points. This is particularly useful in preventing boundary, or edge, effects, a major problem when non-orthogonal polynomial fits are used. Polynomial equations are used to best advantage where either simple or exceedingly complex surfaces are to be generated. If the polynomial to be used is non-orthogonal, the surface cannot be extrapolated out of the control area with any accuracy, and the accuracy of the surface near the edges of the control area is not good. Orthogonal polynomials for surface fitting exist but are quite complex.

As in so many instances, the main consideration in choosing a surface-fitting technique involving Fourier series for this study was its ready availability. Digitgraph Computer Systems Company, Tucson, Arizona, has taken a double-Fourier trend surface analysis program described by James (1966) and placed it on a tape, which is stored in the University of Arizona Computer Center's tape library.

The program is quite simple to use, but several decisions must be made by the user in order to run the program. First, the fundamental wavelengths (H and L) must be chosen. They may be of any value as long as they are larger than the control area. This decision is of great value if some sort of periodicity in the data is suspected. Since no periodicity was suspected in the data used for this study, the fundamental

wavelengths were chosen as twice the value of the control area dimensions on the advice of Dr. J. R. Sturgul of the Department of Geosciences.

Another decision which must be made is the point of origin of the wave form. The location of this point of origin does not affect the shape of the derived surface; it only changes the values of the Fourier coefficients. For this study the point of origin was chosen as the southwest corner of the map area.

The final decision which must be made is the number of terms to be included in the Fourier series. By selecting the number of terms included, the surface can be made to achieve a fit which matches the observed data to a greater or lesser degree. For instance, if the number of terms included in the Fourier series is equal to the number of data points, the surface will fit the data exactly. As the number of terms included is decreased, the surface is smoothed and the more extreme variations in the data are filtered out. It is this smoothing effect which was sought in this study. Since assay data are quite variable, it was necessary to find some way to filter out the "noise" and to obtain a smoothed surface which represents a districtwide zoning pattern. By including the proper number of terms in the Fourier series, the desired amount of filtering may be achieved and a surface which represents districtwide zoning without a lot of noise may be generated.

The surfaces were initially generated using nine terms on the advice of Dr. J. R. Sturgul. This number of terms gave good results. Sixteen- and twenty-five-term surfaces were also generated for several trial examples. For both these number of terms, the resulting surfaces



were extremely noisy, and local variations masked the districtwide zoning patterns. The nine-term surfaces were best for showing overall zoning, and all maps used in this study were generated using nine terms in the Fourier series.

### Statistical Measures--Goodness of Fit

Trend surfacing of data is a procedure of using the least-squares criterion to fit a surface to a set of observed data. However, it is not enough simply to fit a surface to the data; it is essential to get some measure of how well the surface actually fits the observed data, that is, the goodness of fit. Two statistical measures have been used to determine the goodness of fit of the trend surfaces generated: percent sum of the squares contribution (percent SS contribution) and ratio of mean squares (F ratio).

#### Percent Sum of the Squares Contribution

Percent sum of the squares contribution (percent SS contribution) is a measure of how much of the total variation in the data set is accounted for by the trend surface. When the percent SS contribution is low, at 15-30 percent, most of the variation present in the data is not represented by the trend function. However, this does not necessarily invalidate the surface generated. In this study, the purpose was to determine sulfide zoning on a districtwide basis. Local factors which cause a variation in sulfide content are filtered out by the Fourier analysis. A low percent SS contribution indicates that a large part of the variation in sulfide content is due to local controls rather than districtwide zoning.

For a set of data, a single point within the data,  $Z_o$ , will depart from the data mean,  $\bar{Z}$ , by an amount equal to  $Z_o - \bar{Z}$ . A measure of the total variation in a data set is represented by the sum of the square of the departures:

$$S_{t1} = \sum (Z_o - \bar{Z})^2 \quad (22)$$

where,  $S_{t1}$  = total sum of the squares.

The total sum of the squares may be divided into two components, the deviation of observed values from trend values and the deviation of trend values from the mean value. Mathematically,

$$S_d = \sum (Z_o - Z_{tr})^2 \quad (23)$$

$$S_{tr} = \sum (Z_{tr} - \bar{Z})^2 \quad (24)$$

where,  $S_d$  = sum of the squares due to deviation of observed values from trend values, and

$S_{tr}$  = sum of the squares due to deviation of trend values from the mean values.

Now,  $S_d$  and  $S_{tr}$  are the two components which make up  $S_{t1}$ , such that

$$S_{t1} = S_d + S_{tr}. \quad (25)$$

This relationship is true only if the least-squares criterion has been met and the coefficients of the trend function are linear.

Figure 52 may aid in clarifying this relationship. A straight line has been fitted by the least-squares method using the equation:

$$Z_{tr} = mX + b \quad (26)$$

to three points,  $Z_{o1}$ ,  $Z_{o2}$ , and  $Z_{o3}$ . Coefficients  $m$  and  $b$  were determined, as described previously, and  $Z_{tr1}$ ,  $Z_{tr2}$ , and  $Z_{tr3}$ , the trend values, were calculated using equation (26). Distances  $A$ ,  $B$ , and  $C$  represent the following:

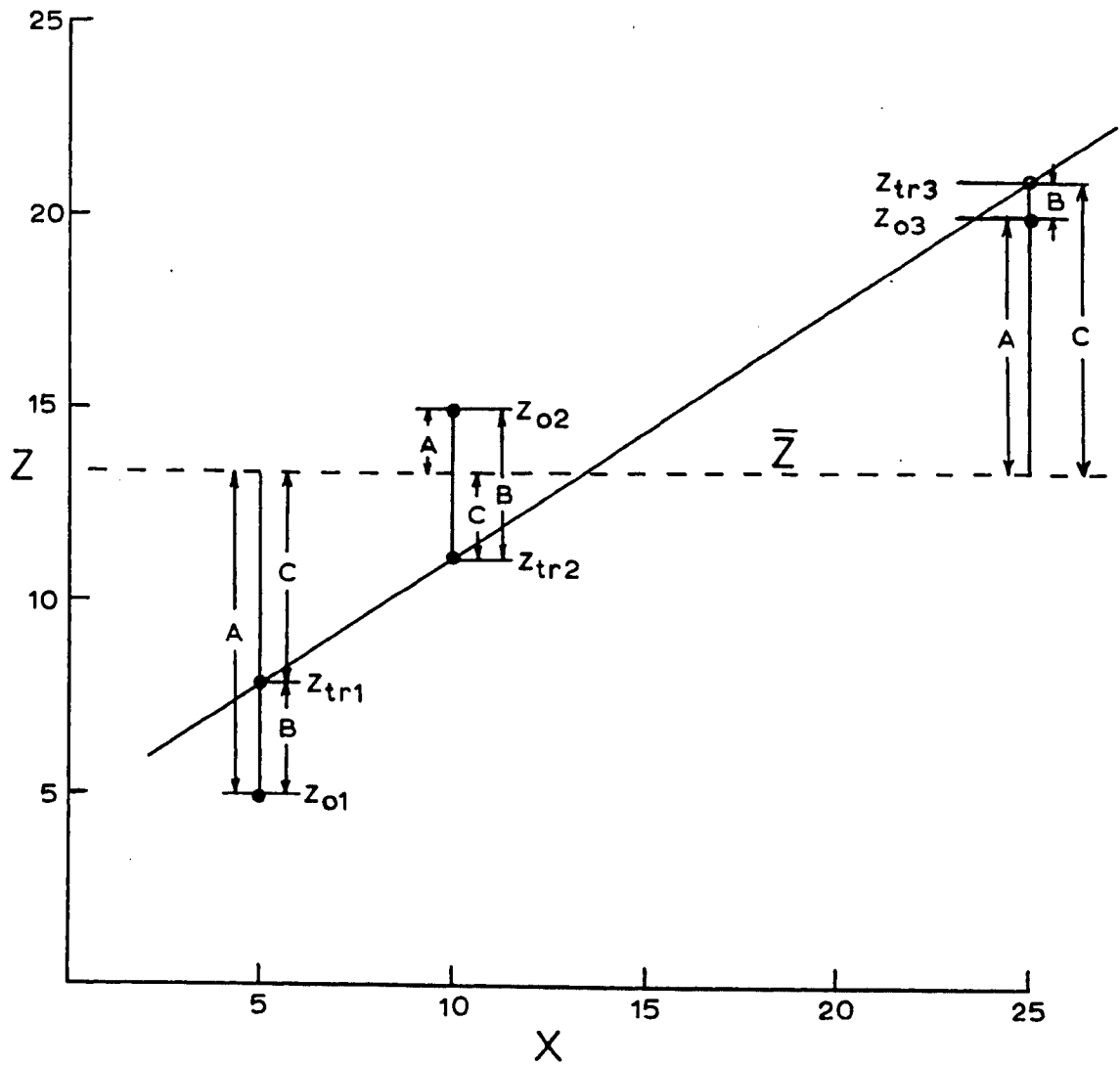


Figure 52. Least-squares Fit of a Line

$$A = Z_o - \bar{Z} \quad (27)$$

$$B = Z_o - Z_{tr} \quad (28)$$

$$C = Z_{tr} - \bar{Z} \quad (29)$$

therefore,

$$\sum A^2 = \sum (Z_o - \bar{Z})^2 = S_{tl} \quad (30)$$

$$\sum B^2 = \sum (Z_o - Z_{tr})^2 = S_d \quad (31)$$

$$\sum C^2 = \sum (Z_{tr} - \bar{Z})^2 = S_{tr} \quad (32)$$

by equations (22)-(24). Thus, the total variation,  $S_{tl}$ , within the data is represented by  $\sum A^2$ , the component of total variation due to the deviation of the observed values from the trend function,  $S_d$ , is represented by  $\sum B^2$ , and the component of total variation due to deviation of the trend function from the average value,  $S_{tr}$ , is represented by  $\sum C^2$ . It is necessary to square the values before summing them in order to remove the effect of their signs. Further, it is only the sum of the squares which are equal,  $\sum A^2 = \sum B^2 + \sum C^2$ . For a single point the squares are not equal. The equality of the sum of the squares is such that  $S_{tl} = S_d + S_{tr}$  only if the least-squares criterion has been met.

The percent SS contribution is a measure of what part of the total variation present in the data is accounted for by the trend surface. It is defined by the equation:

$$\text{percent SS contribution} = 100 \left( 1 - \frac{S_d}{S_{tl}} \right) \quad (33)$$

Thus, for a percent SS contribution of 50 percent, half of the variation in the data is represented by the trend surface and the other half is due to factors not represented by the trend surface.

If the number of terms in the trend function is equal to the number of data points, a percent SS contribution of 100 percent may be obtained, and all of the variation in the data is represented by the trend surface. However, "forcing" a fit in this manner leads to surfaces which have little geological meaning when irregularly spaced data are used, as in this study, as pointed out by Harbaugh and Merriam (1968, p. 67-68).

### F Ratio

The way in which variation occurs in a trend function may be analyzed to define further its statistical significance. The total variation present,  $S_{t1}$ , may be separated into two components,  $S_d$  and  $S_{tr}$ . The objective of variance analysis is to determine if the surface generated by the trend function is statistically significant.

By reducing the deviation sum of the squares,  $S_d$ , and the trend sum of the squares,  $S_{tr}$ , to mean squares, they may be compared as a ratio,  $F$ , which has a known probability distribution. This distribution is related to the manner in which  $S_d$  and  $S_{tr}$  are free to vary, that is, with the degrees of freedom of  $S_d$  and  $S_{tr}$ .

The total number of degrees of freedom are associated with the total variation in a data set. For  $n$  data points there are  $n - 1$  total degrees of freedom and  $n - 1$  degrees of freedom associated with deviations from the mean,  $S_{t1}$ .

For a trend function, the number of degrees of freedom,  $m$ , is equal to the number of terms in the function minus the zeroth term. For the deviations from the trend function, the number of degrees of freedom is equal to the total degrees of freedom,  $n - 1$ , less the number of degrees of freedom for the trend function,  $m$ , that is,  $n - m - 1$ . The mean square for the trend sum of the squares,  $M_1$ , is the trend sum of the

squares divided by the degrees of freedom for the trend function, or

$$M_1 = \frac{S_{tr}}{m} . \quad (34)$$

The mean square for the deviation sum of the squares,  $M_2$ , is the deviation sum of the squares divided by the degrees of freedom for the deviation, or

$$M_2 = \frac{S_d}{n - m - 1} \quad (35)$$

and

$$F = \frac{M_1}{M_2} . \quad (36)$$

The relationship between these various factors is summarized in Table 1.

Once a value for  $F$  has been computed, it can be compared with tabulated values of  $F$  in which values of  $F$  are arranged according to pairs of degrees of freedom at a particular significance level. This comparison is actually a test of the null hypothesis that no regression exists in the trend function, that is, that the trend function arises from chance alone and is not related to the data. If the computed  $F$  ratio exceeds the tabulated  $F$  ratio, the hypothesis is rejected and the alternative hypothesis that the regression does exist and the trend function is related to the data is accepted.

To take an example, assume that the number of degrees of freedom associated with the trend function is 8, the number of degrees of freedom associated with deviation from the trend function is 30, and the computed  $F$  ratio is 2.40. From a table of  $F$  ratios, the tabulated  $F$  ratio for the associated degrees of freedom of 8 and 30 is 2.27 at the 95 percent significance level. Since the computed value of 2.40 exceeds the tabulated value of 2.27, the null hypothesis that no regression exists

Table 1. Information Essential for Analysis of Variance.--From Harbaugh and Merriam (1968, p. 68)

Source of Variation	Degrees of Freedom	Sum of the Squares	Mean Square
Trend-function regression	m	$S_{tr} = \sum (Z_{tr} - \bar{Z})^2$	$M_1 = \frac{S_{tr}}{m}$
Deviations	n - m - 1	$S_d = \sum (Z_o - Z_{tr})^2$	$M_2 = \frac{S_d}{n - m - 1}$
Total	n - 1	$S_{tl} = \sum (Z_o - \bar{Z})^2$	
Ratio of Mean Squares: $F = \frac{M_1}{M_2}$			

m = number of terms in trend component,

n = number of data points,

$S_{tr}$  = sum of the squares due to regression or trend function,

$S_d$  = sum of the squares due to deviations,

$S_{tl}$  = sum of the squares due to total variation,

$Z_{tr}$  = value predicted by trend function,

$Z_o$  = observed data value,

$\bar{Z}$  = arithmetic mean of observed data values,

$M_1$  = mean square associated with regression,

$M_2$  = mean square associated with deviations,

F = ratio of mean squares.

is rejected and the alternative hypothesis that regression does exist is accepted on the 95 percent significance level.

The significance level is a reflection of the validity of the regression surface. For the above example, 95 percent of the regression present in the trend surface is related to the observed data and 5 percent is due to random variation in the fitting technique.



## REFERENCES

- Hammer, D. F., 1961, Geology and ore deposits of the Jackrabbit area, Pinal County, Arizona: unpub. M.S. thesis, University of Arizona.
- Harbaugh, J. W., and Merriam, D. F., 1968, Computer applications in stratigraphic analysis: New York, John Wiley & Sons, Inc.
- Harper, H. E., and Reynolds, J. R., 1969, The Lakeshore copper deposit: Mining Cong. Jour., v. 55, no. 11, p. 26-30.
- Hogue, W. G., 1940, Geology of the northern part of the Slate Mountains, Pinal County, Arizona: unpub. M.S. thesis, University of Arizona.
- James, A. H., 1971, Hypothetical diagrams of several porphyry copper deposits: Econ. Geol., v. 66, no. 1, p. 43-47.
- James, W. R., 1966, Fortran IV program using double-Fourier series for surface fitting of irregularly spaced data: Lawrence, Kansas, Kansas State Geological Survey, Computer Contribution #5.
- Krumbein, W. C., and Graybill, F. A., 1965, Statistical models in geology: New York, McGraw-Hill Book Company, Inc.
- Lowell, J. D., and Guilbert, J. M., 1970, Lateral and vertical alteration-mineralization in porphyry ore deposits: Econ. Geol., v. 65, no. 4, p. 378-408.
- McClymonds, N. E., 1959, Precambrian and Paleozoic sedimentary rocks on the Papago Indian Reservation, Arizona, in Southern Arizona Guidebook II, L. A. Heindl, ed.: Tucson, Arizona, Arizona Geological Society, p. 77-89.
- Rose, A. W., 1970, Zonal relations of wall rock alteration and sulfide distribution at porphyry copper deposits: Econ. Geol., v. 65, no. 8, p. 920-936.
- Wilson, E. D., 1962, A résumé of the geology of Arizona: University of Arizona, Arizona Bureau of Mines Bull. 171.

